Institut für Veterinärbiochemie und Molekularbiologie der
Vetsuisse-Fakultät, Universität Zürich

Direktor: Prof. Dr. med. vet. Ulrich Hübscher

Arbeit unter wissenschaftlicher Betreuung von:
Prof. Dr. med. vet. et phil. II Michael O. Hottiger

Identification of lysine residues as ADP-ribose acceptor sites in core histone tails

Inaugural-Dissertation

zur Erlangung der Doktorwürde der
Vetsuisse-Fakultät, Universität Zürich

vorgelegt von

Andrea Ursula Poživil

Tierärztin
von Niederdorf/BL

Genehmigt auf Antrag von
Prof. Dr. Dr. Michael O. Hottiger (Referent)
Prof. Dr. Thomas Lutz (Korreferent)

Zürich, 2010

Table of content

Summary

In the nucleus of each cell, the DNA is packed with proteins into chromatin. Chromatin consists of DNA wrapped around nucleosomes, which contain two copies of each of the four core histones H2A, H2B, H3 and H4. Histones are composed of one core domain that is flanked by variable N- and C-terminal tails, which can be modified through different posttranslational modifications such as acetylation, methylation, ubiquitylation, phosphorylation and (ADP-ribosyl)ation.

Poly(ADP-ribosyl)ation is catalyzed by poly(ADP-ribose) polymerase 1 (PARP1) by covalent attachment of multiple ADP-ribose units, using NAD^+ as the substrate. PARP1 and its enzymatic activity play a crucial role in many physiological and pathophysiological processes, such as maintenance of genomic stability through DNA repair, transcriptional regulation (e.g. inflammation), cell cycle regulation and cell death through apoptosis or necrosis.

The aim of this thesis was to investigate whether histone tails are (ADP-ribosyl)ated by PARP1, PARP2 and PARP10 and furthermore to identify potential ADP-ribose acceptor sites of the core histone tails.

We found that GST-tagged histone tails are indeed trans(ADP-ribosyl)ated by PARP1 and GST-PARP10(818-1025), but not by PARP2. Furthermore, the minimal deletion mutant required for the interaction with PARP1 was identified for each core histone tail, which correlated with the deletion mutant required for (ADP-ribosyl)ation, except for H2B. High NaCl concentrations reduced the interaction of PARP1 with the GST-tagged histone tails and subsequently also (ADP-ribosyl)ation. Lysines were found to be the most important residues for (ADP-ribosyl)ation of the histone tails, since substitution of distinct lysines resulted in a loss of (ADP-ribosyl)ation. Possible ADP-ribose acceptor sites modified by PARP1 are K13/R20 of H2A as well as K16/20 of H4. Important for the interaction with PARP1 are K15/R20 of H2A, R29/31/33 of H2B, R26 of H3 and K16/20 of H4. The histone tails mainly interact with the automodification domain of PARP1. Finally, same analyses with GST-PARP10(818-1025) suggested possible ADP-ribose acceptor sites modified by PARP10, namely K13/15 of H2A, K27/28/30/34/R29/31/33 of H2B and K16/20, R17/19 of H4.

Together these experiments provide evidence that specific lysine and possibly arginine residues of histone tails are (ADP-ribosyl)ated by PARP1 or PARP10. Parts of this thesis were recently accepted for publication.

Zusammenfassung

DNA ist im Zellkern in Form von Chromatin kondensiert. Das Chromatin besteht aus DNA, die um Nukleosomen gewickelt ist, welche aus jeweils zwei Kopien von jedem Kern-Histon H2A, H2B, H3 and H4 zusammengesetzt sind. Histone bestehen aus einer Kern-Domaine, die N- und C-terminal von einem variablen Ende flankiert wird. Diese Enden können durch verschiedene posttranslationelle Modifikationen, wie Acetylierung, Methylierung, Ubiquitylierung, Phosphorylierung und (ADP-Ribosyl)ierung verändert werden.

Poly(ADP-Ribosyl)ierung wird von Poly(ADP-Ribose) Polymerase 1 (PARP1) durch kovalentes anhängen von mehreren ADP-Ribose-Einheiten, mittels Benutzung von NAD^+ als Substrat katalysiert. PARP1 und seine enzymatische Aktivität spielen eine entscheidende Rolle in vielen physiologischen und pathophysiologischen Vorgängen, wie z.B. dem Erhalt der genomischen Stabilität durch DNA Reparatur, Regulation der Transkription (z.B. im Entzündungsgeschehen), Regulation des Zellzyklus und Zelltod infolge Apoptose oder Nekrose.

Ziel dieser Dissertation war zu erforschen, ob Histonenden durch PARP1, PARP2 oder PARP10 (ADP-ribosyl)iert werden, sowie die potentiellen Akzeptoren von ADP-Ribose auf Kern-Histonenden zu identifizieren.

Wir beobachteten dass GST-Histonenden von PARP1 und GST-PARP10(818-1025), aber nicht von PARP2 (ADP-ribosyl)iert werden. Weiter wurde die minimal nötige Deletionsmutante für erfolgreiche Interaktion der Histonenden mit PARP1 identifiziert. Diese korrelierten mit den Deletionsmutanten, die für erfolgreiche (ADP-Ribosyl)ierung nötig sind, mit Ausnahme für H2B. Hohe Salzkonzentrationen reduzierten die Interaktion von PARP1 mit den GST-Histonenden und deshalb auch die (ADP-Ribosyl)ierung. Wir fanden dass Lysine die wichtigsten Stellen für (ADP-Ribosyl)ierung von Histonenden sind, da bei einer Substitution von spezifischen Lysinen keine (ADP-Ribosyl)ierung mehr stattfinden konnte. Mögliche Akzeptoren von PARP1-regulierter (ADP-Ribosyl)ierung sind K13/R20 von H2A und K16/20 von H4. Wichtig für die Interaktion mit PARP1 sind K15/R20 von H2A, R29/31/33 von H2B, R26 von H3 und K16/20 von H4. Die Histonenden interagieren vor allem mit der Automodifikationsdomäne von PARP1. Schlussendlich haben gleiche Untersuchungen mit PARP10 weitere mögliche Akzeptoren von ADP-Ribose aufgedeckt, nämlich K13/15 von H2A, K27/28/30/34/R29/31/33 von H2B und K16/20, R17/19 von H4.

Zusammen erbringen diese Versuche den Nachweis, dass spezifische Lysine und möglicherweise Arginine der Histonenden von PARP1 oder PARP10 (ADP-ribosyl)iert werden. Teile dieser Dissertation wurden vor kurzem zur Publikation angenommen.

Abbreviations

aa	amino acid
AD	Automodification domain
AIF	Apoptosis-inducing factor
ATP	Adenosine triphosphate
bp	base pairs
BSA	Bovine serum albumine
CAT	Catalytic domain
DBD	DNA-binding domain
DNA	Deoxyribonucleic acid
dNTP's	deoxy Nucleotide-Tri-Phosphates
DSB	Double strand breaks
FL	Full-length
GST	Glutathione S-transferase
h	human
H1	Histone 1
H2A	Histone 2A
H2B	Histone 2B
H3	Histone 3
H4	Histone 4
NAD^+	Nicotinamide adenine dinucleotide
PAR	Poly(ADP-ribose) polymer
PARG	Poly(ADP-ribose) glycohydrolase
PARP	Poly(ADP-ribose) polymerase
PBS	Phosphate buffered saline
PCR	Polymerase chain reaction
RNA	Ribonucleic acid
SDS	Sodium-dodecyl-sulfate
SSB	Single strand breaks
TBS	Tris buffered saline
TBS-T	Tris buffered saline Tween 20
U	Unit
V	Volt
wt	wildtype
ZF	Zinc Finger

1 Introduction

1.1 Chromatin

1.1.1 Introduction

The length of a DNA is 100’000 times longer than a cell. Therefore the DNA has to be arranged in a special manner in form of the chromatin and chromosomes to scope with the size of the cell (1). The chromatin is formed by wrapping DNA around nuclear proteins such as histones and non-histone proteins (2, 3). Importantly, the chromatin structure is an obstacle for genomic activities such as replication, transcription, recombination or repair. Thus, it is important that the DNA is made accessible in response to various stimuli. This is achieved by exchanging or chemical modifying histones, which lead to a change of the chromatin structure (2). Chromatin can be divided into two states, which are called euchromatin and heterochromatin. Euchromatin is less condensed chromatin, which is more accessible for proteins regulating cellular processes. Heterochromatin represents the compact state of chromatin, which is tightly folded and inaccessible for regulatory proteins. Each of these states is associated with a distinct set of histone modifications (4).

1.1.2 Chromatin structure

The compact chromatin structure comprises three different condensation levels (Fig. 1).

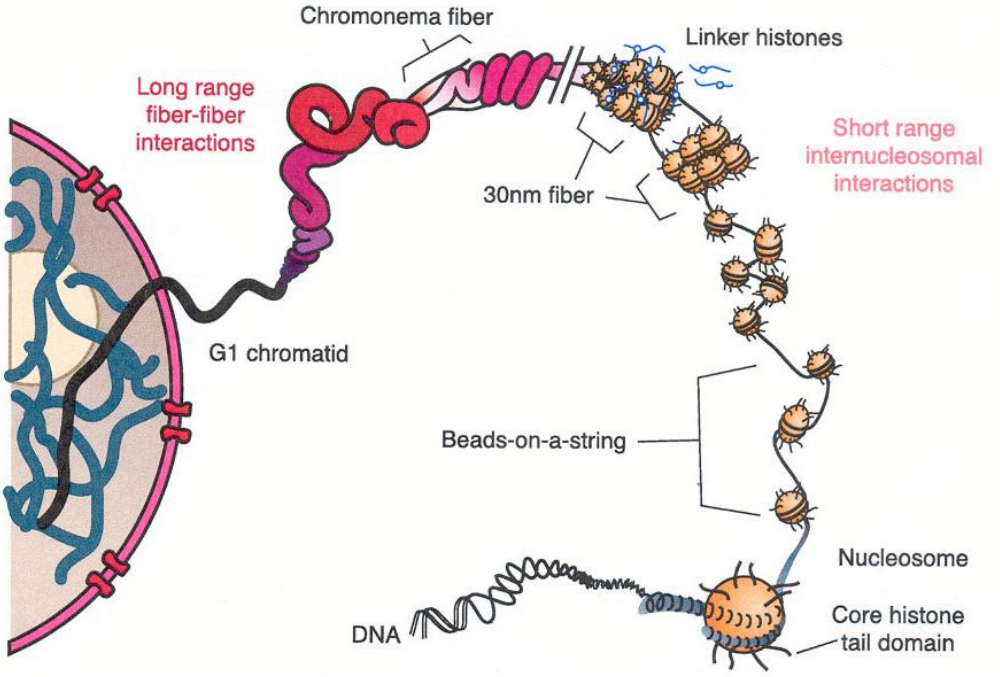

Figure 1: Multiple levels of chromatin folding. DNA compaction within the interphase nucleus occurs through a hierarchy of histone-dependent interactions that can be subdivided into primary, secondary, and tertiary levels of structure. Strings of nucleosomes compose the primary structural unit. Formation of 30nm fibers through histone-tail-mediated nucleosome-nucleosome interactions provides a secondary level of compaction, whereas tail-mediated association of individual fibers produces tertiary structures (such as chromonema fibers) (5).

The first level of condensation, which generates a 7-fold compaction, is achieved by wrapping DNA around histones to form the nucleosome, which has a diameter of 10nm and builds the basic unit of the chromatin (2, 6). One nucleosome contains two copies of each of the four core histones H2A, H2B, H3 and H4, around which are wrapped one and three-quarter superhelical turns of DNA (146 bp) (2). Histones are basic proteins containing a large number of positive charged amino acids, which enable the interaction with the negatively charged DNA. The DNA linker length connecting two nucleosomes is species dependent and varies from 15 to 55 base pairs (1). In presence of the linker histone H1, the chromatin condenses from the fully extended “beads on a string” configuration into a 30nm fiber, for which six nucleosomes are coiled to form one turn, called solenoid structure (2, 6-8). Interactions with additional factors, such as non-histone and nuclear matrix scaffold proteins, establish large chromatin loop domains that can be compacted further to generate interphase and mitotic chromosomes (2). Chromonema fibers represent the highest ordered state of chromatin in vivo (9).

1.1.3 Histone proteins

There are five different histones in mammalian cells which play a role in chromatin formation, namely the nucleosomal or core histones H2A, H2B, H3 and H4 as well as the linker histone H1 (10). Histones are expressed during S-phase and are incorporated into chromatin in a DNA replication-dependent manner. They are composed of one core domain that is flanked by two tail domains. The core domains of histones are responsible for establishing protein-protein interactions and for the compaction of the DNA (11). The N- and C-terminal tail domains can form additional DNA contacts and can be modified by different posttranslational modifications such as acetylation, methylation, ubiquitylation, phosphorylation and (ADP-ribosyl)ation (2, 7, 12, 13). Posttranslational modifications of the tail domains can neutralize the net positive charge of the tails, which reduces the interaction with the negative charged phosphate backbone of the DNA. Modified chromatin is therefore often less condensated and better accessible for proteins involved in transcription, replication and repair (1, 4).

The histones H3 and H4 form a heterotetramer, representing the core of the nucleosome structure that is flanked by two histone H2A and H2B heterodimers. The H3-H4 tetramer is strongly interacting with the nucleosomal DNA and their N-terminal tail domains exit the nucleosome close to the points where the DNA starts to bind or leaves the nucleosome (4, 14-16). In contrast to H3 and H4, histones H2A and H2B are weakly associated with nucleosomal DNA (17-20) and more frequently displaced from nucleosomes (21-27), suggesting that posttranslational modifications on these histones play a less important role (14). Similar to the core histones, linker histone H1 can be covalently modified. The best-studied modification is currently phosphorylation, which weakens the binding of H1 to chromatin and thus destabilizes chromatin structure (10).

1.1.4 Histone variants

Beside remodelling the chromatin by posttranslational modification of histones, there is also another way to regulate the chromatin barrier, namely through incorporation of histone variants into nucleosomes (28). Histone variants are subtypes of core histones and are mainly expressed in other cell cycle phases than the S-phase and incorporated into chromatin in a DNA replication-independent manner (29). The histone variants are suggested to be

located in novel types of nucleosomes, which are located on the chromatin in addition to nucleosomes containing only core histones (30, 31).

One of the best characterized histone variant is H2A.Z, which is a histone variant of histone H2A. The N- and C-terminal domains of H2A.Z have a substantially different sequence from that of the core histone H2A (28, 32, 33). H2A.Z is required for one or more essential roles that cannot be replaced by H2A (32, 33). Several lines of evidence suggest that the incorporation of H2A.Z within chromosomes promotes an actively transcribed chromatin state (28, 34, 35). The theory based on experiments with knockout mice suggests that H2A.Z is important for stabilizing promoters for gene activation (33, 36, 37). The proposed promoter stabilization activity could also be related to the structure of H2A.Z nucleosomes, which prevent internucleosomal interactions and therefore promotes a more open chromatin conformation, which is characteristic for transcriptionally active genes (28, 38). Other variants of H2A are macroH2A, H2A.X and H2ABbd. The function of the variant macroH2A is to silence genes. It is found as a component of the inactivated X-chromosome in female cells (39). The variant H2A.X is modified by phosphate groups after DNA damage and therefore acts as one of the earliest responses to DNA damage by repressing transcription (4, 29). Finally, the variant H2ABbd activates transcription and is located on active X-chromosomes and autosomes (29).

The histone H3 has two histone variants, H3.3 and CENP-A. The variant H3.3 is mainly expressed in genetically active chromatin, whereas CENP-A is localized in centromere-regions of chromosomes (39). Comparable to the core histones, there are also linker histone variants that are nonrandomly incorporated into chromatin and expressed in cell type-specific patterns (40).

Accumulating evidence suggests that the combination of modifications on nucleosomes including core histones and various histone variants, contribute to the epigenetic information, the ultimate regulation of gene expression (41). Epigenetics is defined as heritable changes in the genome function that occurs without alterations of the DNA sequence (42). Therefore, the study of histone proteins and of their posttranslational modifications, has become increasingly important as more investigations are conducted into the “epigenetic signatures” of these important chromosomal proteins (43).

1.1.5 Non-histone proteins

Chromatin-associated non-histone proteins form one-third of the mass of mitotic chromosomes and remain associated with the chromatin, even after removal of the histones (3). Many different proteins belong to the group of non-histone proteins, such as high mobility group (HMG) proteins, scaffold proteins, DNA topoisomerases and DNA polymerases, all regulating different functions (8). One important function is the maintenance of the chromosomal structure (8). Additionally chromosomal non-histone proteins play a role in three important aspects of mitotic events, such as (i) chromosome condensation, (ii) sister chromatid separation and (iii) interaction of the chromosomes with the cytoskeleton during formation of the mitotic spindle (3).

1.2 Posttranslational modifications

1.2.1 Introduction

Posttranslational modifications are reversible modifications of proteins through an enzymatic attachment of special chemical groups, which regulate the biological activity (structure and function) of the modified proteins (8). Different modifications have been described for histones so far, namely: acetylation, methylation, phosphorylation, ubiquitylation, sumoylation, (ADP-ribosyl)ation, deimination and proline isomerization (4). Modifications on histones are usually reversible (4). The vast array of posttranslational modifications provides enormous potential for the regulation of functional responses within the cell (4) and belongs to the mechanisms that define epigenetics (44).

1.2.2 Impact of posttranslational histone modifications on the chromatin

Histones can be modified at over 60 different amino acid residues on their N-terminal tails (4), whereas H3 has the greatest number of currently reported modifications, followed by H4, H2B and H2A. The C-terminal tails also contain posttranslational modifications, but to a lesser extent when compared to the N-terminus (44). Two characteristic alterations are known to be induced by histone modifications. The first alteration is the disruption of contacts between two nucleosomes or between a nucleosome and the DNA, in order to unfold chromatin (4). Acetylation has the highest potential to unfold

chromatin, since it neutralizes the positive charge of the lysines. Therefore actively transcribed euchromatin usually contains high levels of histone acetylation, whereas silent heterochromatin is associated with low levels of histone acetylation (4). The second alteration is the modification-dependent recruitment of non-histone proteins (e.g. remodelling ATPases), which can further modify or alter the chromatin structure through their enzymatic activities. The requirement to recruit an ordered series of enzymatic activities can be explained by the fact that regulatory processes such as transcription, replication and repair are subdivided in several steps. Each one of these steps may require a distinct type of chromatin-remodelling activity and a different set of modifications (4).

Most of the known modifications were identified while studying transcription and can be divided into two groups, those that activate transcription and those that repress transcription. Transcriptional activation is accompanied by acetylation, methylation, phosphorylation or ubiquitylation, and transcriptional repression by methylation, ubiquitylation, sumoylation, deimination or proline isomerization. Thus, any given modification has the potential to activate or repress gene expression depending on the modified residue and the context (e.g. other modifications) (4).

Chromatin also generates a barrier for the repair of damaged DNA. Therefore modifications on histones are also required to facilitate the recognition and the accessibility of sites where DNA needs to be repaired. One of the earliest response to DNA damage in mammalian cells is the phosphorylation of the histone variant H2A.X. Beside phosphorylation, also ubiquitylation, methylation and acetylation of lysines play a role in DNA repair (4). Condensation and decondensation of chromatin are important processes during the replicative cell cycle. This function is regulated by phosphorylation and acetylation of histones (4).

1.2.3 Cross-talk of posttranslational modifications on histones

The main targets of posttranslational modifications on histones are lysines and arginines. Acetylation on histone tails occur at K5 of H2A, K12/15 of H2B, K9/14/18/23/56 of H3 and K5/8/12/16 of H4. Histone H3 and H4 can also be methylated on lysines K4/9/27/36/79 of H3 and K20 of H4 as well as arginines R2/8/17/26 of H3 and R3 of H4 (4). Differential modification of the same lysine residue of the histone tails, makes a cross-talk between modifications very likely. The cross-talk might mechanistically occur at several levels. Firstly, many different modifications occur on the same lysine residues. This will

undoubtedly result in some form of antagonism since distinct types of modifications on lysines are mutually exclusive. Secondly, the binding of a protein could be disrupted by an adjacent modification. The best example is the phosphorylation of H3S10 affecting the binding of HP1 to methylated H3K9 (4, 45). Thirdly, the catalytic activity of an enzyme could be compromised by modification of its substrate recognition site; for example, isomerization of H3P38 affects methylation of H3K36 by Set2 (4, 46). Fourthly, an enzyme could recognize its substrate more effectively in the context of a second modification; the example here is the GCN5 acetyltransferase, which may recognize H3 more effectively when it is phosphorylated at H3S10 (4, 47). Finally, a cross-talk could also be observed, when the modifications are on different histone tails of adjacent histones in an octamer (4).

1.3 Poly(ADP-ribose) polymerases

1.3.1 Introduction

Mammalian Poly(ADP-ribose) polymerase 1 (PARP1), is a 113kDa nuclear chromatin-associated multifunctional enzyme (48). PARP1 catalyzes the covalent transfer of ADP-ribose units from its substrate nicotinamide adenine dinucleotide (NAD^+) to itself and/or other nuclear proteins (49). Through its physical association with, or by poly(ADP-ribosyl)ing target proteins, PARP1 can regulate the chromatin structure and subsequently DNA metabolism. These target proteins include histones, high mobility group (HMG) proteins, topoisomerases I and II, DNA helicases, single strand break repair and base excision repair factors, as well as various transcription factors (50). PARP1 also functions as a survival factor for the maintenance of genomic integrity through recognition and signalling of single strand breaks (SSB) and double strand breaks (DSB) (51-53).

1.3.2 The PARP family

PARP1 is the first and best characterized (ADP-ribosyl)transferase member of a family consisting of 17 mammalian proteins with a sequence homology to the catalytic domain of bacterial Diphteria toxin (48, 54-56). Based on the high sequence similarities of their catalytic domains, the 17 mammalian proteins were named PARP1-17 (55, 56). It has been suggested that the PARP family can be subdivided into two groups, due to the results of

sequence alignments and superpositions of their crystal structures (54). The first group contains 6 PARPs, namely PARP1, PARP2, PARP3, PARP4, PARP5a and PARP5b, and is characterized by the presence of a glutamate in the active site (54, 56). This glutamate (E988 in hPARP1) has been reported to be required for ADP-ribose chain elongation catalyzed by PARP1 (57, 58). Therefore most PARPs in this group are able to catalyze bona fide polymers of ADP-ribose. The second group contains the other 11 PARPs, namely PARP6 to PARP16, which lack the corresponding glutamate in their active site (E988 in hPARP1). These members may thus rather possess mono(ADP-ribosyl)transferase activity than poly(ADP-ribosyl)transferase activity or are even inactive (54, 56). The PARP family members can additionally be classified according to their putative functional domains or established functions, into DNA-dependent PARPs, Tankyrases, CCCH-type PARPs as well as macroPARPs (Fig. 2) (50).

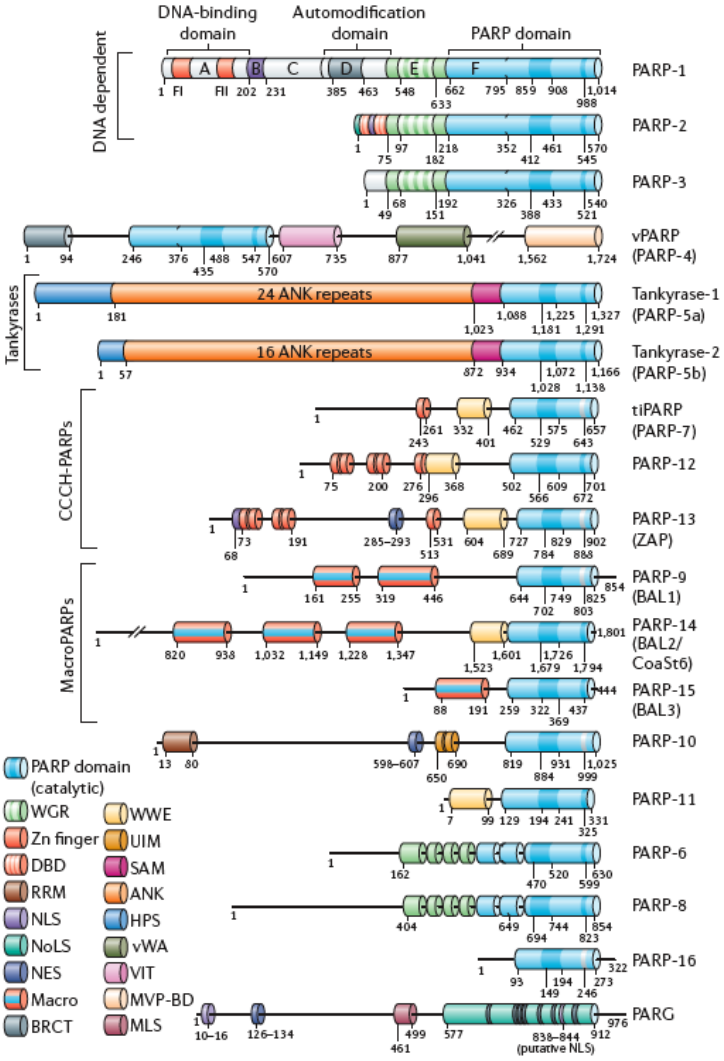

Figure 2: The domain architecture of the 17 members of the poly(ADP-ribose) polymerase (PARP) superfamily and of poly(ADP-ribose) glycohydrolase (PARG). Protein domains that are illustrated by coloured boxes were defined according to the Pfam 19.0 or CCD v2.06 (National Center for Biotechnology Information) databases (50).

1.3.3 Structure of PARP1

PARP1 consists of three functionally distinct domains: a N-terminal DNA-binding domain (DBD), an automodification domain (AD) and a C-terminal domain that includes the catalytic domain (CAT) responsible for poly(ADP-ribose) (PAR) formation (59, 60).

The DNA-binding domain (DBD) contains two structurally and functionally unique zinc fingers (ZFI: amino acid 11-89; ZFII: amino acid 115-199) (54, 60, 61). Recently, a third zinc-binding motif (ZBDIII) was discovered from amino acid 233-373 (62, 63). The PARP1 ZFI and ZFII are thought to recognize altered structures in the DNA and are also involved in protein-protein interactions (60, 64). Several studies indicate that ZFI is required for PARP1

activation by DNA single and double strand breaks, whereas ZFII activates PARP1 only by DNA single strand breaks (54, 60, 61). ZFI is absolutely required for DNA-dependent activation of PARP1, whereas ZFII is dispensable. ZBDIII is essential for the interaction of the DBD with the CAT domain and thus for the activation of PARP1 (60). The DBD also contains a bipartite nuclear localization signal (NLS), between ZFII and ZBDIII, that targets PARP1 to the nucleus (65) and two helix-turn-helix motifs which probably play a role for DNA binding (54, 61).

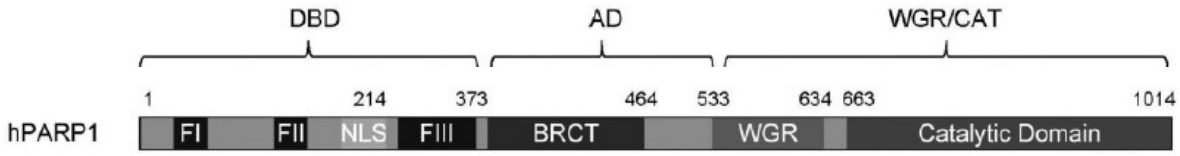

Figure 3: Structure of human PARP1 (60). Different domains are explained in the text.

The automodification domain (AD) of PARP1 is located in the central region of the enzyme (amino acid 373-525) (66, 67) and contains the acceptor amino acids for the covalent attachment of PAR (50). The AD of PARP1 includes a breast cancer 1 protein (BRCA1) C-terminus (BRCT) domain (54), which is found in many proteins acting in DNA repair or cell cycle checkpoint (68). The N-terminal half of the PARP1 AD contains a leucine-zipper motif, which is suggested to be involved in homo- and/or heterodimerization with other nuclear leucine-zipper proteins (69-75). Next to the AD of PARP1 is an 80-90 amino acid long tryptophane-, glycine-, arginine-rich (WGR) domain, which may function as nucleic-acid-binding domain (54, 60). This region has not yet been extensively characterized. But from recent studies, it is known that it is essential for the enzymatic activity of PARP1, although it is not necessary for the interaction between the DBD and the CAT domain (60).

The catalytic domain (CAT) is located at the C-terminal end of PARP1 and catalyzes PAR (59, 60). The WGR/CAT domain in PARP1 cooperates tightly with the N-terminal domain and thus limits the poly(ADP-ribosyl)ation capacity and the ability for automodification (60). Only an intact DBD can interact with the CAT domain in a DNA-dependent manner and induce PAR formation. PAR formation can only take place when ZFI, ZBDIII and the WGR domain are present. Otherwise PARP1 is enzymatic inactive (60).

1.3.4 Enzymatic activity of PARP1

Poly(ADP-ribosyl)ation plays an important role in a wide range of physiological and pathophysiological processes, such as maintenance of genomic stability, transcriptional regulation, centromere function, telomere dynamics and mitotic spindle formation during cell division, energy metabolism and cell death (48). In unstimulated cells the levels of PAR are usually very low (48, 61, 76). However, in response to genotoxic stress or mitogenic stimuli, the PARP activity and the levels of PAR increase 10 to 500 folds (48, 77-80).

1.3.4.1 The poly(ADP-ribosyl)ation reaction

Poly(ADP-ribosyl)ation is a covalent posttranslational modification unique to and remarkably conserved among metazoans, with exception of yeast, which lack PARPs (2, 61). PARPs catalyze the covalent attachment of multiple ADP-ribose units to itself and to a variety of target proteins, using NAD^+ as the substrate and releasing nicotinamide (2, 81). PAR is a homopolymer of ADP-ribose units linked by glycosidic 1" → 2' bonds between the ribose units (81, 82). The synthesis of PAR requires three distinct enzymatic activities, namely (i) the initiation or mono(ADP-ribosyl)ation of the substrate, (ii) the elongation of the polymer and (iii) the branching of the polymer (59-61) (Fig. 4).

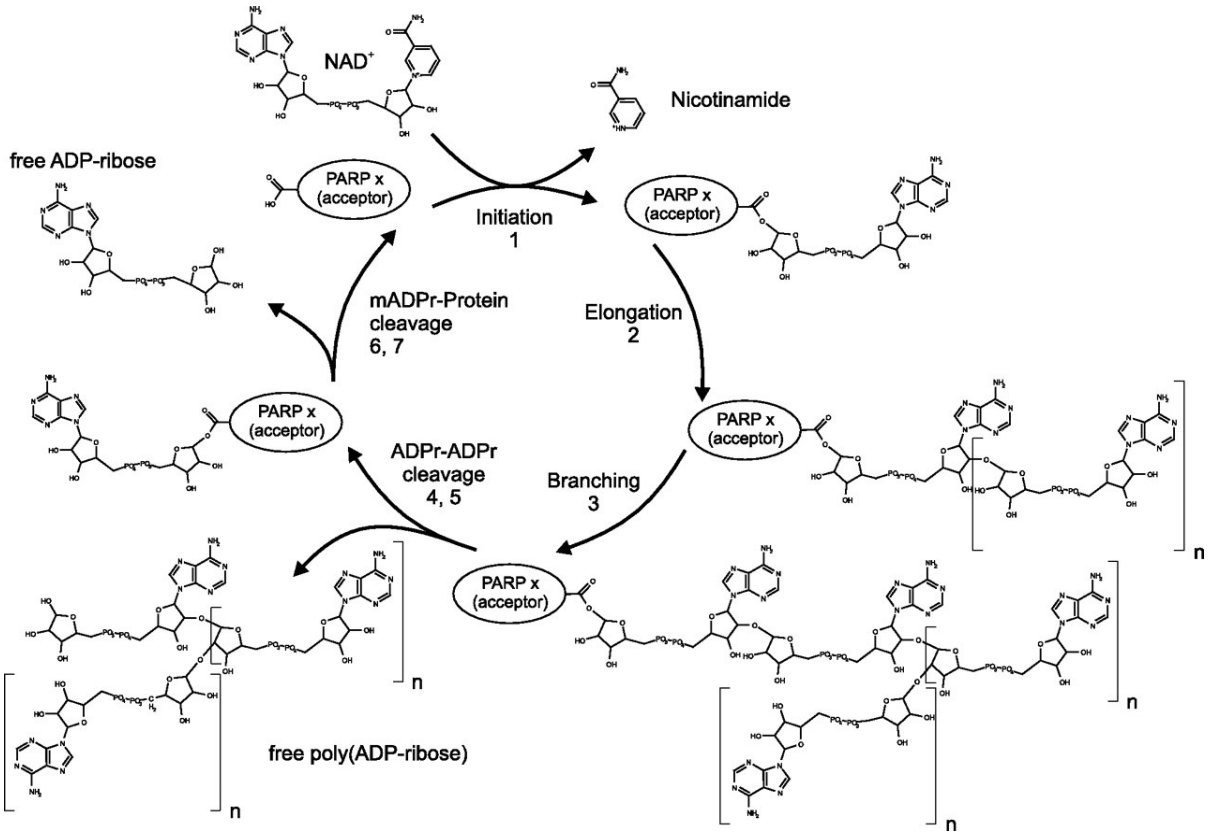

Figure 4: Poly(ADP-ribose) metabolism. Steps 1 to 3 and 4 to 7 represent the anabolic and catabolic reactions, respectively, in the metabolism of PAR. The synthesis of PAR consists of three distinct PARP activities: 1) initiation or mono(ADP-ribosyl)ation of specific residues in the acceptor chain, 2) elongation of the polymer, 3) branching of the polymer. Figure adapted from (54).

The chain length of polymers is heterogeneous and can reach in vitro 200 units. Long polymers are subsequently branched in an irregular manner with a frequency of approximately one branch per linear section of 20-50 units of ADP-riboses (83-85). In the absence of DNA damage the majority of the ADP-ribose units on the acceptor proteins are mono- or oligo(ADP-ribosyl)ated (86, 87). In the presence of DNA strand breaks, the PARP1 activity as well as the levels of PAR are increased, while cellular NAD^+ levels are correspondingly reduced (88-90).

1.3.4.2 Catabolism of poly(ADP-ribose)

Poly(ADP-ribose) has a short half-life and is degraded by the activity of poly(ADP-ribose) glycohydrolase (PARG), which is activated by increasing cellular concentrations of PAR. PARG has an endo- and exoglycosidic activity that cleaves the glycosidic bonds between the ADP-ribose subunits, generating free ADP-ribose units and polymers of ADP-ribose (see Fig. 4). A free ADP-ribose terminus can be further cleaved by PARG or re-

extended by PARP1 (2). The most proximal ADP-ribose unit is suggested to be released from the acceptor protein by either PARG (91) or a ADP-ribosyl protein lyase (92).

1.3.5 Acceptor sites of poly(ADP-ribose)

Ogata et al. reported in 1980 that glutamic acid residues of histone H1 and histone H2B function as ADP-ribose acceptor sites. Additionally glutamic acid residues present in the AD of PARP1 were consequently proposed to be acceptor sites for PARP1-mediated auto(ADP-ribosyl)ation (50, 60). Despite intensive research, the acceptor amino acids in PARP1 have not been confirmed by mutational studies, until 2009. Amino acid substitutions established that not glutamic acid residues within the AD of PARP1 are required for PAR formation but rather lysine residues within this domain are acceptor sites for (ADP-ribosyl)ation (60).

1.3.6 (ADP-ribosyl)ation of histones

Histones have long been known as substrates for (ADP-ribosyl)ation in vivo (93). Histones isolated from rat liver nuclei and HeLa cells incubated with radioactive NAD^+ revealed that the linker histone H1 and all core histones H2A, H2B, H3 and H4, are (ADP-ribosyl)ated, although to a variable extent (94-99). However, an unresolved issue regarding the mechanism of (ADP-ribosyl)ation of histones is, whether this modification primarily occurs at the globular histone domains or at their unstructured amino-terminal tails and which PARP family member is responsible for histone (ADP-ribosyl)ation. Unconfirmed ADP-ribose acceptor amino acids have previously only been proposed for H1 and H2B, but not for H2A, H3 and H4 (97, 99-102). (ADP-ribosyl)ation of histones has been detected during the cell cycle, replication, transcription and DNA repair (88, 103-114).

1.3.7 Cellular functions of PARP1

PARP1 was reported to play a crucial role in many physiological and pathophysiological processes including inter- and intracellular signalling, cell cycle regulation, chromatin remodelling, DNA replication, transcription, DNA repair, V(D)J

recombination, regulation of telomere length, inflammation and cell death through apoptosis or necrosis (49, 54).

PARP1 knockout mice are viable but hypersensitive to ionizing radiation and cells therefore are more sensitive to alkylating agents, strengthening that PARP1 plays an important role in the maintenance of genomic integrity (48, 52, 53, 115, 116).

1.3.7.1 Role of PARP1 in transcription

PARP1 can interact with the transcription machinery by two different ways. The first way is the direct binding of PARP1 to transcription factors to regulate or co-regulate the transcription machinery without its enzymatic activity. PARP1 is not only a component of the transcription initiation complex (117) but also probably involved in regulating the elongation phase of transcription (118). The second way requires the enzymatic activity of PARP1 and poly(ADP-ribosyl)ation of histone proteins. The modification of histones allows chromatin remodelling and increasing accessibility of enzymes to the chromatin for replication, transcription or recombination (61, 119, 120). While decondensation of chromatin was reported in vitro, in vivo condensation of chromatin was observed (114, 121, 122). Through its co-activator-function PARP1 plays also an important role in inflammatory processes, which are regulated by nuclear factor kappa B (NF-κB). Since NF-κB plays an important role in the transcriptional regulation of genes involved in inflammation and cell survival (123). In response to extracellular stimuli, such as LPS or TNFα, PARP1, the acetyltransferase p300, the arginine methyltransferase 1 (CARM1) and the protein arginine methyltransferase 1 (PRMT1) synergistically co-activate NF-κB-dependent gene expression leading to inflammation (123, 124). In contrast PARP1 knockout mice are protected against LPS-induced septic shock or myocardial infarction, reaffirming the vital role of PARP1 in inflammatory disorders through its transcriptional co-activator function (124-126).

1.3.7.2 Role of PARP1 in DNA repair

PARP1 can be directly activated by SSB and DSB or indirectly by the enzymatic excision of damaged bases during DNA repair processes (54, 61). The activation of PARP1 induced by DSB is significantly, but less important than the activation by SSB (61, 127-129). SSB dominate the stimulation of PARP1 due to their larger number (127). Through the attachment of negative charged PAR on histones and other chromatin proteins, the modified

proteins lost in vitro their affinity to DNA and might therefore increase the DNA accessibility for the base excision repair (BER) complex (2).

1.3.7.3 Role of PARP1 in cell death

There are two models how PARP1 regulates cell death. The first model proposed by N. Berger in 1983, suggested that extensive oxidative stress induces overactivation of PARP1 and moreover leads to depletion of the cellular NAD^+ concentrations and subsequently of the ATP levels (48, 130, 131). The physiological consequence of NAD^+ and ATP depletion causes a switch from apoptosis to necrosis (132, 133). This cellular suicide mechanism has been implicated in the pathomechanisms of neurodegenerative disorders, cardiovascular dysfunction and various other forms of inflammation (48, 134). Interestingly, the contribution of poly(ADP-ribosyl)ation reactions to necrotic cell death seems to be dependent on the cell type and cellular metabolic status (48). According to genetic studies with PARP1 knockout mice, there is evidence that energy depletion alone, as suggested in the first model, might not be sufficient to mediate poly(ADP-ribosyl)ation-dependent cell death (135).

The second model suggests that overactivation of PARP1 through genotoxic stress, induces the translocation of apoptosis-inducing factor (AIF) from the mitochondria to the nucleus. This causes DNA condensation, fragmentation and subsequently cell death (48). It has been reported that AIF participates in both caspase-dependent and -independent cell death (136-139).

1.4 Aim of the thesis

The aim of this thesis was to investigate whether histone tails are (ADP-ribosyl)ated by PARP1, PARP2 and PARP10 and furthermore to identify potential ADP-ribose acceptor sites of the core histone tails. Recent findings reported by Altmeyer et al. provided evidence that lysine residues within the AD of PARP1 function as ADP-ribose acceptor sites (60). This led to the question whether lysines in histone tails would function as acceptors for PAR as well, although glutamates were previously suggested as acceptor sites for core histone H2B and linker histone H1 (97, 100).

2 Results

2.1 Core histone tails are (ADP-ribosyl)ated by PARP1 and PARP10, but not by PARP2

Although it was earlier reported that histones can be (ADP-ribosyl)ated, the ADP-ribose acceptor sites were not identified so far. To investigate whether histone tails can be (ADP-ribosyl)ated by PARP1, PARP2 and GST-PARP10(818-1025), histone tails were cloned into pGEX-2T vectors and expressed as GST-fusion proteins in bacteria. The GST-tagged histone tails comprised following amino acid sequences:

A

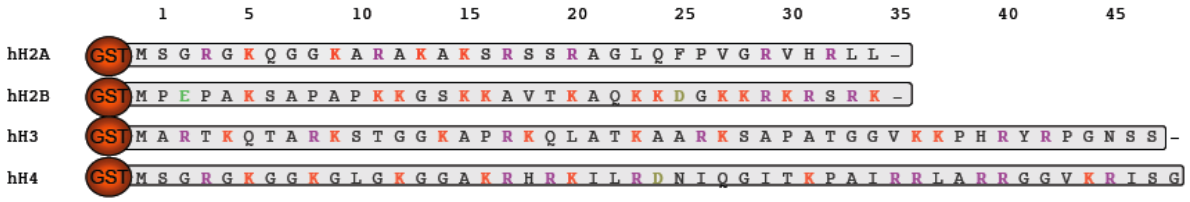

B

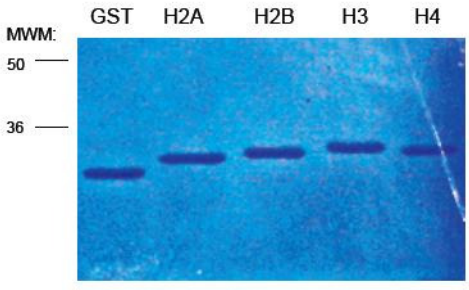

Figure 5: **A:** Amino acid sequences of human core histone tails, tagged with GST. The most important amino acids are colored: K=Lysine, R=Arginine, E=Glutamate.
B: Coomassie stained gel of purified GST-tagged core histone tails. GST was loaded as control. MWM= Molecular Weight Marker

Purified GST-tagged histone tails were incubated in presence of 100nM ^{32}P-NAD^{+}, either with purified PARP1 and PARP2 both expressed and purified from baculo virus or with GST-PARP10(aa:818-1025 = CAT domain) expressed and purified from bacteria. The reaction was stopped and proteins separated by 12% SDS-PAGE. After Coomassie staining, the gels were vacuum dried and exposed to a Phosphor screen to quantify the incorporated

radioactivity, which would correlate with (ADP-ribosyl)ation of the GST-tagged histone tails (Fig. 6).

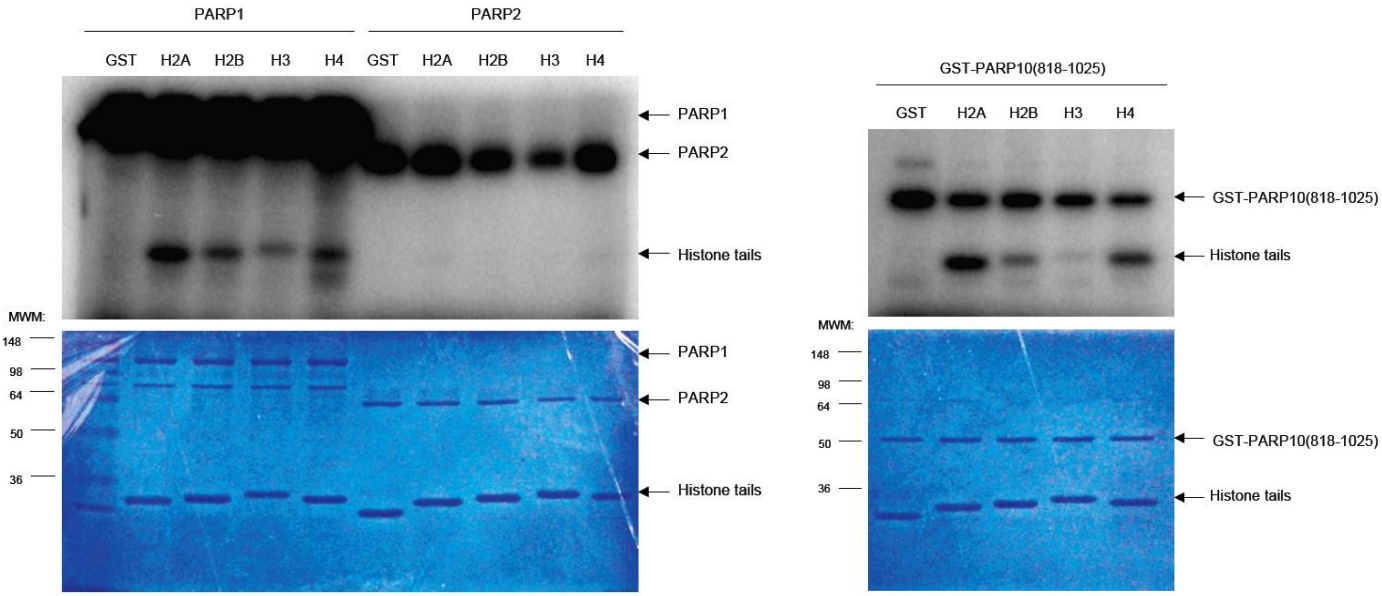

Figure 6: The upper panels show the Phosphor Image of the gels for quantification of radioactivity and the lower panels show Coomassie stained gels for quantification of the protein levels. MWM = Molecular Weight Marker

PARP1 was able to (ADP-ribosyl)ate itself and trans(ADP-ribosyl)ate all cloned core histone tails, although H2A was stronger modified than H2B, H3 and H4 under the tested conditions. PARP2 was also able to efficiently (ADP-ribosyl)ate itself, but in contrast to PARP1, it was not able to trans(ADP-ribosyl)ate the tested histone tails. In contrast to PARP2, GST-PARP10(818-1025) was able to (ADP-ribosyl)ate itself as well as trans(ADP-ribosyl)ate the analyzed histone tails, with the same preference as observed for PARP1. Surprisingly, GST-PARP10(818-1025) also weakly (ADP-ribosyl)ated GST alone (negative control), suggesting that the observed trans(ADP-ribosyl)ation of the GST-tagged H3 tail might just be background labelling. This experiment strongly indicates that all tested core histone tails are trans(ADP-ribosyl)ated by PARP1 and the CAT domain of GST-PARP10 (with the exception of H3), but not by PARP2. Glutamic acid residues were earlier suggested to be ADP-ribose acceptor residues (97, 100). Interestingly, none of the tested GST-tagged histone tails contained a glutamic acid residue except for H2B (E2), indicating that other amino acid residues could function as ADP-ribose acceptor sites.

2.2 Optimization of histone tail trans(ADP-ribosyl)ation

The (ADP-ribosyl)ation reactions were performed so far without NaCl, since the added PARPs contained already NaCl (usually 14-20mM of NaCl). To determine the optimal NaCl concentration, (ADP-ribosyl)ation of GST-tagged H4 tails by PARP1 in presence of 100nM ^{32}P-NAD^{+} and increasing salt concentrations was performed. Six different NaCl concentrations from 0 to 150mM NaCl were tested. The reaction was stopped and the proteins separated by 12% SDS-PAGE. After gel electrophoresis, the gel was stained with Coomassie, vacuum dried and the incorporated radioactivity again quantified by Phosphor screen (Fig. 7).

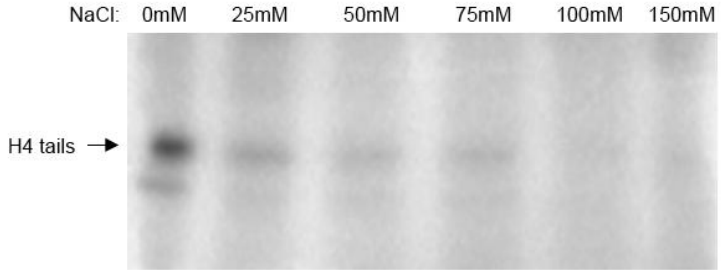

Figure 7: Phosphor Image of the gel to quantify (ADP-ribosyl)ation of GST-tagged H4 tail with different NaCl concentrations.

Complete loss of H4 tail trans(ADP-ribosyl)ation was observed at 100mM NaCl, although a clear reduction of (ADP-ribosyl)ation was already observed at 25mM NaCl. These results indicate that the NaCl concentration either inhibits directly the enzymatic activity of PARP1 or reduces the interaction of PARP1 with the histone tails (see also 2.5). Further assays were subsequently performed without additional NaCl, only containing the NaCl added with PARP1 (approx. 20mM).

To determine the optimal incubation time for PARP1-mediated trans(ADP-ribosyl)ation, an (ADP-ribosyl)ation assay (described in Materials and Methods, 4.2.4) with GST-tagged H3 tail at 30°C and different incubation times was performed. The reaction was stopped at the different indicated time points (see Fig. 8, A) and proteins separated by 12% SDS-PAGE. After gel electrophoresis, the gel was stained with Coomassie, vacuum dried and radioactivity quantified by Phosphor screen (Fig. 8).

A **B**

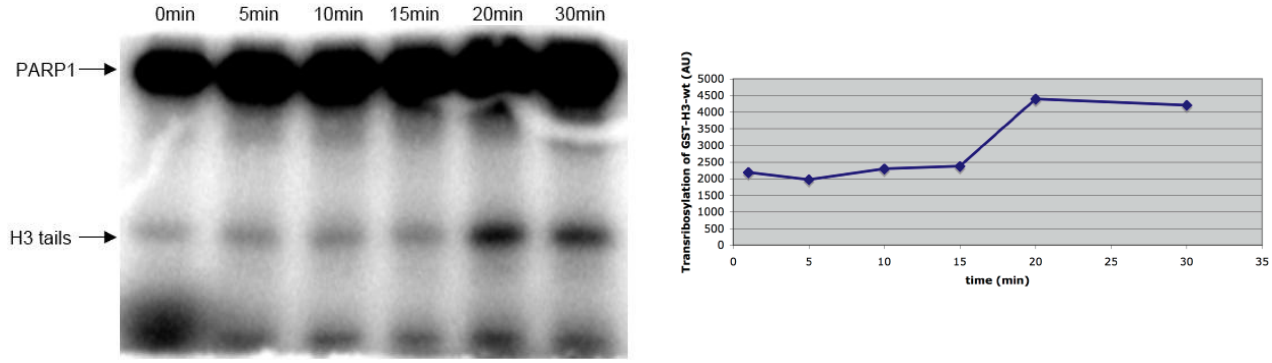

Figure 8: **A:** Phosphor Image of the gel to quantify (ADP-ribosyl)ation with different incubation times of PARP1.
B: Time course representing the intensity of (ADP-ribosyl)ation from Phosphor Image in A.

This experiment revealed that (ADP-ribosyl)ation of GST-tagged H3 tail was increasing over a time period reaching a maximum after 20 minutes. Longer incubation did not further increase the incorporated radioactivity, suggesting that the optimal incubation time under the tested conditions was less than 20 minutes. Earlier publications reported that (ADP-ribosyl)ation can also take place in a non-enzymatic manner through Schiffbase formation. To reduce the possibility of non-enzymatic (ADP-ribosyl)ation of the histone tails, and to measure (ADP-ribosyl)ation in a linear range, subsequent (ADP-ribosyl)ation assays with PARP1 were performed as before with an incubation time of 5 minutes.

2.3 Identification of the minimal histone tail deletion mutant required for PARP1 interaction

To localize the PARP1 interaction and possible ADP-ribose acceptor sites on the histone tails, deletion mutants of the GST-tagged core histone tails were generated. Since Altmeyer et al. recently reported that specific lysine residues in the automodification domain of PARP1 are acceptor amino acids of ADP-ribose (60), different deletions of the core histone tails were constructed always ending two amino acids after a certain lysine (Fig. 9).

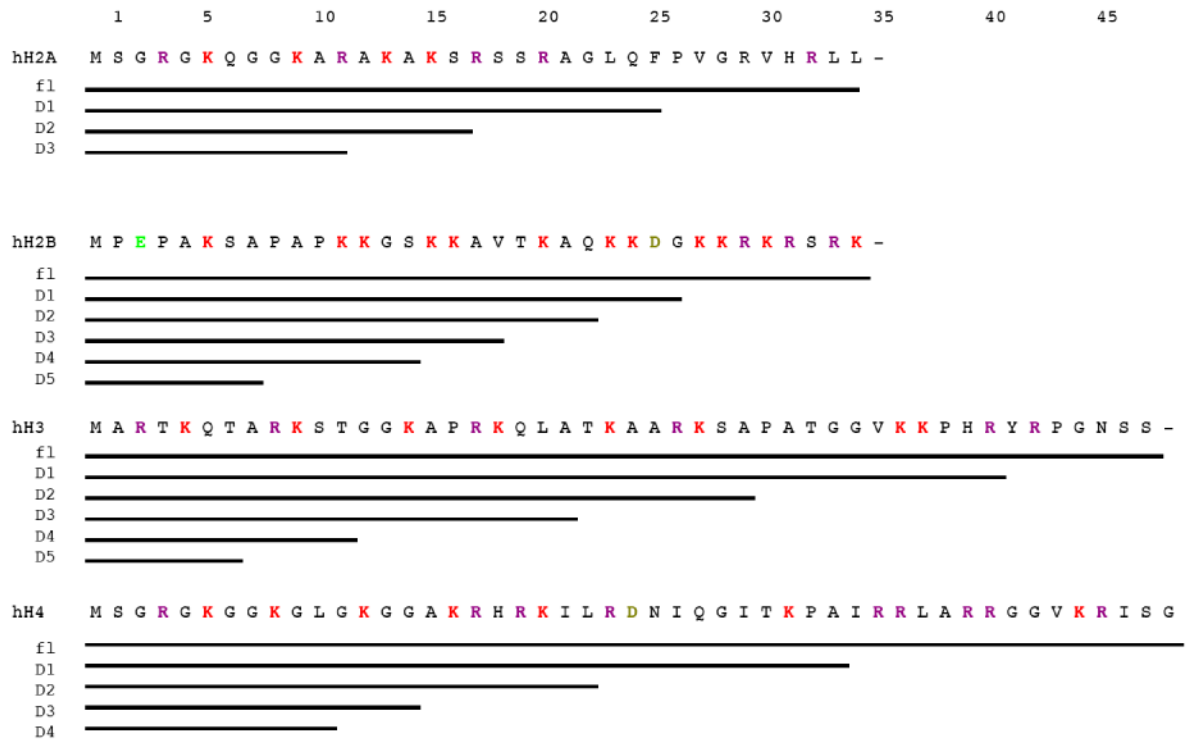

Figure 9: Different deletions of each GST-tagged core histone tail, abbreviated by a D and a number. The important amino acids are coloured: K=Lysine, R=Arginine, E=Glutamate.

To identify the minimal deletion mutant required for PARP1 interaction, interaction analyses with PARP1 and the different GST-tagged histone tail deletion mutants were performed. GST-tagged histone tails or GST alone (as control) were bound from bacterial crude extracts to glutathione-beads and the beads washed five times with two different buffers (as described in Materials and Methods, 4.2.5). 10pmol of PARP1 was incubated to approximately 1-2µg of GST-tagged histone tails bound to beads. After 2 hours incubation, beads were washed 3 times to remove unbound PARP1. The beads were boiled at 95°C to denature the proteins, which were then separated by 12% SDS-PAGE. After gel electrophoresis, proteins were blotted from the gel onto a PVDF membrane and transferred proteins analyzed by western blot using an anti-PARP1 antibody to detect to which deletion mutant PARP1 was still binding. To visualize PARP1, enhanced chemiluminescence was used and the PVDF membranes exposed to an X-ray film (Fig. 10). Purified PARP1 was loaded as positive control in the first lane. Beads loaded with GST and incubated with PARP1 were used as negative control to visualize possible unspecific interaction of PARP1 with GST (loaded in the second lane).

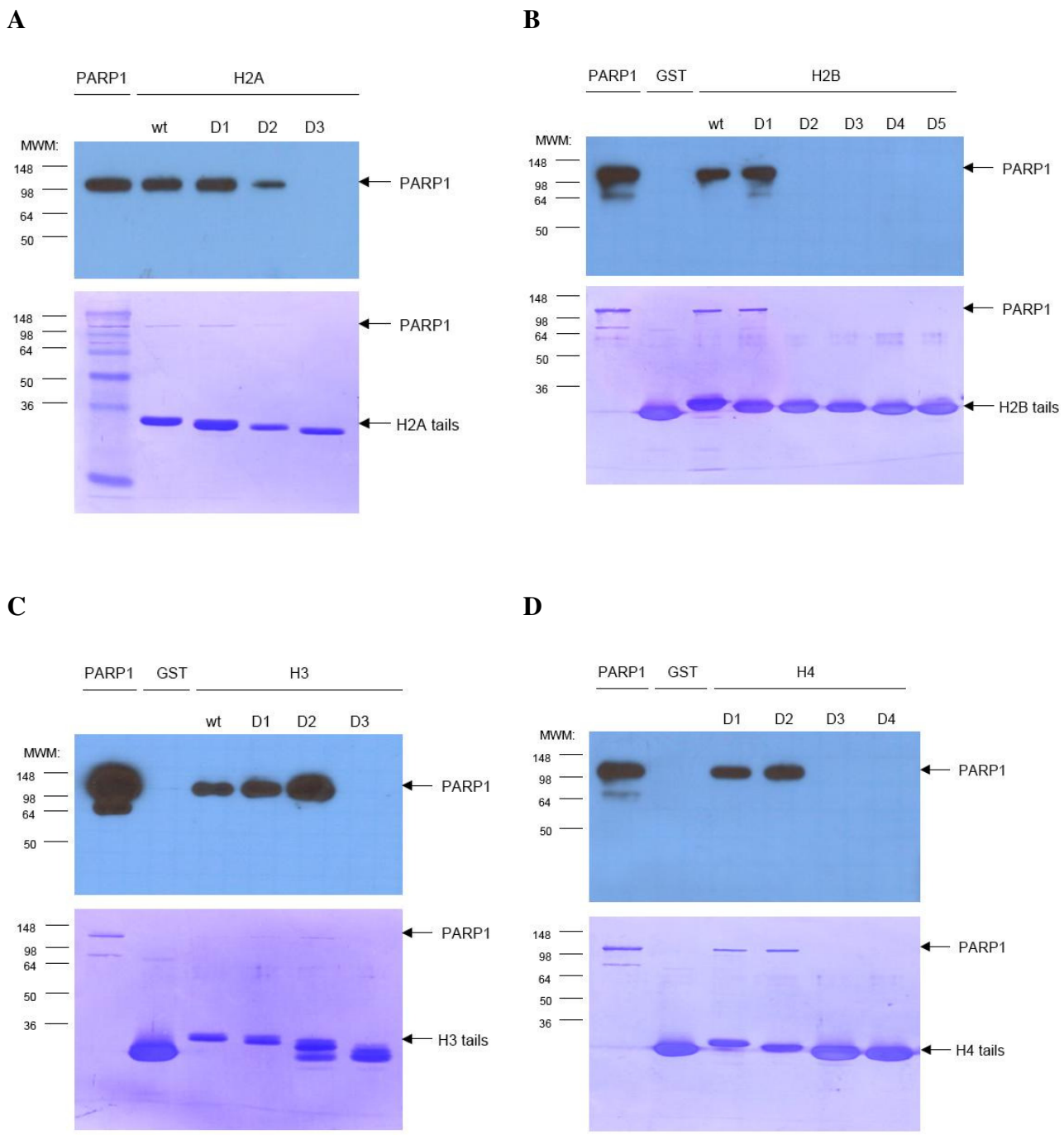

Figure 10: Interaction analyses to identify minimal deletion mutants required for PARP1 interaction. **A:** H2A, **B:** H2B**, C:** H3**, D:** H4. The upper panels are western blot analyses using an anti-PARP1 antibody. PARP1 was used as positive control (lane 1) and GST as negative control (lane 2). The lower panels show Coomassie stained PVDF membranes to quantify the GST-tagged protein levels. MWM = Molecular Weight Marker

PARP1 bound to all tested full-length GST-tagged histone tails (Fig. 10, A-C). Interestingly, interaction with PARP1 was lost for each GST-tagged histone tail with a distinct deletion mutant. The minimal deletion mutants required for interaction with PARP1 are D2 for H2A, D1 for H2B, D2 for H3 and D2 for H4. This experiment indicates that the interaction sites are located at the end of each deletion mutant. The reduced level of PARP1

bound to H2A-D2 is probably due to lower loaded histone tail input as judged by the Coomassie stained PVDF membrane (Fig. 10, A).

2.4 PARP1/Histone tail interaction regulates (ADP-ribosyl)ation of histone tails

To investigate whether the minimal deletion mutants of the GST-tagged histone tails required for the interaction with PARP1 would correlate with the ability to be (ADP-ribosyl)ated, the different mutants were modified by PARP1 in presence of 100nM ^{32}P-NAD^{+}. The reaction was stopped and the histone tail deletion mutants subsequently separated by 12% SDS-PAGE. The gels were stained with Coomassie to visualize the proteins and then exposed to X-ray films or to a Phosphor screen to detect and quantify the incorporated radioactivity. Loss of (ADP-ribosyl)ation was observed for the same deletion mutants, which would not anymore interact with PARP1, indicating that the loss of (ADP-ribosyl)ation is due to lack of interaction (Fig. 11). Only the H2B tail deletions reacted differently. The minimal deletion mutant required for the interaction, was not longer (ADP-ribosyl)ated. Only the full-length H2B tail was (ADP-ribosyl)ated by PARP1, although D1 was still interacting, indicating that the interaction and modification site is not correlating for the H2B tail. Interestingly, H2A-D2 was only modified to 40%, despite the fact that this deletion was still interacting, suggesting that additional modification sites would be located in the sequence covered by D1.

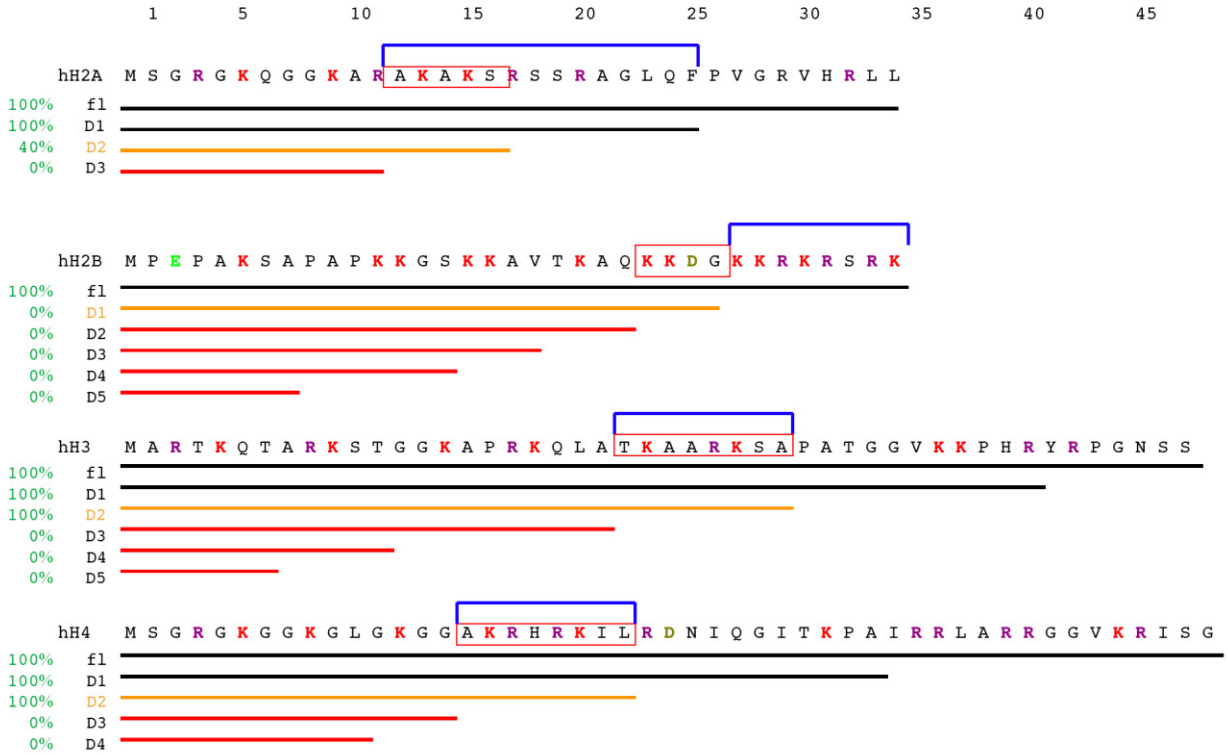

Figure 11: Result of the interaction assay in comparison to the result of (ADP-ribosyl)ation (%) of the histone tail deletions.
Minimal deletion mutants required for the interaction, **full interaction**, no interaction
= indicates location of possible ADP-ribose acceptor sites
= indicates location of possible PARP1 interaction sites

2.5 PARP1/Histone tail interaction is of an electrostatic nature

To strengthen the interaction assay and to analyze if the observed inhibitory effect of NaCl on the enzymatic activity of PARP1 (see chapter 2.2), could be due to an abolished interaction of PARP1 with the GST-tagged histone tails, PARP1 interaction assays with H4 deletions and increasing NaCl concentrations were repeated. GST-tagged histone tail deletions of H4 were bound from bacterial crude extracts to glutathione-beads, washed three times with EBC-buffer and subsequently two times with (ADP-ribosyl)ation-buffer containing three different NaCl concentrations (as indicated in Fig. 12). The different NaCl concentrations were not only used to wash the beads, but were also included for the interaction reaction together with 10pmol of PARP1. After 2 hours incubation, beads were washed again with (ADP-ribosyl)ation-buffer and the indicated NaCl concentration. Bound proteins were eluted from the beads with 10mM glutathione and 200mM NaCl. The eluted samples were boiled at 95°C and separated by 12% SDS-PAGE. After gel electrophoresis the proteins were blotted onto a PVDF membrane and analyzed by western blot using an anti-

PARP1 antibody to detect the interaction of PARP1 with H4 deletions. PARP1 was visualized using enhanced chemiluminescence (Fig. 12). Purified PARP1 was loaded as positive control in the first lane.

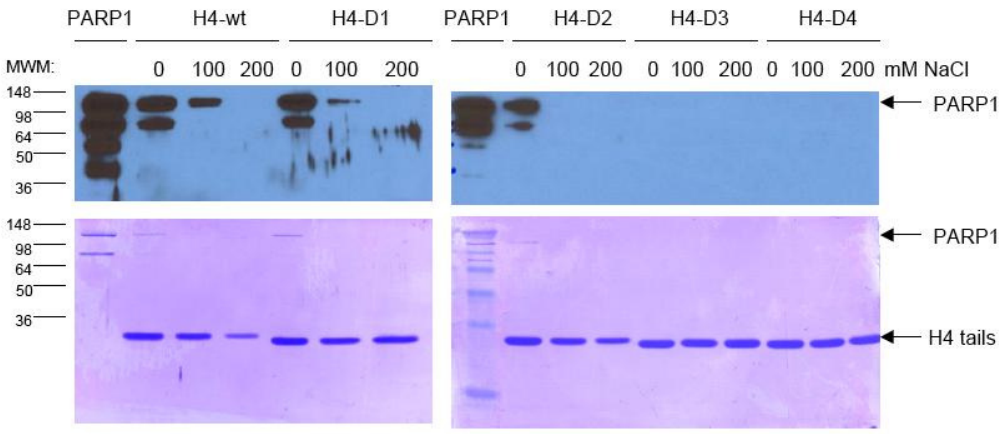

Figure 12: The upper panels are western blot analyses using an anti-PARP1 antibody. PARP1 was used as positive control (lane 1). The lower panels show Coomassie stained PVDF membranes to quantify the protein levels. MWM = Molecular Weight Marker

PARP1 interacted with the tested GST-tagged histone tails in absence of exogenous salt as observed before. As soon as the salt concentration was increased to 100mM NaCl the interaction of PARP1 with H4-D1 was reduced, in comparison to H4-wt. No interaction could be detected at the same NaCl concentration with H4-D2 or a shorter deletion as observed before (Fig. 10, D). Overall, these assays provide evidence that NaCl is indeed affecting the interaction of PARP1 with the GST-tagged histone tails, suggesting that the PARP1/histone tail interaction is of an electrostatic nature. The remaining binding of PARP1 to H4-wt at 100mM NaCl furthermore indicated, that amino acid residues at the very C-terminus of the tail might additionally stabilize the interaction with PARP1. High NaCl concentrations consequently inhibited (ADP-ribosyl)ation. Based on this result, subsequent interaction assays were performed in presence of 50mM NaCl to increase the stringency.

2.6 Lysine replacement in the H3 tail results in a loss of trans(ADP-ribosyl)ation by PARP1

To precisely locate the ADP-ribose acceptor sites within the histone tails, several lysine residues were mutated in the full-length context of GST-tagged H3 tail. Since lysines were recently suggested to be the ADP-ribose acceptor sites by our laboratory, we assumed that a

mutation of lysine residues would cause a loss of (ADP-ribosyl)ation. Five lysine residues (K9, K14, K18, K23 and K27) of the GST-tagged H3 tail were mutated into alanine residues by overlapping PCR (as indicated in Materials and Methods, 4.1.1). The H3 KA mutant contained all five lysine to alanine substitutions. To analyze whether the H3 tail mutants would still be trans(ADP-ribosyl)ated, a PARP1-mediated (ADP-ribosyl)ation assay in presence of 100nM ^{32}P-NAD^{+} was performed. The reaction was stopped after 5min and proteins were separated by 12% SDS-PAGE. After Coomassie staining, the gel was vacuum dried and exposed to a Phosphor screen to quantify the incorporated radioactivity (Fig. 13).

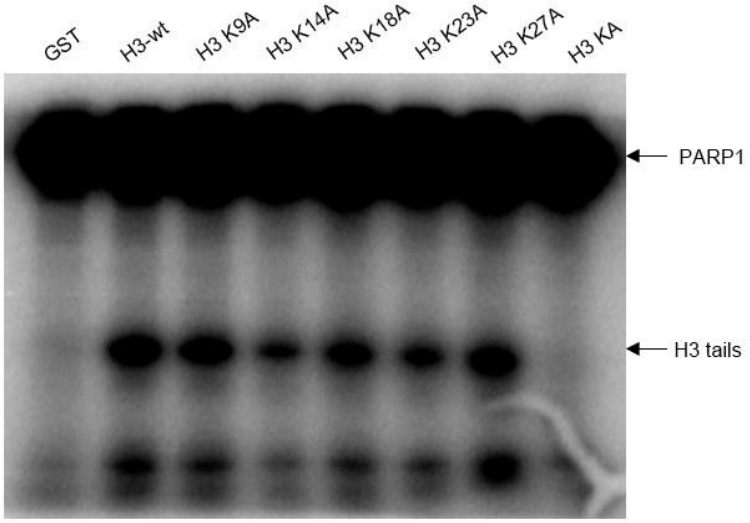

Figure 13: Phosphor Image of the gel to quantify (ADP-ribosyl)ation of different H3 mutations.

None of the single tested mutants showed a loss of (ADP-ribosyl)ation, although some mutations like K14A and K23A showed a slight reduction of (ADP-ribosyl)ation. However, this reduction of (ADP-ribosyl)ation of single or double substitutions could not further be confirmed. Only the H3 KA mutant of the GST-tagged H3 tail was not longer (ADP-ribosyl)ated by PARP1, assuming that lysines are indeed ADP-ribose acceptor sites.

2.7 Addition of DNA does not influence the interaction of PARP1 with GST-tagged histone tails

To analyze whether addition of DNA would affect the interaction of PARP1 with the GST-tagged histone tails, a PARP1 interaction assay in presence or absence of DNA was performed. For this purpose 10pmol of DNA-free PARP1 (purified with Ethidiumbromide to remove co-purified DNA) with or without 5pmol DNA was added to the minimal deletion

mutant of each histone tail bound on beads and incubated for 2 hours. After removing unbound PARP1, beads were boiled and proteins separated by 12% SDS-PAGE. After gel electrophoresis, proteins were blotted from the gel onto a PVDF membrane and analyzed by western blot using an anti-PARP1 antibody to detect interacting PARP1. The presence of PARP1 was visualized using enhanced chemiluminescence (Fig. 14).

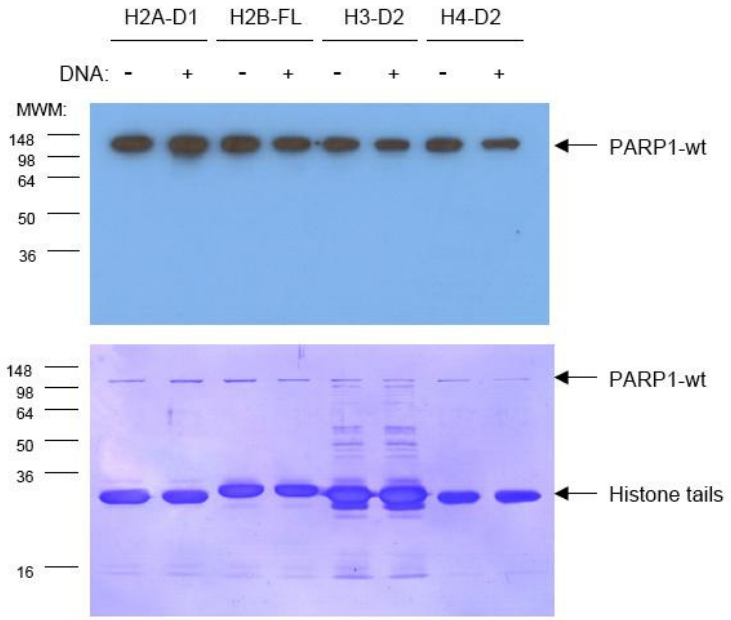

Figure 14: The upper panel shows the western blot analysis using an anti-PARP1 antibody. The lower panel shows a Coomassie stained PVDF membrane to quantify protein levels of PARP and histone tails. MWM = Molecular Weight Marker

PARP1 was interacting with all four tested histone tails independent whether DNA was present or not, indicating that DNA has no impact on the interaction of PARP1 with GST-tagged histone tails. Thus the DNA was omitted for all further interaction experiments.

2.8 Identification of ADP-ribose acceptor sites in histone tails modified by PARP1

To extend the analyses also including the other histone tails, different K to A substitutions were generated by overlapping PCR (as described in Materials and Methods, 4.1.1) in the full-length context or in the minimal interaction mutants of the histone tails and subsequently tested for (ADP-ribosyl)ation and interaction with PARP1. Since arginine residues could potentially also be important for (ADP-ribosyl)ation or interaction, also arginine to alanine substitutions were generated for the different constructs. All generated

mutations were expressed in bacteria, purified and then first tested in PARP1-mediated (ADP-ribosyl)ation assays, to identify substitutions, which are not longer (ADP-ribosyl)ated and would therefore point at possible ADP-ribose acceptor sites. The histone tail mutations were incubated with PARP1 in presence of 100nM ^{32}P-NAD$^+$ for 5min at 30°C. The reaction was stopped and the histone tail mutations subsequently separated by 12% SDS-PAGE. The gels were stained with Coomassie to visualize proteins and then exposed to X-ray films or to a Phosphor screen to detect and quantify the incorporated radioactivity. The (ADP-ribosyl)ation results are summarized in 2.8.1-2.8.4 (Tables 1-4). While several mutants of H2A and H4 were not any longer (ADP-ribosyl)ated by PARP1 (Table 1,4), only one distinct mutant of H2B or H3 was not longer modified (Table 2,3). To elucidate whether the reduced or missing histone (ADP-ribosyl)ation was due to an inhibited interaction with PARP1, interaction assays with the GST-tagged histone tail deletions and mutations were performed. Histone tail deletions and the available mutations or GST alone (negative control) were bound from bacterial crude extracts to glutathione-beads. The beads were washed five times with two buffers and subsequently incubated with 10pmol of PARP1 without addition of DNA or NAD$^+$. After 2 hours incubation time, beads were washed three times to remove unbound PARP1. The beads were boiled and loaded on a 12% SDS-PAGE to separate proteins. After gel electrophoresis, proteins were blotted onto a PVDF membrane and analyzed by western blot using an anti-PARP1 antibody to detect a possible interaction with PARP1. Purified PARP1 was loaded as positive control in the first lane. Beads loaded with GST and incubated with PARP1 were used as negative control and loaded in the second lane. The presence of PARP1 was visualized using enhanced chemiluminescence (see following figures).

2.8.1 K13/R20 of H2A are possible acceptor sites and K15/R20 are important for the interaction with PARP1

Interaction assays with H2A tail deletions and mutations confirmed earlier results, that the interaction of H2A with PARP1 is abolished when using D3 (Fig. 10A and 15).

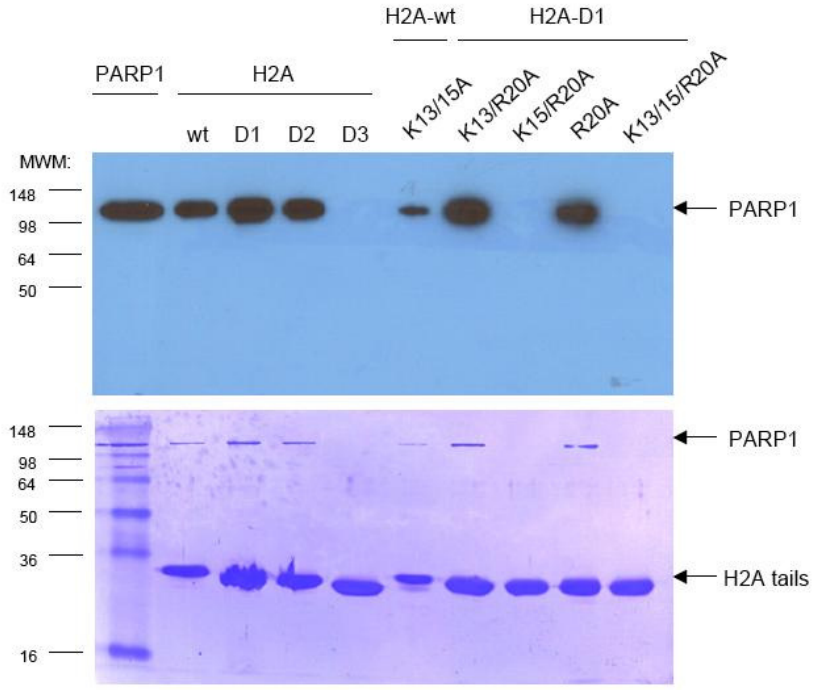

Figure 15: The upper panel is a western blot analysis using an anti-PARP1 antibody. PARP1 was used as positive control (lane 1). The lower panel shows a Coomassie stained PVDF membrane to quantify the protein levels of the H2A tails. MWM = Molecular Weight Marker

In the H2A-D1 context a loss of interaction was observed when K15 and R20 were substituted to alanines and also when K13 and K15 together with R20 were substituted to alanines. Since substitution of R20 alone was not sufficient to abrogate the interaction, either the combination of K15 with R20 or K15 alone would be responsible for the interaction of the H2A tail with PARP1. The level of bound PARP1 was reduced when K13 and K15 were both substituted to alanines, which was, however, probably due to the lower loaded protein input as judged by the Coomassie stained PVDF membrane. This experiment revealed that the H2A tail interacts with PARP1 through K15 and R20.

By comparing these interaction results with the (ADP-ribosyl)ation results, possible acceptor sites were identified for H2A (Table 1).

In the full-length context of H2A a 50% reduction of (ADP-ribosyl)ation was observed when both, K13 and K15, were substituted to alanines. Since this mutant was still interacting with PARP1, these two lysines are indeed possible ADP-ribose acceptor sites. Substitution of R20 alone even showed a higher reduction (80%) of (ADP-ribosyl)ation, although full interaction was observed, suggesting that R20 as well is a possible acceptor site. The combination of K13/R20 reduced (ADP-ribosyl)ation completely, confirming that these two residues are the most important residues for modification in the H2A-D1 context, and that

K15 is most probably not modified but important together with R20 for the interaction of the H2A tail with PARP1.

H2A:

	ADP-ribosylation	Interaction
Full-length	100%	yes
FL: K13/15A (K2A)	50%	yes
D1: R20A	20%	yes
D1: K13 R20A	0%	yes
D1: K15 R20A	0%	no
D1: K13/15 R20A	0%	no

Table 1: Percentage of (ADP-ribosyl)ation and result of the interaction assay for H2A tail. Red labelled are the possible ADP-ribose acceptor sites.

2.8.2 R29/31/33 are important for the interaction of H2B with PARP1

Interaction assays with H2B tail deletions and mutations confirmed earlier results, that the interaction of H2B with PARP1 is abolished when using D2 but not when using D1 as observed for trans(ADP-ribosyl)ation (Fig.10B and 16).

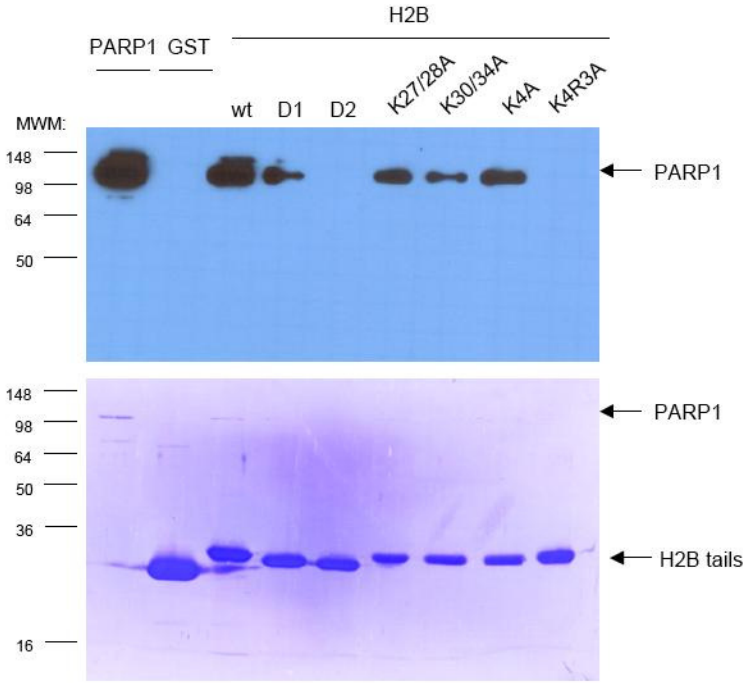

Figure 16: The upper panel is a western blot analysis using an anti-PARP1 antibody. PARP1 was used as positive control (lane 1) and GST as negative control (lane 2). The lower panel shows a Coomassie stained PVDF membrane to quantify the protein levels of the H2B tails. MWM = Molecular Weight Marker

In the full-length context of the H2B tail, substitutions of K27/28 and K30/34 to alanines had no impact on the PARP1 interaction. A loss of interaction was only observed when K27/28/30/34 as well as R29/31/33 were all substituted to alanines (K4R3A). Since substitutions of the four lysines alone (K4A) were not sufficient to abrogate the interaction, either the combination of the four lysines with the three arginines or the three arginines alone are responsible for the interaction of the H2B tail with PARP1. Surprisingly, these seven amino acids are not present in D1, although D1 was still interacting with PARP1. Since the observed interaction site with H2B-D1 is not observed with the mutated H2B-wt (K4R3A), the interaction with D1 might not be physiologically relevant.

For the H2B tail, loss of (ADP-ribosyl)ation was only observed when K27/28/30/34 as well as R29/31/33 were substituted to alanines (K4R3A, Table 2). This mutation was however not interacting any longer with PARP1 (Fig. 16), suggesting that the lack of (ADP-ribosyl)ation was most probably due to a loss of interaction, thus not allowing to determine specific ADP-ribose acceptor sites of H2B with these experiments.

H2B:

	ADP-ribosylation	**Interaction**
Full-length	100%	yes
FL: K27A	100%	not tested
FL: K28A	100%	not tested
FL: K30A	100%	not tested
FL: K34A	100%	not tested
FL: K27/28A	100%	yes
FL: K30/34A	100%	yes
FL: K27/28/30/34A (K4A)	100%	yes
FL: R29/31/33A (R3A)	100%	not tested
FL: K27/28/30/34 R29/31/33A (K4R3A)	0%	no

Table 2: Percentage of (ADP-ribosyl)ation and result of the interaction assay for H2B tail.

2.8.3 R26 is important for the interaction of H3 with PARP1

Interaction assays with H3 tail deletions and mutations confirmed earlier results, that the interaction of H3 with PARP1 is abolished when using D3 (Fig.10C and 17). The slight interaction seen with D3 seemed to be background binding, since this interaction was not observed in other assays (e.g. Fig. 10C).

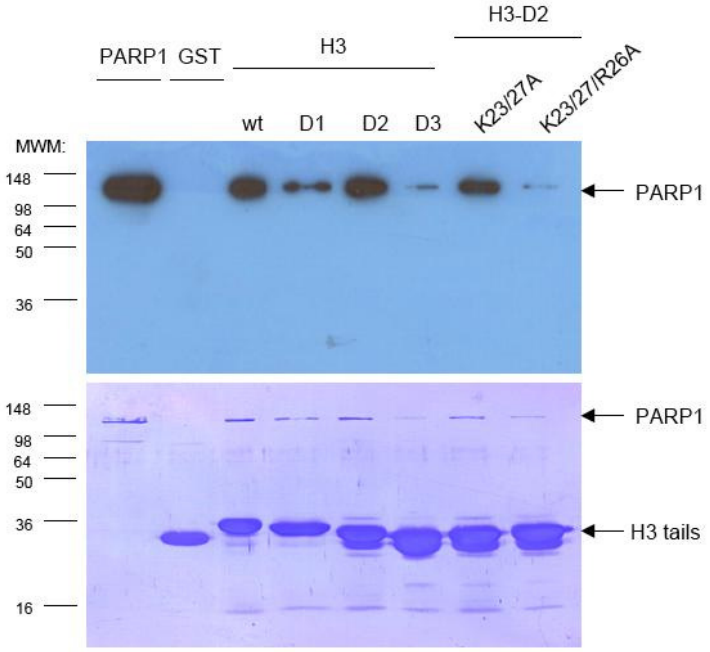

Figure 17: The upper panel is a western blot analysis using an anti-PARP1 antibody. PARP1 was used as positive control (lane 1) and GST as negative control (lane 2). The lower panel shows a Coomassie stained PVDF membrane to quantify the protein levels of the H3 tails. MWM = Molecular Weight Marker

In the H3-D2 context, a loss of interaction was only observed when K23/27 as well as R26 were substituted to alanines (K23/27/R26A). Substitution of only K23/27 to alanines had no impact on the interaction, indicating that R26 is responsible for the interaction of the H3 tail with PARP1.

For the H3 tail, loss of (ADP-ribosyl)ation was only observed when K23/27 as well as R26 were substituted to alanines (K23/27/R26A, Table 3). Since this mutant was also not interacting any longer with PARP1 (Fig. 17), the lack of (ADP-ribosyl)ation was likely due to a loss of interaction, thus not allowing to determine specific ADP-ribose acceptor sites of H3 with these experiments.

H3:

	ADP-ribosylation	**Interaction**
Full-length	100%	yes
D2: K23A	100%	not tested
D2: K27A	100%	not tested
D2: K23/27A	100%	yes
D2: R26A	100%	not tested
D2: K23/27 R26A	0%	no

Table 3: Percentage of (ADP-ribosyl)ation and result of the interaction assay for H3 tail.

2.8.4 K16/20 are possible acceptor sites as well as important for the interaction of H4 with PARP1

Interaction assays with H4 tail deletions and mutations confirmed earlier results, that the interaction of H4 with PARP1 is abolished when using D3 (Fig.10D and 18).

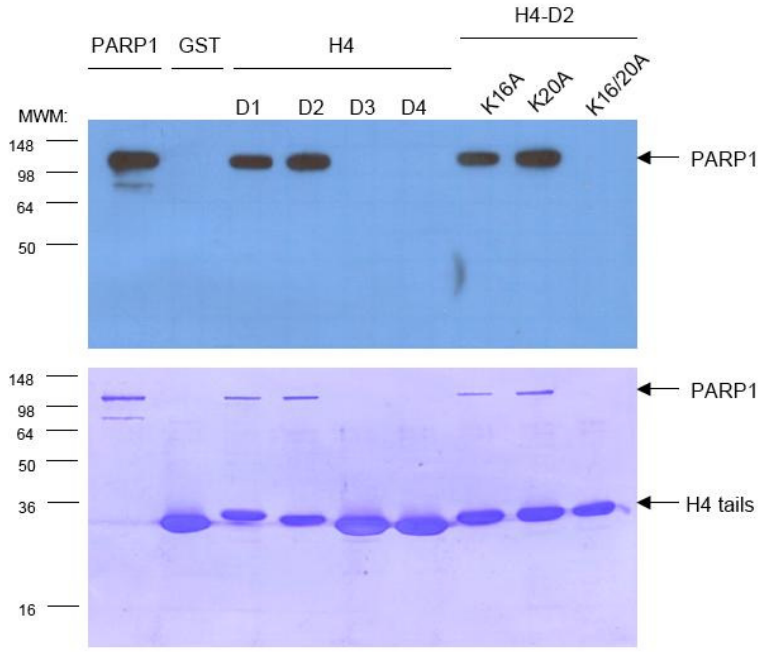

Figure 18: The upper panel is a western blot analysis using an anti-PARP1 antibody. PARP1 was used as positive control (lane 1) and GST as negative control (lane 2). The lower panel shows a Coomassie stained PVDF membrane to quantify the protein levels of the H4 tails. MWM = Molecular Weight Marker

In the H4-D2 context a loss of interaction was observed when K16/20 were substituted to alanines. Single lysine substitutions (K16A and K20A) did not cause a loss of interaction, indicating that both lysines are required for the interaction of the H4 tail with PARP1.

By comparing these interaction results with the (ADP-ribosyl)ation results, possible acceptor sites were identified for H4 (Table 4).

For the H4 tail, single lysine substitutions (K16A, K20A) showed a 50% reduction of (ADP-ribosyl)ation, but were still interacting with PARP1, suggesting that these residues are possible ADP-ribose acceptor sites. Since substitution combination of both lysines K16/20 to alanines revealed that (ADP-ribosyl)ation as well as interaction with PARP1 was not longer possible, these two lysines are possible acceptor sites and also important for the interaction with PARP1 (Fig. 18).

H4:

	ADP-ribosylation	Interaction
Full-length	100%	yes
D2: K16A	50%	yes
D2: K20A	50%	yes
D2: K16/20A	0%	no
D2: R17/19A	0%	no
D2: K16/20 R17/19A (K2R2A)	0%	no

Table 4: Percentage of (ADP-ribosyl)ation and result of the interaction assay for H4 tail. Red labelled are the possible ADP-ribose acceptor sites.

2.9 GST-tagged histone tails mainly interact with the BRCT domain of PARP1

To determine which PARP1 domain is responsible for the interaction with the GST-tagged histone tails, interaction assays with PARP1-fragments and the minimal histone tail deletions required for PARP1 interaction were performed. Five different myc-tagged PARP1-fragments were used, comprising amino acid 1-214 which includes ZFI and II, amino acid 215-371 which includes the ZBDIII, amino acid 372-525 which includes the BRCT domain, amino acid 525-656 which includes the WGR domain and a fragment including amino acid 656-1014, which expresses the CAT domain. A PARP1-fragment interaction assay with 30pmol of PARP1-fragments in absence of DNA was performed with all GST-tagged histone tails bound to glutathione-beads (as described in Materials and Methods, 4.2.5). Since some fragments were small, a 13% SDS-PAGE was used to separate bound PARP1-fragments by gel electrophoresis. After blotting the proteins onto a PVDF membrane, a western blot analysis using an anti-Myc antibody was performed. The presence of PARP1-fragments was visualized using enhanced chemiluminescence (Fig. 20). As input control, 30pmol of all PARP1-fragments were separated by 13% SDS-PAGE, blotted onto a PVDF membrane and analyzed by western blot using an anti-Myc antibody (Fig. 19).

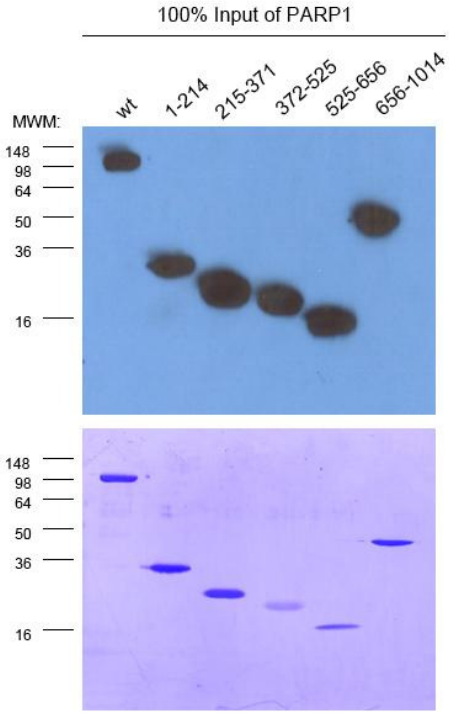

Figure 19: The upper panel shows 100% Input of the PARP1-fragments detected by western blot using an anti-Myc antibody. The lower panel shows a Coomassie stained PVDF membrane with the protein levels of the separated PARP1-fragments. MWM = Molecular Weight Marker

H2A-D1:

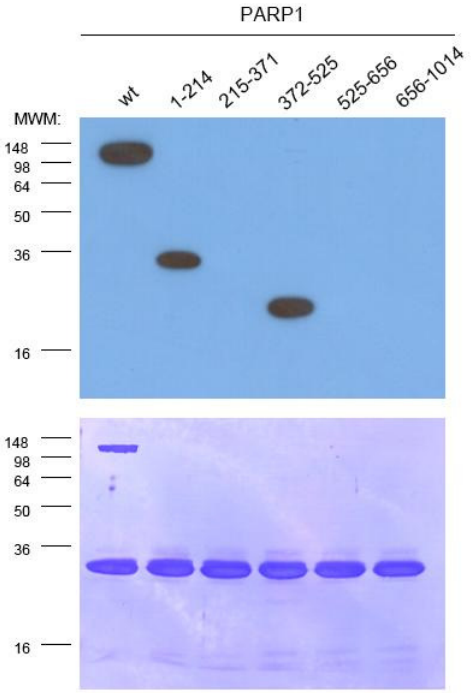

H2B-FL:

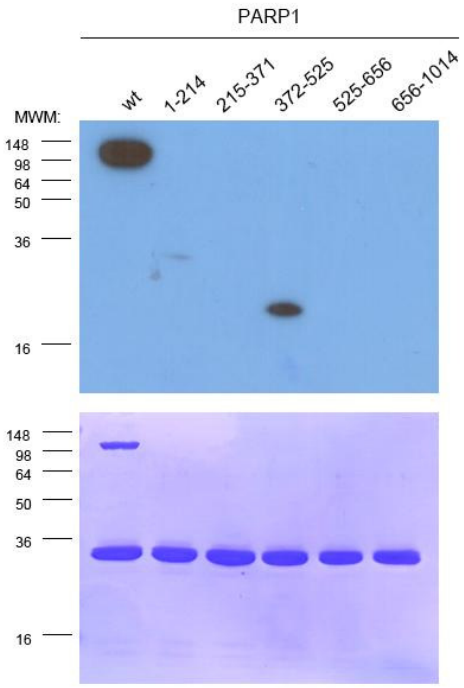

H3-D2: H4-D2:

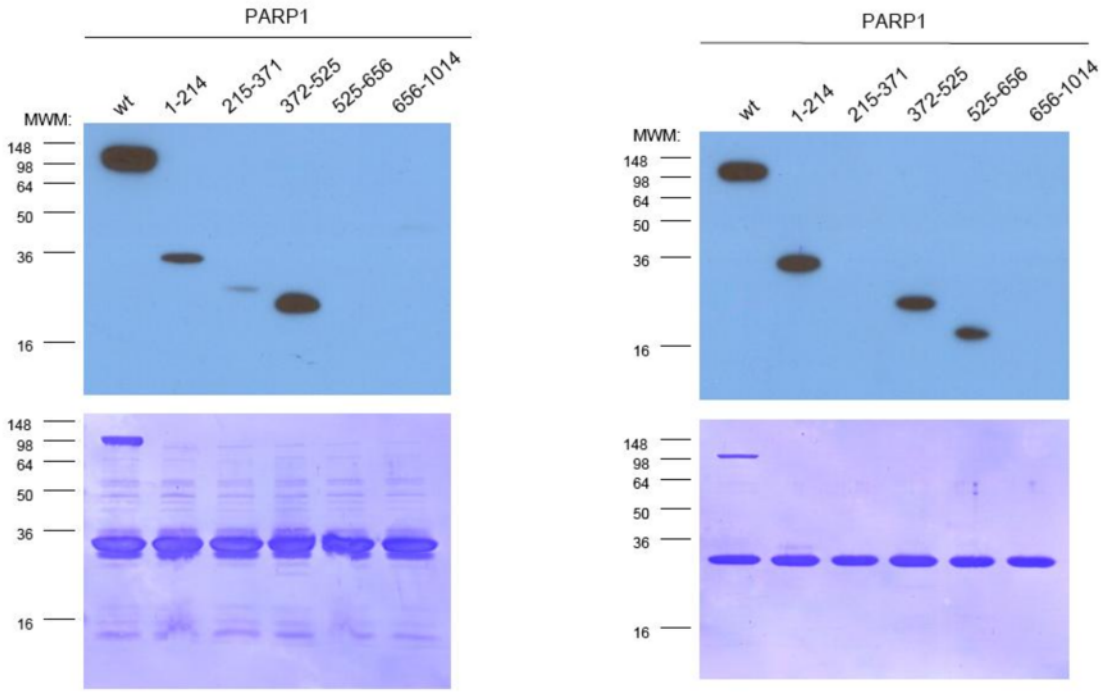

Figure 20: The upper panels are western blot analyses using an anti-Myc antibody against Myc-tagged PARP1-fragments and the lower panels show Coomassie stained PVDF membranes to quantify the protein levels of the histone tails. MWM = Molecular Weight Marker

All four histone tails interacted under the tested conditions with the BRCT domain of PARP1 (aa: 372-525). H2A-D1, H3-D2 and H4-D2 interacted also with the fragment expressing the ZFI and ZFII, H2B-FL showed only a slight interaction with this domain. Since ZFI and ZFII were reported to bind to DNA, the observed interaction with this fragment might be due to DNA from bacterial crude extract, which was co-purified with the histone tails. H4-D2 interacted additionally with the fragment expressing the WGR domain. This interaction could however not be confirmed, since full-length PARP1 lacking the WGR domain was still interacting with the histone tail (see Fig. 21).

2.10 GST-tagged H4 tail mainly interacts with the AD of PARP1

To confirm that the AD and especially the BRCT and Ac domain of PARP1 are important for the interaction with the histone tails, interactions of the H4 tail with different full-length PARP1 mutants lacking only different domains were performed. Following PARP1-deletions were used: ΔZFII (= FL without ZFII), ΔZBDIII (= FL without ZBDIII), ΔBRCT (= FL without breast cancer C-terminal domain), ΔWGR (= FL without WGR

domain), ΔAcD (= FL without Ac domain (C-terminal of BRCT domain)). GST-tagged H4 tail was bound from bacterial crude extracts to glutathione-beads and washed as indicated earlier. 10pmol of each PARP1-deletion in presence of 5pmol DNA was added to the beads and incubated 2 hours. After removing unbound PARP1-deletions, bound proteins were eluted with 10mM glutathione. The eluted protein samples were boiled at 95°C and separated by 12% SDS-PAGE. After gel electrophoresis, proteins were blotted onto a PVDF membrane and subsequently analyzed by western blot using an anti-HIS antibody to detect the interaction of the HIS-tagged PARP1-deletions. The presence of a PARP1-deletion was visualized by enhanced chemiluminescence (Fig. 21).

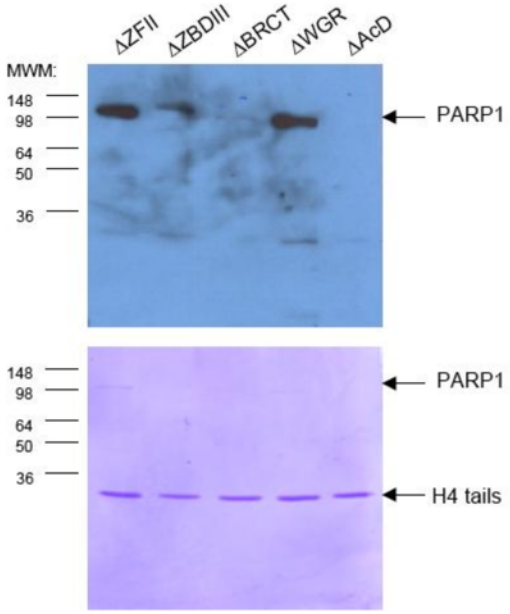

Figure 21: The upper panel is a western blot analysis using an anti-HIS antibody against HIS-tagged PARP1-deletions and the lower panel shows a Coomassie stained PVDF membrane to quantify protein levels of the H4 tails. MWM = Molecular Weight Marker

While full-length PARP1 was interacting with the histone tails, the PARP1-deletion missing either the BRCT or the Ac domain was no longer able to interact with the GST-tagged H4 tail, confirming that the automodification domain of PARP1 (both BRCT and AcD) is important for the interaction with the H4 tail and most probably also for the interaction with the other histone tails.

2.11 GST-PARP10(818-1025) (ADP-ribosyl)ate itself and histone tails in presence of eNAD$^+$

Trans(ADP-ribosyl)ation analysis of GST-tagged histone tails was further more extended by using ethenoNAD$^+$ as substrate for PARP1 or a protein fragment of PARP10 comprising amino acids 818-1025, which includes the CAT domain. The usage of eNAD$^+$ would allow first to perform (ADP-ribosyl)ation experiments without radioactive labelled NAD$^+$ and the corresponding protection equipment, and second to detect eNAD$^+$ incorporation by western blot. (ADP-ribosyl)ation assays with different eNAD$^+$ concentrations and full-length GST-tagged H4 tail were performed. Samples were incubated with 10pmol of PARP1 for 5min at 30°C or with 10pmol of GST-PARP10(818-1025) for 30min at 30°C in presence of different amounts of eNAD$^+$ (as indicated in Fig. 22). The reaction was stopped and proteins separated by 12% SDS-PAGE. After gel electrophoresis, the proteins were blotted onto a PVDF membrane and analyzed by western blot using the IG4 antibody, which detects the etheno mojety of eNAD$^+$. The labelled proteins were visualized by enhanced chemiluminescence (Fig. 22).

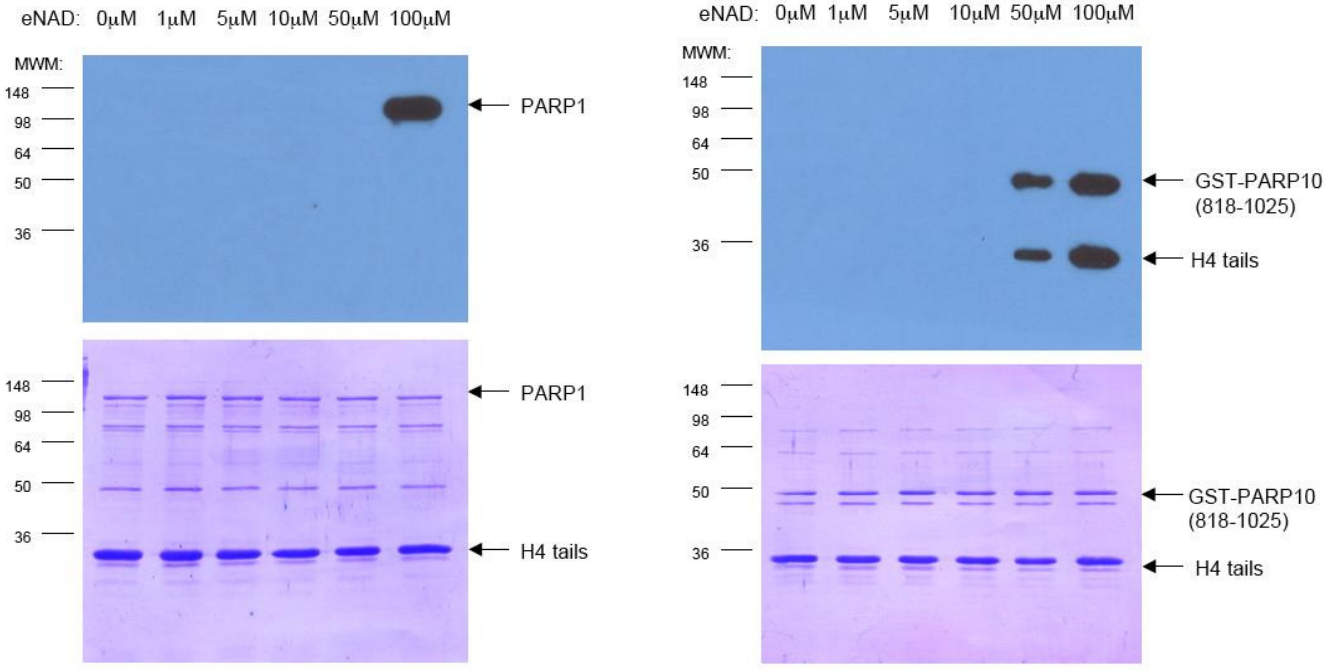

Figure 22: The upper panels are western blot analyses using the IG4 antibody to detect at which concentration of eNAD$^+$, (ADP-ribosyl)ation is performed. The lower panels show Coomassie stained PVDF membranes to quantify protein levels of PARP and the histone tails. MWM = Molecular Weight Marker

For PARP1 only auto(ADP-ribosyl)ation was observed using 100µM $eNAD^+$. In contrast, GST-PARP10(818-1025) was able to perform auto(ADP-ribosyl)ation as well as trans(ADP-ribosyl)ation of the GST-tagged H4 tail under the same conditions. Also the minimal $eNAD^+$ concentration for the enzymatic activation of PARP1 and GST-PARP10(818-1025) differed. While PARP1 only (ADP-ribosyl)ated itself at a concentration of 100µM $eNAD^+$, GST-PARP10(818-1025) auto- and trans(ADP-ribosyl)ation was observed already at a concentration of 50µM $eNAD^+$, indicating that only GST-PARP10(818-1025)-mediated (ADP-ribosyl)ation could potentially be further analyzed under these conditions. To confirm this result, a (ADP-ribosyl)ation assay with GST-PARP10(818-1025) and all other GST-tagged histone tails was repeated in presence of 100µM $eNAD^+$ (Fig. 23).

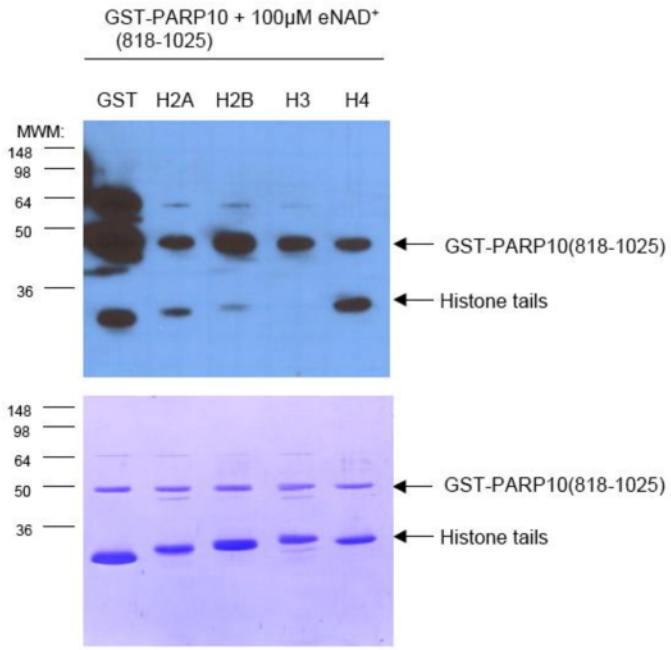

Figure 23: The upper panel is a western blot analysis using the IG4 antibody. The lower panel shows a Coomassie stained PVDF membrane to quantify protein levels of PARP and the histone tails. MWM = Molecular Weight Marker

GST-PARP10(818-1025) was able to trans(ADP-ribosyl)ate all tested GST-tagged histone tails except of H3, which was comparable to the results obtained in Fig. 6. However, GST (negative control) was also modified by GST-PARP10(818-1025) under the tested conditions, suggesting that the modification of the GST-tagged histone tails was only unspecific labelling. Since GST-tag modification of the histone tails cannot be excluded, further experiments were again performed with ^{32}P-NAD^+.

2.12 Trans(ADP-ribosyl)ation of histone deletions and mutants by GST-PARP10(818-1025)

To test whether GST-PARP10(818-1025) would (ADP-ribosyl)ate the different histone tail deletions and mutations at all and to identify possible ADP-ribose acceptor sites, GST-PARP10(818-1025)-mediated (ADP-ribosyl)ation assays in presence of 100nM ^{32}P-NAD^{+} and the available histone tails were performed. After 30min incubation at 30°C, reaction was stopped and the proteins separated by 12% SDS-PAGE. The gel was subsequently stained with Coomassie, vaccum dried and exposed to a Phosphor screen to quantify the incorporated radioactivity (see figures below).

2.12.1 K13/15 are possible ADP-ribose acceptor sites of H2A modified by GST-PARP10(818-1025)

The minimal deletion mutant required for (ADP-ribosyl)ation by GST-PARP10(818-1025) was H2A-D2, which correlated with the one found for PARP1 (Fig. 24).

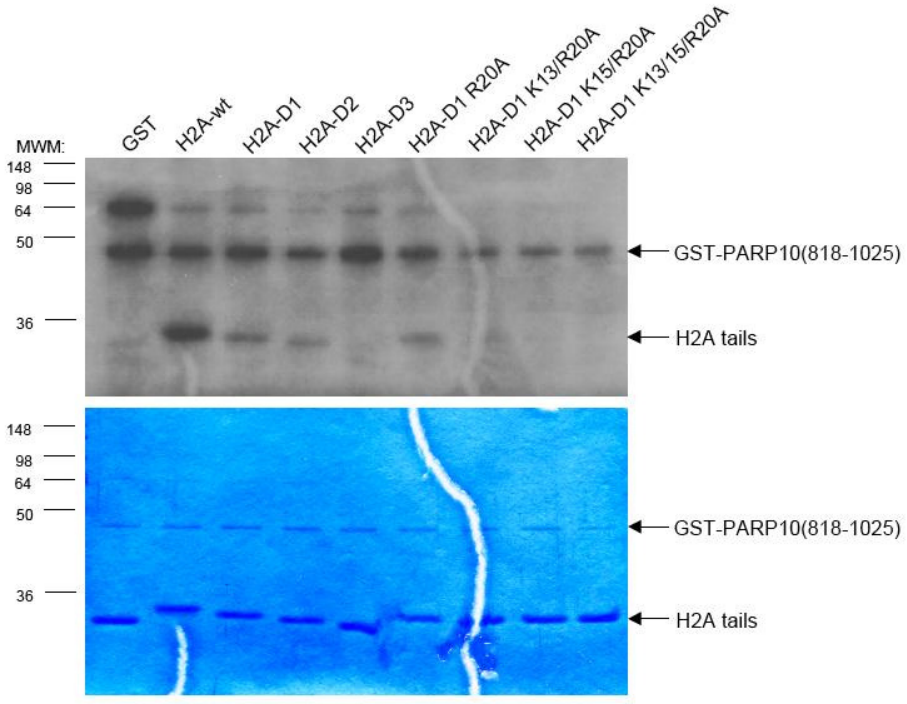

Figure 24: The upper panel shows the x-ray film to quantify the radioactivity coupled with (ADP-ribosyl)ation and the lower panel shows a Coomassie stained gel to quantify the protein levels of PARP and H2A tails. MWM = Molecular Weight Marker

In the H2A-D1 context a loss of (ADP-ribosyl)ation was observed when K13/R20 and K15/R20 were substituted to alanines, but also when all three amino acids were substituted (K13/15/R20A). Since substitution of R20 alone did not reduce (ADP-ribosyl)ation in the H2A-D1 context, the substitution of K13 and K15 is most probably responsible for the loss of (ADP-ribosyl)ation, thus pointing at K13 and K15 as acceptor sites. However, since a reduction of about 50% of (ADP-ribosyl)ation was observed when H2A-wt was deleted to D1, additional modification sites for PARP10 are suggested to be located between amino acids 26-34.

2.12.2 K27/28/30/34/R29/31/33 are possible ADP-ribose acceptor sites of H2B modified by GST-PARP10(818-1025)

In the full-length context of the H2B tail a loss of (ADP-ribosyl)ation by GST-PARP10(818-1025) was observed when K27/28/30/34 as well as R29/31/33 were substituted to alanines (K4R3A, Fig. 25).

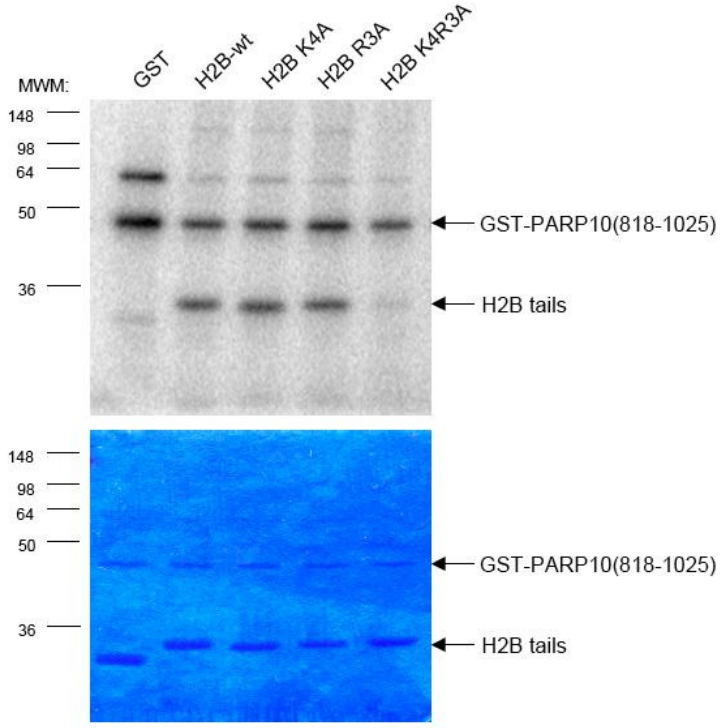

Figure 25: The upper panel shows the Phosphor Image of the gel to quantify the radioactivity coupled with (ADP-ribosyl)ation and the lower panel shows a Coomassie stained gel to quantify the protein levels of PARP and H2B tails. MWM = Molecular Weight Marker

H2B tails with substitutions of the four lysines (K4A) or the three arginines (R3A) alone were still (ADP-ribosyl)ated. Only when all seven substitutions were combined, (ADP-

ribosyl)ation was completely lost, suggesting that all seven amino acids together are important for (ADP-ribosyl)ation. This (ADP-ribosyl)ation pattern correlated with the one observed for PARP1. The only difference was the slight modification of GST (negative control), which was already seen in earlier experiments (Fig. 6 and 23). Together, these results suggest that K27/28/30/34 as well as R29/31/33 of H2B are the most important residues for trans(ADP-ribosyl)ation by the CAT domain of PARP10.

2.12.3 H3 tail is not modified by GST-PARP10(818-1025)

All tested H3 tail deletions and mutations showed the same low (ADP-ribosyl)ation levels, which correlated with the signal observed for GST (negative control, Fig. 26), indicating that GST-PARP10(818-1025) is not able to trans(ADP-ribosyl)ate the H3 tail.

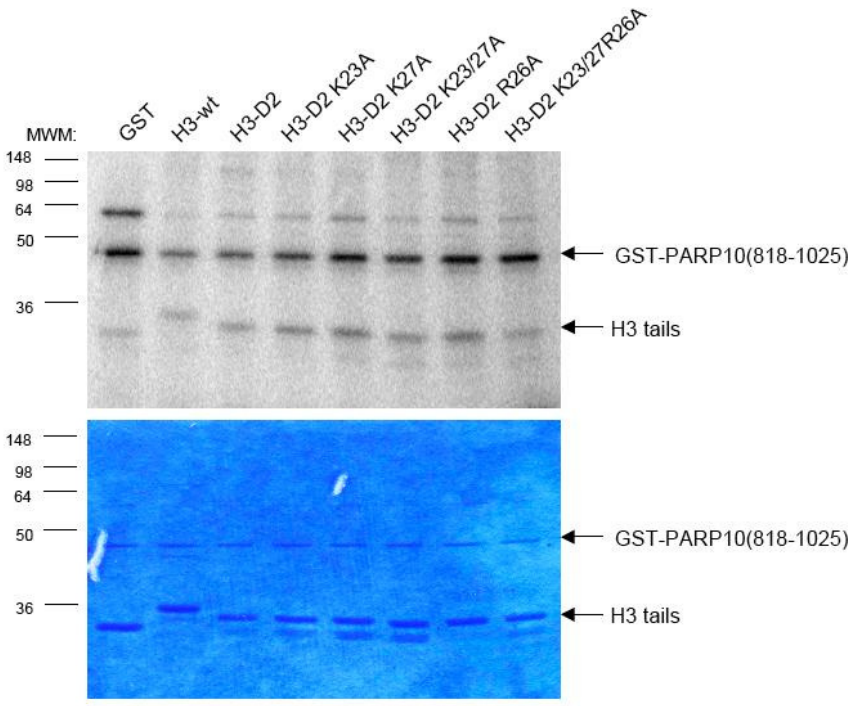

Figure 26: The upper panel shows the Phosphor Image of the gel to quantify the radioactivity coupled with (ADP-ribosyl)ation and the lower panel shows a Coomassie stained gel to quantify the protein levels of PARP and H3 tails. MWM = Molecular Weight Marker

2.12.4 K16/20 and R17/19 are possible ADP-ribose acceptor sites of H4 modified by GST-PARP10(818-1025)

Since H4-D2 was the minimal modified deletion mutant by PARP1, it was speculated that this might also be the one modified by GST-PARP10(818-1025). Indeed, H4-D2 was also (ADP-ribosyl)ated by GST-PARP10(818-1025) (Fig. 27).

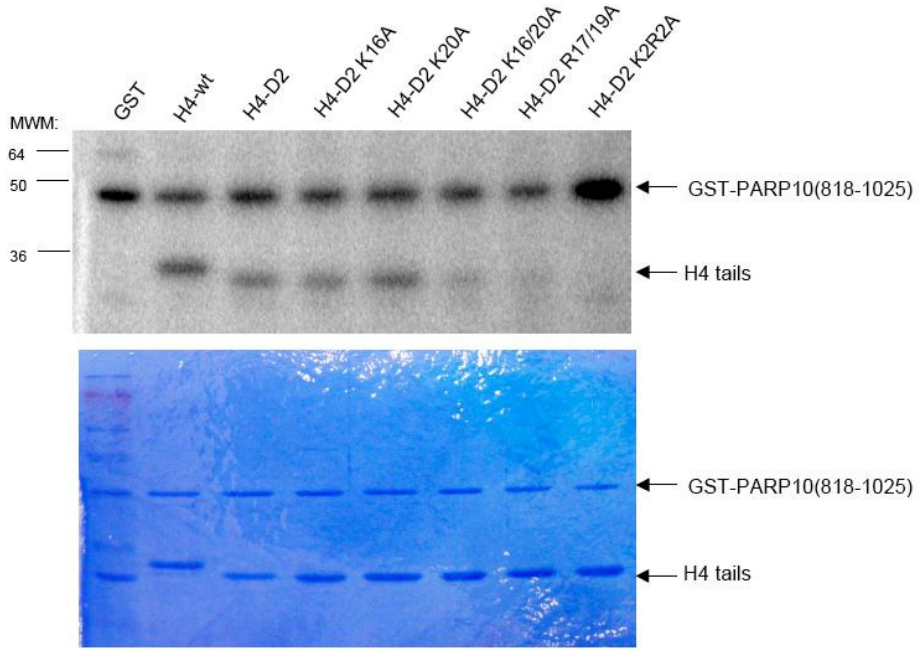

Figure 27: The upper panel shows the Phosphor Image of the gel to quantify the radioactivity coupled with (ADP-ribosyl)ation and the lower panel shows a Coomassie stained gel to quantify the protein levels of PARP and H4 tails. MWM = Molecular Weight Marker

In the H4-D2 context a loss of (ADP-ribosyl)ation was observed when K16/20 or R17/19 or all four amino acids together (K2R2A) were substituted to alanines. The H4 tail with single lysine substitutions (K16A or K20A) was still (ADP-ribosyl)ated, suggesting that multiple lysines are modified by PARP10. This (ADP-ribosyl)ation pattern correlated with the one observed for PARP1. Taken together, K16/20 and R17/19 seemed to be important residues for trans(ADP-ribosyl)ation by the CAT domain of PARP10.

All together these experiments provide evidence that distinct lysine and arginine residues are important for (ADP-ribosyl)ation by GST-PARP10(818-1025). Whether this is due to a lack of interaction has to be further analyzed (including single amino acid mutants), but is less likely to be the case, since mass spectrometric analyses confirmed these sites for H4 (see Discussion).

3 Discussion

The aim of this thesis was to investigate whether histone tails are (ADP-ribosyl)ated by PARP1, PARP2 and PARP10 and furthermore to identify potential ADP-ribose acceptor sites of the core histone tails. Core histone tails were cloned into pGEX-2T vectors and expressed as GST-fusion proteins to perform PARP-mediated (ADP-ribosyl)ation and interaction assays. Trans(ADP-ribosyl)ation of histone tails was only observed for PARP1 and GST-PARP10(818-1025), but not for PARP2, although all three PARPs were able to perform auto(ADP-ribosyl)ation. High NaCl concentrations inhibited the enzymatic activity of PARP1, by inhibiting its interaction with histone tails, suggesting that the interaction is of an electrostatic nature. The minimal deletion mutants of all GST-tagged histone tails required for the interaction with PARP1 were identified and correlated with the ones required for trans(ADP-ribosyl)ation, except for H2B, where a second interaction site was identified, which seemed to be unphysiological. Furthermore, substitutions of lysines and arginines to alanines in the full-length as well as deletion mutant, which could still interact, were used to identify potential ADP-ribose acceptor sites of the histone tails. These experiments revealed that distinct lysines and arginines are responsible for the modification. Addition of DNA had no impact on the interaction of PARP1 with GST-tagged histone tails and the BRCT as well as Ac domain of PARP1 were identified as the responsible domains for interaction with histone tails. The same experiments were repeated with GST-PARP10(818-1025). (ADP-ribosyl)ation assays revealed that distinct lysines and arginines are also the most important residues for modification by GST- PARP10(818-1025).

(ADP-ribosyl)ation of histone tails

This is the first time that (ADP-ribosyl)ation of histone tails has been reported, since only (ADP-ribosyl)ation of full-length histones has been described so far. Some studies reported that H1 is the most modified histone followed by H2B, H2A, H4 and H3. This differs from our result, in which the H2A tail was modified stronger than the other tails. The difference might be explained by the fact that full-length histones have additional modification sites, besides the one identified in the tail.

PARP2 was not able no trans(ADP-ribosyl)ate histone tails, which is probably because of structural differences in the CAT domain. This is strengthened by the fact that a different substrate specifity for PARP1 and 2 was already described (140). GST-PARP10(818-1025) trans(ADP-ribosyl)ated the histone tails with the same specifity as observed for PARP1,

despite the fact that the glutamate in the catalytic site is missing in this protein, providing evidence that the glutamate itself is not important for substrate specifity.

Lysines are ADP-ribose acceptor sites

Together our studies identified lysines as ADP-ribose acceptor amino acids of the histone tails and not the glutamic acid residues as suggested by Ogata et al. (97, 100). In the 1970s several laboratories identified glutamic acid residues in histone H1 and H2B to be modified when they incubated chromatin from rat liver with radioactive NAD^+ (97, 100-102). At that time, no other PARP family member except PARP1 was identified yet, and no knockdown-system was available (99). The modification of glutamic acid residues as acceptor sites was never verified using purified enzymes (e.g. PARP1) nor confirmed by mutagenesis or mass spectrometry (141). Thus, it is possible that other PARP family members or even unrelated NAD^+ consuming enzymes were responsible for the modification at the identified glutamates and that PARP1 modifies lysine residues (99). For some histone tails, defined lysines could be identified as acceptor site, by (ADP-ribosyl)ation assays as well as mass spectrometric analyses. While for other histone tails additional single mutations or mass spectrometric analyses would be required to determine the exact acceptor site modified by PARP1 or PARP10. For this kind of analysis, (ADP-ribosyl)ated peptides were acetone precipitated and analyzed by liquid-chromatography coupled mass spectrometry. The modified peptides were analyzed by ETD (electron transfer dissociation) resulting in an almost complete fragmentation of the multiple charged histone peptides (99). Fragmentation of the mono(ADP-ribosyl)ated H3 peptide revealed specific (ADP-ribosyl)ation of K27 and K37 by PARP1. For the H4 peptide, mass spectrometric analysis identified K16 to be (ADP-ribosyl)ated by PARP1. These sites represent two known sites of frequent histone modification (H3K27 and H4K16), as described in 1.2.3 and below, as well as a novel modification site (H3K37) (99).

Since the attachment of an ADP-ribose reverses the positive charge of an amino acid into a negative charge, the functional consequence of lysine (ADP-ribosyl)ation can be assumed to be even more drastic than other posttranslational modifications. Therefore, the possible effects on chromatin architecture, histone dynamics, histone degradation and histone variant incorporation may be dramatic (99).

Furthermore, certain posttranslated ADP-ribose acceptor sites are also important for the interaction with PARP1 (e.g. R20 of H2A or K16 and K20 of H4), indicating that the modified lysine is contacting in the active site a negative amino acid, which would stabilize

the interaction but also allow Schiffbase formation with the ADP-ribose. To provide evidence that the observed (ADP-ribosyl)ation of lysine residues is not a result of non-enzymatic Schiffbase formation, but rather specifically mediated by PARP1, mass spectrometric analyses were performed using peptides incubated with NAD^+ alone or in presence of ADP-ribose and PARP1. These analyses provided evidence that the modification of lysines is indeed specifically catalyzed by PARP1 (99).

Cross-talk with other modifications

Since we identified K16 of the H4 tail as ADP-ribose acceptor site, which was already reported to be an acceptor site for acetylation, cross-talk between these two modifications can be expected. Acetylation of H4K16 occurs frequently in eukaryotic cells and has been correlated with chromatin decompaction (4, 99). If H4K16 is indeed an acceptor site for PARP1-mediated (ADP-ribosyl)ation, acetylation at this site should impair (ADP-ribosyl)ation. Our laboratory tested this hypothesis with H4 chemically acetylated at K16 in mass spectrometry and in (ADP-ribosyl)ation assays with radioactive NAD^+. Both assays revealed that PARP1 was not any longer able to induce (ADP-ribosyl)ation of the acetylated peptide. These results support the conclusion that H4K16 is indeed modified by PARP1 and that acetylation of K16 inhibits (ADP-ribosyl)ation of the H4 peptide. To test in vivo whether PARP1 would interfere with this histone modification, PARP1 was transiently knocked down in asynchronous HeLa cells and extracted histones were assessed for cellular H4K16ac levels. Interestingly the levels of H4K16ac were increased in PARP1-depleted extracts, suggesting that PARP1-mediated (ADP-ribosyl)ation interferes with H4K16 acetylation also in vivo (99).

Possibly, (ADP-ribosyl)ation of histone H3 and H4 also interferes with other posttranslational modifications on the same lysines. For example, H3K27 is methylated by EZH2 (enhancer of zeste homolog 2), which is in the polycomb group complex that is involved in maintenance of the inactive X-chromosome (99, 142). Interestingly, PARP1 was demonstrated to participate in the maintenance of X-chromosome silencing as well (99, 143). On the other hand, the stretch between K16 and K20 of the H4 tail, was shown to be required for chromatin fiber formation and for interaction with various non-histone modulators, such as Alc1, which needs this stretch for it's activity (99, 144). Interestingly, recent reports provide evidence that the ATPase activity of Alc1 is highly stimulated by binding to poly(ADP-ribosyl)ated PARP1 (99, 144, 145). Whether (ADP-ribosyl)ated H4 would activate Alc1, remains to be investigated.

Interaction site on PARP1

Addition of DNA to the PARP1 interaction assays had no impact on PARP1's interaction with the tested tails. Interaction assays with PARP1-fragments revealed that histone tails mainly interact with the automodification domain of PARP1. The automodification domain was already reported to be an interaction site of several different proteins (61, 146). Interaction of ZFI and II with histone tails was also observed, but this interaction seems to be likely unspecific, since ZFI and ZFII can bind DNA and a co-purification of DNA with the histone tails from bacteria can currently not be excluded. Also the WGR domain that interacted with the H4 tail seems not to be important for the interaction of PARP1 with H4, since a deletion of PARP1 lacking the WGR domain was still able to interact with the H4 tail.

(ADP-ribosyl)ation of histones by PARP10

Furthermore, additional assays were performed with the CAT domain of PARP10, since it is not possible to express the full-length PARP10 in bacteria. In presence of 50µM $eNAD^+$, only GST-PARP10(818-1025) was able to perform trans(ADP-ribosyl)ation, while PARP1 could not. Automodification of both PARPs were observed, however only at high concentration of $eNAD^+$ and only allowing mono(ADP-ribosyl)ation, but not poly(ADP-ribosyl)ation. This result suggests that $eNAD^+$ compared to unmodified NAD^+, is not an ideal substrate for both, PARP1 and PARP10.

By performing GST-PARP10(818-1025)-mediated (ADP-ribosyl)ation assays possible ADP-ribose acceptor sites of histone tails were identified. However, due to a lack of interaction studies with GST-PARP10(818-1025), which is not possible under these conditions since PARP10 and the tails are both GST-tagged and would bind to the same beads, these acceptor sites can currently not be confirmed.

Outlook and medical relevance

Histone interaction studies with PARP10 would be interesting to perform and to confirm the putative identified ADP-ribose acceptor sites. These experiments would also allow further comparisons with results obtained for PARP1. Furthermore, performing mass spectrometry would be useful to detect further specific ADP-ribose acceptor sites of the histone tails. It would also be interesting to extend the analysis and to investigate (ADP-ribosyl)ation of histones in the nucleosome context in presence of DNA or to analyze the ADP-ribose acceptor sites in regard to different cellular stress conditions (e.g. genotoxic stress).

PARP1 plays a crucial role in genotoxic stress signalling by poly(ADP-ribosyl)ing core histones. Cancer cells rely very much on the activity of PARP1, since inhibition of PARP1 induces cell death in cells deficient for homologous recombination regulated by BRCA1 and BRCA2 (147). Extending this analysis of acceptor sites for histones but also for other nuclear proteins in cancer cells, with the aim to identify more acceptor sites, would possibly help to further elucidate the beneficial effect of PARP inhibition in cancer therapy.

4 Material and Methods

4.1 Molecular Biology Methods

4.1.1 Overlapping PCR

Overlapping PCR was used in this thesis to introduce a site specific mutation in a DNA strand (e.g. lysines and arginines were substituted to alanines). For this purpose 4 different primers were designed. In this thesis, a BstBI-primer (5'AATGTTCGAAGATC GTTTATGTC3') and a PstI-primer (5'ATTGCTGCAGGCATC GTGGTGTCAC3') on the plasmid were used for flanking the whole amplified region, together with a reverse as well as a forward primer, which encoded the desired mutation (sequence of alanine). In a first PCR, two PCR products were amplified using one flanking primer and one mutation primer. The first product (5' to the mutation site) was produced by BstBI-primer and the reverse primer, and the second product (3' to the mutation site) was produced by the forward primer and PstI-primer. The PCR-Mix contained 1µM of each primer, 200µM of dNTP's, 5µl of 5xPhusion buffer HF, 100ng of DNA-template and 1Unit of Phusion-polymerase (Finnzyme) and was adjusted with H_2O to a sample volume of 25µl. The first PCR began with 5min at 95°C, followed by 25 cycles of 30sec at 95°C, 30sec at 55°C and 30sec at 72°C, and finished with 7min at 72°C. The second product was slightly longer and therefore the incubation time was extended to 1min (at 72°C) instead of 30sec.

After the first PCR, 10µl of each PCR product was loaded on a 1% Agarose gel (Agarose from Promega Corporation) to control the amplified products. The Agarose gel was run with 1x TAE buffer (40mM Tris acetate, 1mM EDTA, 0.1% Acetic acid) for 20min at 80V. These PCR products were further used in a second PCR round, which was an overlapping PCR using both PCR products from the first round and only the flanking primers, to generate one combined PCR product. Due to the complementarity of the primers at the mutation site, overlapping PCR elongation occurs, combining the first and the second product spanning the region from the BstBI to the PstI restriction site. For this overlapping PCR 0.5µl of the first PCR product and 1µl of the second PCR product was used together with 1µM of BstBI-primer, 1µM of PstI-primer, 200µM of dNTP's, 10µl of 5xPhusion buffer HF and 1 Unit of the Phusion-polymerase and was adjusted with H_2O to a sample volume of 50µl. The thermo cycles for this amplification were the same as above for the second product. After

PCR, 10µl of the PCR product were loaded again on a 1% Agarose gel to control the amplification.

4.1.2 DNA extraction from Agarose Gel

A PCR product with the correct length was cut out of the Agarose gel (Agarose from Promega Corporation). 200µl of NT-binding-buffer (MACHEREY-NAGEL, Switzerland) per 100mg gel were added to dissolve the Agarose gel and to equilibrate the binding conditions of DNA for the column. After addition of NT-binding-buffer, the sample was heated to 50°C until the gel was solubilized. After that, the sample was transferred onto a NucleoSpin column (MACHEREY-NAGEL, Switzerland) and centrifuged for 1min at 11'000rpm (12'900rcf), to allow DNA binding to the silicia membrane of the column. Next, 600µl of washing buffer NT3 (MACHEREY-NAGEL, Switzerland) was added and the column was again centrifuged for 1min at 11'000rpm (12'900rcf). After the washing buffer was discarded, the silicia membrane was dried with a 2min centrifugation run at 11'000rpm (12'900rcf). Then the column was placed into a fresh tube and 15µl of autoclaved H_2O was added to the silicia membrane. After incubation for 1min at room temperature the column was again centrifuged with 11'000rpm (12'900rcf) for 1min, to elute the DNA from the membrane into the fresh tube.

4.1.3 Restriction digest

To prepare the ends of the amplified DNA-fragments for cloning, restriction digest was performed. Since the BstBI-primer and the PstI-primer included the sequence of the restriction enzymes BstBI and PstI, PCR products were therefore cut with the same two restriction enzymes (BstBI; New England Biolabs, 20U/µl; and PstI; New England Biolabs, 20U/µl). The restriction digest was performed with 10 Units of BstBI, 10 Units of PstI, 0.3µl BSA (100x concentrated, FLUKA Analytical) and 3µl of New England Biolabs 3 Buffer (10x concentrated) and was adjusted to a volume of 30µl with the eluted DNA. It was incubated in a thermo-cycler for 90min at 37°C and 90min at 65°C. The pGEX-2T vector was cut with the same enzymes in a different tube.

4.1.4 Ligation of DNA fragments into a vector

After the restriction digest, the PCR-products and the vector were separately loaded on NucleoSpin columns and again eluted (as described in 4.1.2). For the ligation of the PCR-product into a vector, approximately 50ng of the eluted DNA and 50ng of cutted (BstBI/PstI) pGEX-2T vector together with 1µl of 10x T4-DNA-Ligase Buffer (Fermentas) and 1 Weiss Unit of T4-Ligase (Fermentas) were used. The ligation mix was incubated overnight at 18°C. Chemo-competent E.coli strain XL-10 was used to transform the ligation mix. 10µl of ligation mix was added and incubated with 100µl of bacteria for 10min on ice, then heat shock was done for 40sec at 42°C. The samples were subsequently placed again on ice for 2min and 1ml of LB-medium without ampicillin was added. The samples were put in an incubator and shaked for 1hour at 37°C to allow bacterial recovery and to produce proteins important for the selection. The samples were centrifuged for 1min at 11'000rpm (12'900rcf) to pellet the bacteria. The pellet was resuspended in 100µl of LB-medium and plated on an ampicillin (50µg/ml) containing LB-Agar-plate. The plate was incubated overnight at 37°C. Only bacteria with the vector containing the ampicillin resistance marker could form colonies. The next day, bacteria colonies were picked and inoculated into 3ml of LB-medium (50µg/ml ampicillin). The LB-medium was incubated overnight on a shaker at 37°C and 220rpm.

4.1.5 Small scale-Plasmid Isolation (Miniprep)

2ml of the overnight grown LB-medium with bacteria, which contained the pGEX plasmid and would therefore grow under selective conditions, were centrifuged at 5'000rpm (2'700rcf) for 5min. The pellet was resuspended with 300µl of S1-solution (MACHEREY-NAGEL, Switzerland). After resuspension, 300µl of S2-solution (MACHEREY-NAGEL, Switzerland) was added to lyse the bacterial cell membrane. The sample was tilted once and then incubated for 3-5min at room temperature. Next, 400µl of S3-solution (MACHEREY-NAGEL, Switzerland) was added to neutralize the sample, tilted twice and then incubated 10min on ice. After incubation, the sample was centrifuged for 10min at 14'000rpm (20'800rcf) at 4°C. The supernatant was transferred to a fresh tube and the centrifugation step was repeated. After centrifugation, the supernatant was again transferred into a fresh tube and 650µl of Isopropanol (100%) was added to precipitate the plasmid-DNA. The sample was vortexed and incubated for 10min on ice. After centrifugation for 10min at 14'000rpm

(20'800rcf) and 4°C, the supernatant was discarded. Next, 200µl of Ethanol (70%) was added and the tube was incubated on ice for 5min. A centrifugation step followed as above (10min at 14'000rpm and 4°C). The Ethanol was discarded and the pellet containing the plasmid-DNA was vacuum dried in a speed vac for 20min. Finally, 20µl of autoclaved H_2O was added and the pellet resuspended by shaking gently for 20-60min at room temperature.

4.2 Biochemical Methods

4.2.1 Expression of GST-tagged histone tails in bacteria

An appropriate amount of plasmid-DNA was transformed into competent E.coli strain BL21(DE3) through heat shock (see also 4.1.4). 100µl of BL21(DE3) and 10-100ng of the plasmid-DNA were incubated for 10min on ice. The mix was heat shocked for 40sec at 42°C and then incubated on ice again for 2min. To allow bacterial growth, 1ml LB-medium without ampicillin was added and the samples subsequently shaked for 1hour at 37°C. After this incubation, the samples were centrifuged 1min at 11'000rpm (12'900rcf) and the pellet resuspended in 100µl LB-medium. 80µl of these bacteria were used to inoculate 3ml of LB-medium (50µg/ml ampicillin) and incubated overnight at 37°C. The next morning a larger culture of 50ml LB-medium (50µg/ml ampicillin) was inoculated with 2ml of the overnight culture. The bacteria were grown at 30°C until OD_{600} reached 0.6. Then 1M IPTG (I-8000 Isopropyl-beta-D-thiogalactopyranoside, Biosynth) was added to a final concentration of 1mM IPTG to induce the expression of the GST-fusion protein and the bacterial growth was continued at 30°C for another 3hours. The bacteria were collected by centrifugation with 4'000rpm (5'299rcf) during 15min at 4°C. Per 50ml of culture, 2.5ml of EBC-buffer (120mM NaCl, 50mM Tris-HCl (pH 8.0), 0.5% (v/v) NP-40, 5mM DTT, 1mM PMSF) was added to the pellet and resuspended by pipetting. Once the pellet was resolved 0.5mg/ml freshly dissolved lysozyme (Sigma Aldrich) was added to the resuspension and incubated 20min on rolls at room temperature to lyse the bacterial cell membrane. To shear the bacterial DNA, the solution then was sonicated with 15 pulses of 30 % duty cycles. The sonicated solution was centrifuged for 10min at 12'000rpm (17'600rcf) with a SS34 rotor to spin down the bacterial debris. Finally the supernatant, corresponding to as "crude protein extract", which contains the GST-tagged histone tails, was aliquoted and stored at -20°C.

4.2.2 Purification of GST-tagged histone tail proteins

To purify the GST-tagged histone tails, 1ml of the crude protein extract was diluted with 2.5ml of EBC-buffer (120mM NaCl, 50mM Tris-HCl (pH 8.0), 0.5% (v/v) NP-40, 5mM DTT, 1mM PMSF) in a 15ml falcon tube. Next, 70µl slurry of glutathione-beads (Glutathione-Sepharose^{TM}4B, in 20% Ethanol: GE Healthcare) were equilibrated with 1ml of EBC-buffer. After centrifugation for 2min at 2'000rpm (1'002rcf) the supernatant was discarded and the diluted crude protein extract containing the GST-tagged histone tail proteins was incubated with the beads for 1h at 4°C on rolls. The falcons were subsequently centrifuged at 2'000rpm (1'002rcf) for 2min. The supernatant was discarded and the beads were washed 3 times with 5ml of EBC-buffer. Between the washing steps the falcons were centrifuged for 2min at 2'000rpm (1'002 rcf). Usually charged beads were also equilibrated once with 7ml of (ADP-ribosyl)ation-buffer (50mM Tris-HCl (pH 8.0), 4mM $MgCl_2$, 1µg/ml pepstatin, 1µg/ml bestatin, 1µg/ml leupeptin, 250µM DTT). After discarding the supernatant, 300µl of (ADP-ribosyl)ation-buffer with 10mM glutathione (L-Glutathione reduced, minimum 99%, Sigma-Aldrich) was added to the beads to elute the GST-tagged histone tail proteins from the beads. It was incubated overnight at 4°C or for 45min at room temperature on rolls. Finally the samples were centrifuged for 2min at 2'000rpm (1'002rcf) and the supernatant with the purified protein was stored in liquid nitrogen.

4.2.3 Bradford Protein Assay

To measure the protein concentrations of the eluted proteins, Bradford assay was used. This assay uses BIO-RAD solution (BIO-RAD Protein Assay, Bio-Rad Laboratories GmbH), which stains proteins blue. Color change can be detected in a Spectrometer at 595nm. For this assay the 5x concentrated BIO-RAD solution was diluted with ddH_2O to a 1x concentrated solution. To 1ml of 1x concentrated BIO-RAD solution, 5-20µl of protein were added. As standard concentrations, 20µl of 4 known BSA (FLUKA Analytical) concentrations were used, 0.2mg/ml, 0.36mg/ml, 0.54mg/ml and 0.72mg/ml respectively. The values at 595nm of these protein concentrations, served as a standard curve, with which an unknown protein concentration could be determined.

4.2.4 (ADP-ribosyl)ation assay with ^{32}P-NAD$^+$

This assay was used to investigate the (ADP-ribosyl)ation activity of different PARPs (e.g. PARP1/2/10). For an (ADP-ribosyl)ation assay 1.5µg of protein (GST-tagged histone tails), 10pmol of PARP, 5pmol of EcoRI-linker DNA, (ADP-ribosyl)ation-buffer (50mM Tris-HCl (pH 8.0), 4mM $MgCl_2$, 1µg/ml pepstatin, 1µg/ml bestatin, 1µg/ml leupeptin, 250µM DTT) and 100nM of ^{32}P-NAD$^+$ (Perkin Elmer) were used. The sample volume was usually 25µl or 30µl. The amount of the added protein varied due to the different protein concentrations measured by Bradford protein assay (as described in 4.2.3). To adjust the difference of sample volumes and to prevent degradation of proteins through proteases, (ADP-ribosyl)ation-buffer that contained protease-inhibitors was added. First the (ADP-ribosyl)ation-buffer was added to the reaction, then the GST-tagged histone tails followed by PARP and finally the EcoRI-linker DNA. In the C-laboratory 100nM ^{32}P-NAD$^+$ was added to start the (ADP-ribosyl)ation-reaction. The NAD$^+$ is labelled with ^{32}P to detect the (ADP-ribosyl)ation of the GST-tagged histone tails catalyzed by PARPs by radiography. After addition of ^{32}P-NAD$^+$, the samples containing PARP1 were incubated for 5min at 30°C and the samples containing PARP2 or 10, were usually incubated for 30min at 30°C. To stop the reaction, 2.7-3.3µl of 10x SDS-sample-buffer (600mmol/l Tris-HCl (pH 6.8), 20% (w/v) Na-dodecylsulfate, 20% (v/v) Glycerol, 0.05% (w/v) Bromphenol blue, 20% (v/v) Mercaptoethanol, 25mmol/l DTT) was added. As soon as 10x SDS-sample-buffer was added, the samples were put into a heat block for 5min at 95°C to denature the proteins. After this step, the proteins were separated by a SDS-Polyacrylamide gel (see 4.2.6) and incorporated radioactivity quantified (as described in 4.2.7).

4.2.5 PARP1 interaction assay with GST-tagged histone tails

To check whether PARP1 can interact with GST-tagged histone tails or deletions and mutations thereof, PARP1 interaction assays were performed. 10-30µl of GST-tagged histone tail crude protein extracts were bound to 10-15µl of equilibrated glutathione-beads (Glutathione-Sepharose™4B, in 20% Ethanol: GE Healthcare) for 1hour at 4°C on rolls. To dilute the extract and to adjust binding conditions, 200-600µl of EBC-buffer (120mM NaCl, 50mM Tris-HCl (pH 8.0), 0.5% (v/v) NP-40, 5mM DTT, 1mM PMSF) was added. After 1hour, unbound proteins were removed through different washing steps. First, the GST-beads were washed 3 times with 1ml of EBC-buffer, then 2 times with 1ml of 0-50mM NaCl-

containing (ADP-ribosyl)ation-buffer (50mM Tris-HCl (pH 8.0), 4mM $MgCl_2$, 1µg/ml pepstatin, 1µg/ml bestatin, 1µg/ml leupeptin, 250µM DTT). Between the washing steps the samples were centrifuged for 1min at 5'000rpm (2'655rcf) at 4°C. Interaction with PARP1 was performed by addition of 10pmol of PARP1 with or without 5pmol of EcoRI-linker DNA to the beads while the volume was adjusted with 0-50mM NaCl-containing (ADP-ribosyl)ation-buffer to 300µl. The samples were incubated for 2hours on the rotating wheel at 4°C. To remove the unbound PARP1, the samples were washed 3 times with 1ml of 0-50mM NaCl-containing (ADP-ribosyl)ation-buffer. The supernatant was discarded and 20µl of 2x SDS-sample-buffer was added to the beads. After boiling for 5min at 95°C, the beads were loaded on a SDS-PAGE, followed by western blot (see 4.2.8) to analyze if PARP1 had interacted with the different GST-tagged target proteins.

4.2.6 SDS-Polyacrylamide Gel Electrophoresis (SDS-PAGE)

The sodium dodecyl sulfate polyacrylamide gel (SDS-PAGE), is used to separate proteins based on their molecular weight. First, one glass plate (10 x 8.5cm) and one teflon plate were cleaned with Ethanol (70%) and two spacers (10 x 0.15cm) placed in between them. The assembled plates were put into a gel preparation unit and was filled with about 8ml of separation gel solution (12% SDS-PAGE: 3.6ml ddH_2O, 2.0ml Solution B (1.5M Tris-HCl (pH 8.8), 0.4% (w/v) Na-dodecylsulfate), 2.4ml Acrylamide (Acrylamide-Bis solution (37.5:1), 40% (w/v), SERVA Electrophoresis GmbH), 80µl APS (10%), 8µl TEMED). As soon as the chamber was filled, 1ml of H_2O was added to generate a plain surface of the gel. After 20min the gel was normally polymerized, allowing the water to be replaced by 3ml of stacking gel solution (3ml of 4% (v/v) stacking solution (65ml ddH_2O, 25ml Solution C (0.5M Tris-HCl (pH 6.8), 0.4% (w/v) Na-dodecylsulfate and a tip of Bromphenol blue), 10ml of 40% Acrylamide), 30µl APS (10%), 3µl TEMED). A comb containing 10 or 15 flaps was inserted into the stacking gel solution before polymerization, to generate the sample pockets. Usually, the SDS-gels were poured freshly, that means about 30min before usage. Sometimes, the gel was poured earlier and stored at 4°C overnight. The polymerized gel was placed into a running unit, which was filled with 1x SDS running buffer (25mM Tris base, 200mM Glycine, 0.1% (w/v) Na-dodecylsulfate). The comb was removed and the sample pockets rinsed with the 1x SDS running buffer. Into the first sample pocket 4µl of See Blue ® Plus 2 Prestained Standard (1x from invitrogen) was loaded, which is a marker of distinct molecular weights. Into the other pockets the different samples were loaded and run for 20min at 90V to

allow proteins to stack and reach the beginning of the separation gel. After that the voltage was raised to 130V for 1 hour. Finally slides were removed from the gel, which was either stained or blotted (as described in 4.2.8). For staining, the gel was soaked in Coomassie (0.25% (w/v) Coomassieblue R250, 40% (v/v) Methanol, 10% (v/v) Acetic acid) for 10min, destained with Fast Destain (12% (v/v) Methanol, 10% (v/v) Acetic acid) and then used for Quantification by Phosphor Imaging (as described in 4.2.7).

4.2.7 Quantification by Phosphor Imaging

Phosphor Imaging was used to quantify the amount of radioactivity. The phosphor screens retain emitted energy from beta particles, X-rays and gamma rays. The retained energy is emitted as light from the phosphor screen upon laserinduced stimulation, in proportion to the amount of stored radioactivity. The emitted light is collected and converted to an electrical signal by a photomultiplier. The electrical signal is digitized to permit image display and analysis. Phosphor Imaging was specifically used to measure the amount of radioactivity, which was incorporated by (ADP-ribosyl)ation of the GST-tagged histone tails. The gel was exposed to a Phosphor screen (Molecular Dynamics) overnight or at least for 2hours. Afterwards the screen was scanned by a Typhoon 9400 (Amersham Biosciences) and the resulting digital file was edited with the program ImageQuant 5.0 (Molecular Dynamics).

4.2.8 Western Blot Analysis

Western blot analysis is used to specifically detect proteins or posttranslational modifications such as poly(ADP-ribosyl)ation. For a western blot a “sandwich” was assembled in a bath of 1x Transfer buffer (20% (v/v) Methanol, 70% ddH_2O, 10% (v/v) 10x Transfer buffer (25mmol/l Tris-base, 192mmol/l Glycine, dissolved in ddH_2O)) as follows: one wetted sponge, two pre-wetted Wattman-papers, one PVDF membrane (Millipore, Pore size: 0.45um), which was first activated by 100% Methanol, the polyacrylamide gel with the separated proteins, followed by two pre-wetted Wattman-papers and one wetted sponge. The plastic frame with the sandwich was put into a western blot chamber, which was filled with 1x Transfer buffer and an ice bloc. The blotting was done for 90min at 100V at 4°C. To confirm that proteins were blotted successfully from the gel onto the PVDF membrane, the membrane was stained shortly with 1x Ponceau and destained with deionized water and TBS-

T (10mmol/l Tris HCl (pH 7.5), 150mmol/l NaCl, ddH_2O, 0.05% (v/v) Tween 20) for about 10min. 5ml of a 5% blocking solution to avoid unspecific binding of the antibody, consisting of skim milk powder (Migros) and TBS-T, was added to each membrane and incubated for 1hour on a shaker at room temperature. After blocking, 5ml of a 1% blocking solution with the primary antibody was added. The selection of the primary antibody depended on the protein to be detected. Anti-PARP1 (1:3000, homemade) was used to detect PARP1, anti-PAR (1:3000, LP 96-H, BD Biosciences) was used to detect poly(ADP-ribosyl)ation, IG4 (1:20) was used to detect ethenoNAD$^+$ (Sigma, N2630), αHIS (1:1000, diluted in 3% BSA, Qiagen) was used to detect HIS-tagged PARPs and cMYC (1:1000, LP 9E10, Roche) was used to detect MYC-tagged PARPs. After incubation for 1 or 2 hours, the membrane was washed with TBS-T to remove the primary antibody. The washing step was repeated 2 times with 5ml of TBS-T over 15min. Next, the secondary antibody was added in presence of 5ml of 1% blocking solution. The selection of the secondary antibody depended on the primary antibody to be detected. For anti-PARP1 and anti-PAR, an anti-rabbit IgG (GE Healthcare, Horseradish Peroxidase-linked whole antibody from donkey) was used and for IG4, cMYC and αHIS, an anti-mouse IgG (GE Healthcare, Horseradish Peroxidase-linked whole antibody from sheep) was used. The incubation time of the secondary antibody was 1hour on a shaker at room temperature in presence of 1% skim milk and TBS-T. The membranes were washed again with TBS-T to remove unspecific antibody binding. The membranes were subsequently drained and 1ml of normal ECL (1ml of UptiLight HRP Blot Substrate Reagent A, from Uptima and 1drop of UptiLight HRP Blot Reagent B, from Uptima) was dropped onto the membrane to induce a chemiluminescence reaction, which was visualized by an X-ray film exposure.

5 References

1. Hottiger, M. O. (2005) Cell biology script.
2. Rouleau, M., Aubin, R. A., and Poirier, G. G. (2004) Poly(ADP-ribosyl)ated chromatin domains: access granted. J Cell Sci **117**, 815-825
3. Earnshaw, W. C., and Mackay, A. M. (1994) Role of nonhistone proteins in the chromosomal events of mitosis. FASEB J **8**, 947-956
4. Kouzarides, T. (2007) Chromatin modifications and their function. Cell **128**, 693-705
5. Horn, P. J., and Peterson, C. L. (2002) Molecular biology. Chromatin higher order folding--wrapping up transcription. Science **297**, 1824-1827
6. Wolffe, A. (1998) Chromatin: Structure and Function. London: Academic Press
7. Holde, K. v. (1988) Chromatin. Berlin: Springer Verlag
8. Alberts, B. (1983) Molecular biology of the cell.
9. Belmont, A. S., Dietzel, S., Nye, A. C., Strukov, Y. G., and Tumbar, T. (1999) Large-scale chromatin structure and function. Curr Opin Cell Biol **11**, 307-311
10. Izzo, A., Kamieniarz, K., and Schneider, R. (2008) The histone H1 family: specific members, specific functions? Biol Chem **389**, 333-343
11. Arents, G., and Moudrianakis, E. N. (1995) The histone fold: a ubiquitous architectural motif utilized in DNA compaction and protein dimerization. Proc Natl Acad Sci U S A **92**, 11170-11174
12. Wu, J., and Grunstein, M. (2000) 25 years after the nucleosome model: chromatin modifications. Trends Biochem Sci **25**, 619-623
13. Zlatanova, J., Caiafa, P., and Van Holde, K. (2000) Linker histone binding and displacement: versatile mechanism for transcriptional regulation. FASEB J **14**, 1697-1704
14. Wyrick, J. J., and Parra, M. A. (2009) The role of histone H2A and H2B post-translational modifications in transcription: a genomic perspective. Biochim Biophys Acta **1789**, 37-44
15. Mellor, J. (2006) Dynamic nucleosomes and gene transcription. Trends Genet **22**, 320-329
16. Shimada, M., Niida, H., Zineldeen, D. H., Tagami, H., Tanaka, M., Saito, H., and Nakanishi, M. (2008) Chk1 is a histone H3 threonine 11 kinase that regulates DNA damage-induced transcriptional repression. Cell **132**, 221-232
17. Oohara, I., and Wada, A. (1987) Spectroscopic studies on histone-DNA interactions. I. The interaction of histone (H2A, H2B) dimer with DNA: DNA sequence dependence. J Mol Biol **196**, 389-397
18. Oohara, I., and Wada, A. (1987) Spectroscopic studies on histone-DNA interactions. II. Three transitions in nucleosomes resolved by salt-titration. J Mol Biol **196**, 399-411
19. Park, Y. J., Dyer, P. N., Tremethick, D. J., and Luger, K. (2004) A new fluorescence resonance energy transfer approach demonstrates that the histone variant H2AZ stabilizes the histone octamer within the nucleosome. J Biol Chem **279**, 24274-24282
20. Hoch, D. A., Stratton, J. J., and Gloss, L. M. (2007) Protein-protein Forster resonance energy transfer analysis of nucleosome core particles containing H2A and H2A.Z. J Mol Biol **371**, 971-988
21. Aragay, A. M., Diaz, P., and Daban, J. R. (1988) Association of nucleosome core particle DNA with different histone oligomers. Transfer of histones between DNA-(H2A,H2B) and DNA-(H3,H4) complexes. J Mol Biol **204**, 141-154

22. Kimura, H., and Cook, P. R. (2001) Kinetics of core histones in living human cells: little exchange of H3 and H4 and some rapid exchange of H2B. J Cell Biol **153**, 1341-1353
23. Kireeva, M. L., Walter, W., Tchernajenko, V., Bondarenko, V., Kashlev, M., and Studitsky, V. M. (2002) Nucleosome remodeling induced by RNA polymerase II: loss of the H2A/H2B dimer during transcription. Mol Cell **9**, 541-552
24. Vicent, G. P., Nacht, A. S., Smith, C. L., Peterson, C. L., Dimitrov, S., and Beato, M. (2004) DNA instructed displacement of histones H2A and H2B at an inducible promoter. Mol Cell **16**, 439-452
25. Kimura, H. (2005) Histone dynamics in living cells revealed by photobleaching. DNA Repair (Amst) **4**, 939-950
26. Thiriet, C., and Hayes, J. J. (2005) Replication-independent core histone dynamics at transcriptionally active loci in vivo. Genes Dev **19**, 677-682
27. Jamai, A., Imoberdorf, R. M., and Strubin, M. (2007) Continuous histone H2B and transcription-dependent histone H3 exchange in yeast cells outside of replication. Mol Cell **25**, 345-355
28. Svotelis, A., Gevry, N., and Gaudreau, L. (2009) Regulation of gene expression and cellular proliferation by histone H2A.Z. Biochem Cell Biol **87**, 179-188
29. Li, B., Carey, M., and Workman, J. L. (2007) The role of chromatin during transcription. Cell **128**, 707-719
30. Henikoff, S., Ahmad, K., Platero, J. S., and van Steensel, B. (2000) Heterochromatic deposition of centromeric histone H3-like proteins. Proc Natl Acad Sci U S A **97**, 716-721
31. Meluh, P. B., Yang, P., Glowczewski, L., Koshland, D., and Smith, M. M. (1998) Cse4p is a component of the core centromere of Saccharomyces cerevisiae. Cell **94**, 607-613
32. Clarkson, M. J., Wells, J. R., Gibson, F., Saint, R., and Tremethick, D. J. (1999) Regions of variant histone His2AvD required for Drosophila development. Nature **399**, 694-697
33. Santisteban, M. S., Kalashnikova, T., and Smith, M. M. (2000) Histone H2A.Z regulats transcription and is partially redundant with nucleosome remodeling complexes. Cell **103**, 411-422
34. Allis, C. D., Glover, C. V., Bowen, J. K., and Gorovsky, M. A. (1980) Histone variants specific to the transcriptionally active, amitotically dividing macronucleus of the unicellular eucaryote, Tetrahymena thermophila. Cell **20**, 609-617
35. Stargell, L. A., Bowen, J., Dadd, C. A., Dedon, P. C., Davis, M., Cook, R. G., Allis, C. D., and Gorovsky, M. A. (1993) Temporal and spatial association of histone H2A variant hv1 with transcriptionally competent chromatin during nuclear development in Tetrahymena thermophila. Genes Dev **7**, 2641-2651
36. Adam, M., Robert, F., Larochelle, M., and Gaudreau, L. (2001) H2A.Z is required for global chromatin integrity and for recruitment of RNA polymerase II under specific conditions. Mol Cell Biol **21**, 6270-6279
37. Larochelle, M., and Gaudreau, L. (2003) H2A.Z has a function reminiscent of an activator required for preferential binding to intergenic DNA. EMBO J **22**, 4512-4522
38. Fan, J. Y., Gordon, F., Luger, K., Hansen, J. C., and Tremethick, D. J. (2002) The essential histone variant H2A.Z regulates the equilibrium between different chromatin conformational states. Nat Struct Biol **9**, 172-176
39. Knippers, R. (2006) Molekulare Genetik.

40. Parseghian, M. H., Newcomb, R. L., Winokur, S. T., and Hamkalo, B. A. (2000) The distribution of somatic H1 subtypes is non-random on active vs. inactive chromatin: distribution in human fetal fibroblasts. Chromosome Res **8**, 405-424
41. Nightingale, K. P., O'Neill, L. P., and Turner, B. M. (2006) Histone modifications: signalling receptors and potential elements of a heritable epigenetic code. Curr Opin Genet Dev **16**, 125-136
42. Riggs, A. D., Martiennssen, R.A., Russo, V.E.A. (1996) Epigenetic Mechanisms of Gene Regulation. Cold Spring Harbor Laboratory Press
43. Shechter, D., Dormann, H. L., Allis, C. D., and Hake, S. B. (2007) Extraction, purification and analysis of histones. Nat Protoc **2**, 1445-1457
44. Wood, C., Snijders, A., Williamson, J., Reynolds, C., Baldwin, J., and Dickman, M. (2009) Post-translational modifications of the linker histone variants and their association with cell mechanisms. FEBS J **276**, 3685-3697
45. Fischle, W., Tseng, B. S., Dormann, H. L., Ueberheide, B. M., Garcia, B. A., Shabanowitz, J., Hunt, D. F., Funabiki, H., and Allis, C. D. (2005) Regulation of HP1-chromatin binding by histone H3 methylation and phosphorylation. Nature **438**, 1116-1122
46. Nelson, C. J., Santos-Rosa, H., and Kouzarides, T. (2006) Proline isomerization of histone H3 regulates lysine methylation and gene expression. Cell **126**, 905-916
47. Clements, A., Poux, A. N., Lo, W. S., Pillus, L., Berger, S. L., and Marmorstein, R. (2003) Structural basis for histone and phosphohistone binding by the GCN5 histone acetyltransferase. Mol Cell **12**, 461-473
48. Hassa, P. O., and Hottiger, M. O. (2008) The diverse biological roles of mammalian PARPS, a small but powerful family of poly-ADP-ribose polymerases. Front Biosci **13**, 3046-3082
49. Hassa, P. O., and Hottiger, M. O. (2002) The functional role of poly(ADP-ribose)polymerase 1 as novel coactivator of NF-kappaB in inflammatory disorders. Cell Mol Life Sci **59**, 1534-1553
50. Schreiber, V., Dantzer, F., Ame, J. C., and de Murcia, G. (2006) Poly(ADP-ribose): novel functions for an old molecule. Nat Rev Mol Cell Biol **7**, 517-528
51. de Murcia, J. M., Niedergang, C., Trucco, C., Ricoul, M., Dutrillaux, B., Mark, M., Oliver, F. J., Masson, M., Dierich, A., LeMeur, M., Walztinger, C., Chambon, P., and de Murcia, G. (1997) Requirement of poly(ADP-ribose) polymerase in recovery from DNA damage in mice and in cells. Proc Natl Acad Sci U S A **94**, 7303-7307
52. Wang, Z. Q., Stingl, L., Morrison, C., Jantsch, M., Los, M., Schulze-Osthoff, K., and Wagner, E. F. (1997) PARP is important for genomic stability but dispensable in apoptosis. Genes Dev **11**, 2347-2358
53. Masutani, M., Nozaki, T., Nishiyama, E., Shimokawa, T., Tachi, Y., Suzuki, H., Nakagama, H., Wakabayashi, K., and Sugimura, T. (1999) Function of poly(ADP-ribose) polymerase in response to DNA damage: gene-disruption study in mice. Mol Cell Biochem **193**, 149-152
54. Hassa, P. O., Haenni, S. S., Elser, M., and Hottiger, M. O. (2006) Nuclear ADP-ribosylation reactions in mammalian cells: where are we today and where are we going? Microbiol Mol Biol Rev **70**, 789-829
55. Ame, J. C., Spenlehauer, C., and de Murcia, G. (2004) The PARP superfamily. Bioessays **26**, 882-893
56. Otto, H., Reche, P. A., Bazan, F., Dittmar, K., Haag, F., and Koch-Nolte, F. (2005) In silico characterization of the family of PARP-like poly(ADP-ribosyl)transferases (pARTs). BMC Genomics **6**, 139

57. Marsischky, G. T., Wilson, B. A., and Collier, R. J. (1995) Role of glutamic acid 988 of human poly-ADP-ribose polymerase in polymer formation. Evidence for active site similarities to the ADP-ribosylating toxins. J Biol Chem **270**, 3247-3254
58. Rolli, V., O'Farrell, M., Menissier-de Murcia, J., and de Murcia, G. (1997) Random mutagenesis of the poly(ADP-ribose) polymerase catalytic domain reveals amino acids involved in polymer branching. Biochemistry **36**, 12147-12154
59. Ruf, A., Mennissier de Murcia, J., de Murcia, G., and Schulz, G. E. (1996) Structure of the catalytic fragment of poly(AD-ribose) polymerase from chicken. Proc Natl Acad Sci U S A **93**, 7481-7485
60. Altmeyer, M., Messner, S., Hassa, P. O., Fey, M., and Hottiger, M. O. (2009) Molecular mechanism of poly(ADP-ribosyl)ation by PARP1 and identification of lysine residues as ADP-ribose acceptor sites. Nucleic Acids Res **37**, 3723-3738
61. D'Amours, D., Desnoyers, S., D'Silva, I., and Poirier, G. G. (1999) Poly(ADP-ribosyl)ation reactions in the regulation of nuclear functions. Biochem J **342 (Pt 2)**, 249-268
62. Tao, Z., Gao, P., Hoffman, D. W., and Liu, H. W. (2008) Domain C of human poly(ADP-ribose) polymerase-1 is important for enzyme activity and contains a novel zinc-ribbon motif. Biochemistry **47**, 5804-5813
63. Langelier, M. F., Servent, K. M., Rogers, E. E., and Pascal, J. M. (2008) A third zinc-binding domain of human poly(ADP-ribose) polymerase-1 coordinates DNA-dependent enzyme activation. J Biol Chem **283**, 4105-4114
64. Pion, E., Ullmann, G. M., Ame, J. C., Gerard, D., de Murcia, G., and Bombarda, E. (2005) DNA-induced dimerization of poly(ADP-ribose) polymerase-1 triggers its activation. Biochemistry **44**, 14670-14681
65. Schreiber, V., Molinete, M., Boeuf, H., de Murcia, G., and Menissier-de Murcia, J. (1992) The human poly(ADP-ribose) polymerase nuclear localization signal is a bipartite element functionally separate from DNA binding and catalytic activity. EMBO J **11**, 3263-3269
66. Desmarais, Y., Menard, L., Lagueux, J., and Poirier, G. G. (1991) Enzymological properties of poly(ADP-ribose)polymerase: characterization of automodification sites and NADase activity. Biochim Biophys Acta **1078**, 179-186
67. Schreiber, V., Ame, J. C., Dolle, P., Schultz, I., Rinaldi, B., Fraulob, V., Menissier-de Murcia, J., and de Murcia, G. (2002) Poly(ADP-ribose) polymerase-2 (PARP-2) is required for efficient base excision DNA repair in association with PARP-1 and XRCC1. J Biol Chem **277**, 23028-23036
68. Yang, X. J. (2005) Multisite protein modification and intramolecular signaling. Oncogene **24**, 1653-1662
69. Uchida, K., Hanai, S., Ishikawa, K., Ozawa, Y., Uchida, M., Sugimura, T., and Miwa, M. (1993) Cloning of cDNA encoding Drosophila poly(ADP-ribose) polymerase: leucine zipper in the auto-modification domain. Proc Natl Acad Sci U S A **90**, 3481-3485
70. Uchida, K., Morita, T., Sato, T., Ogura, T., Yamashita, R., Noguchi, S., Suzuki, H., Nyunoya, H., Miwa, M., and Sugimura, T. (1987) Nucleotide sequence of a full-length cDNA for human fibroblast poly(ADP-ribose) polymerase. Biochem Biophys Res Commun **148**, 617-622
71. Kim, J. W., Kim, K., Kang, K., and Joe, C. O. (2000) Inhibition of homodimerization of poly(ADP-ribose) polymerase by its C-terminal cleavage products produced during apoptosis. J Biol Chem **275**, 8121-8125

72. Uchida, K., and Miwa, M. (1994) Poly(ADP-ribose) polymerase: structural conservation among different classes of animals and its implications. Mol Cell Biochem **138**, 25-32
73. Uchida, K., Uchida, M., Hanai, S., Ozawa, Y., Ami, Y., Kushida, S., and Miwa, M. (1993) Isolation of the poly(ADP-ribose) polymerase-encoding cDNA from Xenopus laevis: phylogenetic conservation of the functional domains. Gene **137**, 293-297
74. Koyama, Y., Katagiri, S., Hanai, S., Uchida, K., and Miwa, M. (1999) Poly(ADP-ribose) polymerase interacts with novel Drosophila ribosomal proteins, L22 and l23a, with unique histone-like amino-terminal extensions. Gene **226**, 339-345
75. Masutani, M., Nozaki, T., Hitomi, Y., Ikejima, M., Nagasaki, K., de Prati, A. C., Kurata, S., Natori, S., Sugimura, T., and Esumi, H. (1994) Cloning and functional expression of poly(ADP-ribose) polymerase cDNA from Sarcophaga peregrina. Eur J Biochem **220**, 607-614
76. Hassa, P. O., and Hottiger, M. O. (2005) An epigenetic code for DNA damage repair pathways? Biochem Cell Biol **83**, 270-285
77. Ziegler, M. (2000) New functions of a long-known molecule. Emerging roles of NAD in cellular signaling. Eur J Biochem **267**, 1550-1564
78. Berger, F., Ramirez-Hernandez, M. H., and Ziegler, M. (2004) The new life of a centenarian: signalling functions of NAD(P). Trends Biochem Sci **29**, 111-118
79. Magni, G., Amici, A., Emanuelli, M., Orsomando, G., Raffaelli, N., and Ruggieri, S. (2004) Structure and function of nicotinamide mononucleotide adenylyltransferase. Curr Med Chem **11**, 873-885
80. Magni, G., Amici, A., Emanuelli, M., Orsomando, G., Raffaelli, N., and Ruggieri, S. (2004) Enzymology of NAD+ homeostasis in man. Cell Mol Life Sci **61**, 19-34
81. Chambon, P., Weill, J. D., and Mandel, P. (1963) Nicotinamide mononucleotide activation of new DNA-dependent polyadenylic acid synthesizing nuclear enzyme. Biochem Biophys Res Commun **11**, 39-43
82. Reeder, R. H., Ueda, K., Honjo, T., Nishizuka, Y., and Hayaishi, O. (1967) Studies on the polymer of adenosine diphosphate ribose. II. Characterization of the polymer. J Biol Chem **242**, 3172-3179
83. Miwa, M., Saikawa, N., Yamaizumi, Z., Nishimura, S., and Sugimura, T. (1979) Structure of poly(adenosine diphosphate ribose): identification of 2'-[1"-ribosyl-2"-(or 3"-)(1'"-ribosyl)]adenosine-5',5",5'"-tris(phosphate) as a branch linkage. Proc Natl Acad Sci U S A **76**, 595-599
84. Kawaichi, M., Ueda, K., and Hayaishi, O. (1981) Multiple autopoly(ADP-ribosyl)ation of rat liver poly(ADP-ribose) synthetase. Mode of modification and properties of automodified synthetase. J Biol Chem **256**, 9483-9489
85. Alvarez-Gonzalez, R., and Jacobson, M. K. (1987) Characterization of polymers of adenosine diphosphate ribose generated in vitro and in vivo. Biochemistry **26**, 3218-3224
86. Ferro, A. M., and Oppenheimer, N. J. (1978) Structure of a poly (adenosine diphosphoribose) monomer: 2'-(5"-hosphoribosyl)-5'-adenosine monophosphate. Proc Natl Acad Sci U S A **75**, 809-813
87. Benjamin, R. C., and Gill, D. M. (1980) Poly(ADP-ribose) synthesis in vitro programmed by damaged DNA. A comparison of DNA molecules containing different types of strand breaks. J Biol Chem **255**, 10502-10508
88. Wielckens, K., George, E., Pless, T., and Hilz, H. (1983) Stimulation of poly(ADP-ribosyl)ation during Ehrlich ascites tumor cell "starvation" and suppression of concomitant DNA fragmentation by benzamide. J Biol Chem **258**, 4098-4104

89. Alvarez-Gonzalez, R., and Althaus, F. R. (1989) Poly(ADP-ribose) catabolism in mammalian cells exposed to DNA-damaging agents. Mutat Res **218**, 67-74
90. Simonin, F., Poch, O., Delarue, M., and de Murcia, G. (1993) Identification of potential active-site residues in the human poly(ADP-ribose) polymerase. J Biol Chem **268**, 8529-8535
91. Desnoyers, S., Shah, G. M., Brochu, G., Hoflack, J. C., Verreault, A., and Poirier, G. G. (1995) Biochemical properties and function of poly(ADP-ribose) glycohydrolase. Biochimie **77**, 433-438
92. Oka, J., Ueda, K., Hayaishi, O., Komura, H., and Nakanishi, K. (1984) ADP-ribosyl protein lyase. Purification, properties, and identification of the product. J Biol Chem **259**, 986-995
93. Ueda, K., Omachi, A., Kawaichi, M., and Hayaishi, O. (1975) Natural occurrence of poly(ADP-ribosyl) histones in rat liver. Proc Natl Acad Sci U S A **72**, 205-209
94. Otake, H., Miwa, M., Fujimura, S., and Sugimura, T. (1969) Binding of ADP-ribose polymer with histone. J Biochem **65**, 145-146
95. Adamietz, P., Bredehorst, R., and Hilz, H. (1978) ADP-ribosylated histone H1 from HeLa cultures. Fundamental differences to (ADP-ribose)n-histone H1 conjugates formed into vitro. Eur J Biochem **91**, 317-326
96. Minaga, T., Romaschin, A. D., Kirsten, E., and Kun, E. (1979) The in vivo distribution of immunoreactive larger than tetrameric polyadenosine diphosphoribose in histone and non-histone protein fractions of rat liver. J Biol Chem **254**, 9663-9668
97. Ogata, N., Ueda, K., and Hayaishi, O. (1980) ADP-ribosylation of histone H2B. Identification of glutamic acid residue 2 as the modification site. J Biol Chem **255**, 7610-7615
98. Boulikas, T. (1988) At least 60 ADP-ribosylated variant histones are present in nuclei from dimethylsulfate-treated and untreated cells. EMBO J **7**, 57-67
99. Messner, S., Altmeyer, M., Zhao, H., and Pozivil, A. (2010) PARP1 ADP-ribosylates lysine residues in core histone tails. submitted
100. Ogata, N., Ueda, K., Kagamiyama, H., and Hayaishi, O. (1980) ADP-ribosylation of histone H1. Identification of glutamic acid residues 2, 14, and the COOH-terminal lysine residue as modification sites. J Biol Chem **255**, 7616-7620
101. Burzio, L. O., Riquelme, P. T., and Koide, S. S. (1979) ADP ribosylation of rat liver nucleosomal core histones. J Biol Chem **254**, 3029-3037
102. Riquelme, P. T., Burzio, L. O., and Koide, S. S. (1979) ADP ribosylation of rat liver lysine-rich histone in vitro. J Biol Chem **254**, 3018-3028
103. Adolph, K. W. (1985) Cell cycle variations in ADP-ribosylation of HeLa nuclear proteins. Arch Biochem Biophys **243**, 427-438
104. Jump, D. B., Butt, T. R., and Smulson, M. (1979) Nuclear protein modification and chromatin substructure. 3. Relationship between poly(adenosine diphosphate) ribosylation and different functional forms of chromatin. Biochemistry **18**, 983-990
105. Colyer, R. A., Burdette, K. E., and Kidwell, W. R. (1973) Poly ADP-ribose synthesis and DNA replication in synchronized mouse L-cells. Biochem Biophys Res Commun **53**, 960-966
106. Kidwell, W. R., and Mage, M. G. (1976) Changes in poly(adenosine diphosphate-ribose) and poly(adenosine diphosphate-ribose) polymerase in synchronous HeLa cells. Biochemistry **15**, 1213-1217
107. Miwa, M., Sugimura, T., Inui, N., and Takayama, S. (1973) Poly(adenosine diphosphate ribose) synthesis during the cell cycle of transformed hamster lung cells. Cancer Res **33**, 1306-1309

108. Singh, N., and Cerutti, P. (1985) Poly ADP-ribosylation of histones in tumor promoter phorbol-12-myristate-13-acetate treated mouse embryo fibroblasts C3H10T1/2. Biochem Biophys Res Commun **132**, 811-819
109. Kun, E., Kirsten, E., Bauer, P. I., and Ordahl, C. P. (2006) Quantitative correlation between cellular proliferation and nuclear poly (ADP-ribose) polymerase (PARP-1). Int J Mol Med **17**, 293-300
110. Chabert, M. G., Niedergang, C. P., Hog, F., Partisani, M., and Mandel, P. (1992) Poly(ADPR)polymerase expression and activity during proliferation and differentiation of rat astrocyte and neuronal cultures. Biochim Biophys Acta **1136**, 196-202
111. Krishnakumar, R., Gamble, M. J., Frizzell, K. M., Berrocal, J. G., Kininis, M., and Kraus, W. L. (2008) Reciprocal binding of PARP-1 and histone H1 at promoters specifies transcriptional outcomes. Science **319**, 819-821
112. Mullins, D. W., Jr., Giri, C. P., and Smulson, M. (1977) Poly(adenosine diphosphate-ribose) polymerase: the distribution of a chromosome-associated enzyme within the chromatin substructure. Biochemistry **16**, 506-513
113. Petesch, S. J., and Lis, J. T. (2008) Rapid, transcription-independent loss of nucleosomes over a large chromatin domain at Hsp70 loci. Cell **134**, 74-84
114. Timinszky, G., Till, S., Hassa, P. O., Hothorn, M., Kustatscher, G., Nijmeijer, B., Colombelli, J., Altmeyer, M., Stelzer, E. H., Scheffzek, K., Hottiger, M. O., and Ladurner, A. G. (2009) A macrodomain-containing histone rearranges chromatin upon sensing PARP1 activation. Nat Struct Mol Biol **16**, 923-929
115. Wang, Z. Q., Auer, B., Stingl, L., Berghammer, H., Haidacher, D., Schweiger, M., and Wagner, E. F. (1995) Mice lacking ADPRT and poly(ADP-ribosyl)ation develop normally but are susceptible to skin disease. Genes Dev **9**, 509-520
116. Trucco, C., Oliver, F. J., de Murcia, G., and Menissier-de Murcia, J. (1998) DNA repair defect in poly(ADP-ribose) polymerase-deficient cell lines. Nucleic Acids Res **26**, 2644-2649
117. Slattery, E., Dignam, J. D., Matsui, T., and Roeder, R. G. (1983) Purification and analysis of a factor which suppresses nick-induced transcription by RNA polymerase II and its identity with poly(ADP-ribose) polymerase. J Biol Chem **258**, 5955-5959
118. Rawling, J. M., and Alvarez-Gonzalez, R. (1997) TFIIF, a basal eukaryotic transcription factor, is a substrate for poly(ADP-ribosyl)ation. Biochem J **324 (Pt 1)**, 249-253
119. Kraus, W. L., and Lis, J. T. (2003) PARP goes transcription. Cell **113**, 677-683
120. Hassa, P. O., and Hottiger, M. O. (1999) A role of poly (ADP-ribose) polymerase in NF-kappaB transcriptional activation. Biol Chem **380**, 953-959
121. de Murcia, G., Huletsky, A., Lamarre, D., Gaudreau, A., Pouyet, J., Daune, M., and Poirier, G. G. (1986) Modulation of chromatin superstructure induced by poly(ADP-ribose) synthesis and degradation. J Biol Chem **261**, 7011-7017
122. Huletsky, A., de Murcia, G., Muller, S., Hengartner, M., Menard, L., Lamarre, D., and Poirier, G. G. (1989) The effect of poly(ADP-ribosyl)ation on native and H1-depleted chromatin. A role of poly(ADP-ribosyl)ation on core nucleosome structure. J Biol Chem **264**, 8878-8886
123. Hassa, P. O., Covic, M., Bedford, M. T., and Hottiger, M. O. (2008) Protein arginine methyltransferase 1 coactivates NF-kappaB-dependent gene expression synergistically with CARM1 and PARP1. J Mol Biol **377**, 668-678
124. Hassa, P. O., Buerki, C., Lombardi, C., Imhof, R., and Hottiger, M. O. (2003) Transcriptional coactivation of nuclear factor-kappaB-dependent gene expression by p300 is regulated by poly(ADP)-ribose polymerase-1. J Biol Chem **278**, 45145-45153

125. Eliasson, M. J., Sampei, K., Mandir, A. S., Hurn, P. D., Traystman, R. J., Bao, J., Pieper, A., Wang, Z. Q., Dawson, T. M., Snyder, S. H., and Dawson, V. L. (1997) Poly(ADP-ribose) polymerase gene disruption renders mice resistant to cerebral ischemia. Nat Med **3**, 1089-1095
126. Oliver, F. J., Menissier-de Murcia, J., Nacci, C., Decker, P., Andriantsitohaina, R., Muller, S., de la Rubia, G., Stoclet, J. C., and de Murcia, G. (1999) Resistance to endotoxic shock as a consequence of defective NF-kappaB activation in poly (ADP-ribose) polymerase-1 deficient mice. EMBO J **18**, 4446-4454
127. Weinfeld, M., Chaudhry, M. A., D'Amours, D., Pelletier, J. D., Poirier, G. G., Povirk, L. F., and Lees-Miller, S. P. (1997) Interaction of DNA-dependent protein kinase and poly(ADP-ribose) polymerase with radiation-induced DNA strand breaks. Radiat Res **148**, 22-28
128. Panzeter, P. L., and Althaus, F. R. (1994) DNA strand break-mediated partitioning of poly(ADP-ribose) polymerase function. Biochemistry **33**, 9600-9605
129. D'Silva, I., Pelletier, J. D., Lagueux, J., D'Amours, D., Chaudhry, M. A., Weinfeld, M., Lees-Miller, S. P., and Poirier, G. G. (1999) Relative affinities of poly(ADP-ribose) polymerase and DNA-dependent protein kinase for DNA strand interruptions. Biochim Biophys Acta **1430**, 119-126
130. Berger, N. A. (1985) Poly(ADP-ribose) in the cellular response to DNA damage. Radiat Res **101**, 4-15
131. Berger, N. A., Sims, J. L., Catino, D. M., and Berger, S. J. (1983) Poly(ADP-ribose) polymerase mediates the suicide response to massive DNA damage: studies in normal and DNA-repair defective cells. Princess Takamatsu Symp **13**, 219-226
132. Eguchi, Y., Shimizu, S., and Tsujimoto, Y. (1997) Intracellular ATP levels determine cell death fate by apoptosis or necrosis. Cancer Res **57**, 1835-1840
133. Leist, M., Single, B., Castoldi, A. F., Kuhnle, S., and Nicotera, P. (1997) Intracellular adenosine triphosphate (ATP) concentration: a switch in the decision between apoptosis and necrosis. J Exp Med **185**, 1481-1486
134. Jagtap, P., and Szabo, C. (2005) Poly(ADP-ribose) polymerase and the therapeutic effects of its inhibitors. Nat Rev Drug Discov **4**, 421-440
135. Goto, S., Xue, R., Sugo, N., Sawada, M., Blizzard, K. K., Poitras, M. F., Johns, D. C., Dawson, T. M., Dawson, V. L., Crain, B. J., Traystman, R. J., Mori, S., and Hurn, P. D. (2002) Poly(ADP-ribose) polymerase impairs early and long-term experimental stroke recovery. Stroke **33**, 1101-1106
136. Wang, H., Yu, S. W., Koh, D. W., Lew, J., Coombs, C., Bowers, W., Federoff, H. J., Poirier, G. G., Dawson, T. M., and Dawson, V. L. (2004) Apoptosis-inducing factor substitutes for caspase executioners in NMDA-triggered excitotoxic neuronal death. J Neurosci **24**, 10963-10973
137. Yu, S. W., Andrabi, S. A., Wang, H., Kim, N. S., Poirier, G. G., Dawson, T. M., and Dawson, V. L. (2006) Apoptosis-inducing factor mediates poly(ADP-ribose) (PAR) polymer-induced cell death. Proc Natl Acad Sci U S A **103**, 18314-18319
138. Yu, S. W., Wang, H., Poitras, M. F., Coombs, C., Bowers, W. J., Federoff, H. J., Poirier, G. G., Dawson, T. M., and Dawson, V. L. (2002) Mediation of poly(ADP-ribose) polymerase-1-dependent cell death by apoptosis-inducing factor. Science **297**, 259-263
139. Ye, H., Cande, C., Stephanou, N. C., Jiang, S., Gurbuxani, S., Larochette, N., Daugas, E., Garrido, C., Kroemer, G., and Wu, H. (2002) DNA binding is required for the apoptogenic action of apoptosis inducing factor. Nat Struct Biol **9**, 680-684

140. Johansson, M. (1999) A human poly(ADP-ribose) polymerase gene family (ADPRTL): cDNA cloning of two novel poly(ADP-ribose) polymerase homologues. Genomics **57**, 442-445
141. Messner, S. (2010) Histone ADP-ribosylation revisited. unpublished
142. Heard, E. (2005) Delving into the diversity of facultative heterochromatin: the epigenetics of the inactive X chromosome. Curr Opin Genet Dev **15**, 482-489
143. Nusinow, D. A., Hernandez-Munoz, I., Fazzio, T. G., Shah, G. M., Kraus, W. L., and Panning, B. (2007) Poly(ADP-ribose) polymerase 1 is inhibited by a histone H2A variant, MacroH2A, and contributes to silencing of the inactive X chromosome. J Biol Chem **282**, 12851-12859
144. Ahel, D., Horejsi, Z., Wiechens, N., Polo, S. E., Garcia-Wilson, E., Ahel, I., Flynn, H., Skehel, M., West, S. C., Jackson, S. P., Owen-Hughes, T., and Boulton, S. J. (2009) Poly(ADP-ribose)-dependent regulation of DNA repair by the chromatin remodeling enzyme ALC1. Science **325**, 1240-1243
145. Gottschalk, A. J., Timinszky, G., Kong, S. E., Jin, J., Cai, Y., Swanson, S. K., Washburn, M. P., Florens, L., Ladurner, A. G., Conaway, J. W., and Conaway, R. C. (2009) Poly(ADP-ribosyl)ation directs recruitment and activation of an ATP-dependent chromatin remodeler. Proc Natl Acad Sci U S A **106**, 13770-13774
146. Buki, K. G., Bauer, P. I., Hakam, A., and Kun, E. (1995) Identification of domains of poly(ADP-ribose) polymerase for protein binding and self-association. J Biol Chem **270**, 3370-3377
147. Bolderson, E., Richard, D. J., Zhou, B. B., and Khanna, K. K. (2009) Recent advances in cancer therapy targeting proteins involved in DNA double-strand break repair. Clin Cancer Res **15**, 6314-6320

6 Curriculum Vitae

Name:	Požívil
Vorname:	Andrea Ursula
Geburtsdatum:	30. September 1986
Geburtsort:	Basel
Nationalität:	Schweizerin
Heimatort:	Niederdorf, BL

Ausbildung:

1993-1998	Primarschule Allschwil
1998-2002	Progymnasium Allschwil
2002-2005	Gymnasium am Münsterplatz, Basel
01.07.2005	Zweisprachige Matura (Englisch/Deutsch) im Schwerpunkt Latein am Gymnasium am Münsterplatz in Basel
2005-2010	Veterinärmedizin Studium an der Vetsuisse-Fakultät der Universität Zürich mit Schwerpunkt Biomedizinische Forschung
02.03.09 - 15.01.10	Anfertigung der Dissertation unter Leitung von Prof. Dr. med. vet. et phil. II Michael O. Hottiger am Institut für Veterinärbiochemie und Molekularbiologie der Vetsuisse-Fakultät Universität Zürich (Direktor: Prof. Dr. med. vet. Ulrich Hübscher)

7 Acknowledgements

First I want to thank Prof. Dr. Michael Hottiger for the opportunity to work in his laboratory and to perform this thesis, as well as for his support and guidance.

My special thanks goes to Simon Messner, he was a great supervisor and the person who introduced me into the laboratory work. He had always time for me either for the planning of my experiments, for answering my questions or solving methodical problems. I'm very thankful for his support and patience.

Furthermore I would like to thank the whole Hottiger group, Suheda, Matthias, Ingrid, Moni, Karolin, Florian, Claudio, Raffaella and Andrej, for helping me when I was searching something or just for nice words. It was great to work in this harmonical group atmosphere and to be a part of it.

I also want to acknowledge all other institute members, since it was a nice working environment here at the institute.

Last I would like to thank my family, my boyfriend and my colleagues, who supported me during this time and were willing to spare me for some time.

8 Manuscript

My contribution to the attached manuscript (accepted in Nucleic Acids Research), was to perform GST-pulldown as well as (ADP-ribosyl)ation assays as described on page 6 and 7. Some of my results are described on page 10, 13 and 14. One of my (ADP-ribosyl)ation assays is seen in Figure 1C.

PARP1 ADP-ribosylates lysine residues of the core histone tails

Simon Messner[1,2,*], Matthias Altmeyer[1,2,*], Hongtao Zhao[4], Andrea Pozivil[1], Bernd Roschitzki[3], Peter Gehrig[3], Dorothea Rutishauser[3], Danzhi Huang[4], Amedeo Caflisch[4] and Michael O. Hottiger[1,§]

[1]Institute of Veterinary Biochemistry and Molecular Biology
University of Zurich, Winterthurerstrasse 190,
8057 Zurich, Switzerland
Phone: +41-44-635 54 74, Fax: +41-44-635 68 40
Email: hottiger@vetbio.uzh.ch

[2]Life Science Zurich Graduate School, Molecular Life Science Program,
University of Zurich

[3]Functional Genomics Center Zurich, University of Zurich, Winterthurerstrasse 190,
8057 Zurich, Switzerland

[4]Department of Biochemistry, University of Zurich, Winterthurerstrasse 190,
8057 Zurich, Switzerland

* These authors contributed equally to this work

§ Corresponding author

Abstract

The chromatin-associated enzyme PARP1 has previously been suggested to ADP-ribosylate histones, but the specific ADP-ribose acceptor sites have remained enigmatic. Here, we show that PARP1 covalently ADP-ribosylates the amino-terminal histone tails of all core histones. Using biochemical tools and novel ETD mass spectrometric protocols, we identify for the first time K13 of H2A, K30 of H2B, K27 and K37 of H3, as well as K16 of H4 as ADP-ribose acceptor sites. Multiple explicit water molecular dynamics simulations of the H4 tail peptide into the catalytic cleft of PARP1 indicate that two stable intermolecular salt bridges hold the peptide in an orientation that allows K16 ADP-ribosylation. Consistent with a functional cross-talk between ADP-ribosylation and other histone tail modifications, acetylation of H4K16 inhibits ADP-ribosylation by PARP1. Taken together, our computational and experimental results provide strong evidence that PARP1 modifies important regulatory lysines of the core histone tails.

Keywords: PARP-1, H3K27, H4K16, chromatin, ADP-ribosylation

Introduction

Histone proteins form the nucleosome, which is the fundamental repeating unit of chromatin (1,2). Each nucleosome contains two heterodimers of the core histones H2A and H2B, one tetramer of the core histones H3 and H4, and 146 base pairs of DNA (3). Dynamic chromatin structures are governed in part by post-translational modifications of the histones, modification of nucleotides, remodeling of nucleosomes, and by non-coding RNAs or non-histone DNA-binding proteins (4). The amino-terminal tails of the core histone proteins protrude from the nucleosome. They appear to be unstructured and are believed to participate in the formation of higher order chromatin structures by mediating internucleosomal interactions and to contact the linker DNA (3,5). A large number of residues within the histones are modified by post-translational modifications including acetylation, phosphorylation, methylation, ubiquitination and ADP-ribosylation, which occur in distinct patterns (6). Recent work has provided compelling evidence that these modifications influence the functional properties of chromatin.

Histones have long been known as substrates for ADP-ribosylation *in vivo* (7). Histones isolated from rat liver nuclei and HeLa cells incubated with radioactive NAD^+ revealed that the linker histone H1 and all core histones, H2A, H2B, H3 and H4, are ADP-ribosylated, although to a variable extent (8-12). An unresolved issue regarding the mechanism of ADP-ribosylation of histones is whether this modification primarily occurs at the globular histone domains or at their unstructured amino-terminals tails. Moreover, unconfirmed ADP-ribose acceptor amino acids have previously only been proposed for H1 and H2B, but not for H2A, H3 and H4 (11,13-15).

Poly(ADP-ribose) polymerase 1 (ARTD1/PARP1) is a nuclear chromatin-associated multifunctional enzyme that is present in most eukaryotes apart from yeast (16). The enzyme is responsible for most of the cellular poly(ADP-ribose) formation. Targets of PARP1's enzymatic activity include a variety of nuclear proteins, most prominently PARP1 itself, as well as histone proteins (17). Among the six PARP family members, PARP2 has the highest similarity with PARP1 (43% sequence identity in the catalytic domain) (18). PARP2 displays similar automodification properties as PARP1 and may account for the residual poly(ADP-ribose) synthesis observed in PARP1 knockout mice.

Recently, we showed that individual lysine residues of PARP1 and PARP2

function as acceptor sites for auto-ADP-ribosylation and not, as previously assumed, glutamic acid residues (19,20). Here, we report PARP1-mediated ADP-ribosylation of the core histone proteins. We found that PARP1, but not PARP2, ADP-ribosylates core histone proteins at their amino-terminal tails. Mass spectrometry of ADP-ribosylated histone peptides revealed that the lysine residues K13 of H2A, K30 of H2B, K27 and K37 of H3, as well as K16 of H4, are specifically ADP-ribosylated by PARP1. Acetylation of H4K16 or mutation of this residue to an alanine abrogated ADP-ribosylation. Molecular dynamics (MD) simulations of tetra- and octapeptide segments of the amino terminal tail of H4 indicated that two positively charged side chains at position n and n+1 in the histone sequence, which point in opposite directions, are engaged in favorable electrostatic interactions with two acidic PARP1 residues at the positions 988 and 756, buried in the catalytic cleft and on a loop at the entrance of the cleft, respectively. Taken together, our results reveal that PARP1 specifically modifies lysine residues of the core histone tails, which are known to control chromatin structure and function.

Materials and Methods

Chemicals and antibodies

^{32}P-NAD^{+} was purchased from PerkinElmer. NAD^{+} was obtained from Sigma-Aldrich. Anti-PAR (LP-96-10) antibody was from Becton Dickinson. Anti-PARP1 antibody was generated in this laboratory. PARP-inhibitor DAM-TIQ-A was obtained from Alexis Biochemicals, PJ34 was purchased from Enzo Life Science, 3-amino-benzamide (3AB) was from Sigma-Aldrich. Peptides were from PiProteomics. Probond^{TM} nickel beads were from Invitrogen. Glutathione-Sepharose 4B affinity beads were from GE-healthcare.

Plasmids

The baculovirus expression vectors pQE-TriSystem (Qiagen) and BacPak8 (Clontech) were used for the expression of recombinant proteins in Sf21 cells as described (21,22). pGEX-2T vectors (GE healthcare) were used for the cloning and expression of GST-fusion proteins. Full-length and truncated histone proteins were expressed in pET3a or pET3d vectors, as described (3). Sequencing of plasmids was performed by Microsynth (Balgach, CH).

Cloning, expression and purification of recombinant proteins

Human PARP1 and PARP2 were cloned, expressed and purified as described (19). Full length histone proteins were generated as described (3). GST-histone tail fusion proteins were generated by PCR and cloned into pGEX-2T vector. Truncated and mutated versions of GST-fusion proteins were generated by cloning with BstBI and EcoRI restriction sites. Primers for PCR and direct cloning were obtained from Sigma-Aldrich and Microsynth. pGEX-2T plasmids were transformed into BL21(DE3) bacteria and expression was induced by addition of 1 mM IPTG into LB-medium for 3 hours at 30°C. After centrifugation and resuspension in EBC-buffer (120 mM NaCl, 50 mM Tris-pH 8.0, 0.5% NP-40, 5 mM DTT, 1 mM PMSF), bacteria were lysed by the addition of lysozyme (0.5 mg/ml) and the DNA was sheared by a French Press. After centrifugation the supernatant was taken and the proteins were bound to GST-beads and washed extensively with EBC-buffer. The GST-beads with the bound GST-fusion proteins were equilibrated with ADP-ribosylation buffer (50 mM Tris-HCl, pH 8.0, 4 mM $MgCl_2$, 250 μM DTT, 20 mM

NaCl, 1 μg/ml protease inhibitors pepstatin, leupeptin and bestatin) and after extensive washing eluted from the GST-beads with 10 mM reduced glutathione in ADP-ribosylation buffer.

ADP-ribosylation assays

^{32}P-NAD^{+} ADP-ribosylation was performed as previously described (19). Briefly, 20 μg histone mix from calf thymus (Roche) were incubated with 10 pmol PARP1 or PARP2 in a 25 μl reaction, containing 5 pmol annealed EcoRI-linker DNA and 100 nM ^{32}P-NAD^{+} in ADP-ribosylation buffer (50 mM Tris-HCl, pH 8.0, 4 mM $MgCl_2$, 250 μM DTT, 20 mM NaCl, 1 μg/ml protease inhibitors pepstatin, leupeptin and bestatin) for 10 min at 30°C. ADP-ribosylation of full-length or truncated single histones was performed with 3 μg full-length or truncated histone proteins and 10 pmol PARP1 in a 25 μl reaction. ADP-ribosylation of GST-histone tail fusion proteins was performed with 1.5 μg purified fusion protein, together with 10 pmol of PARP1. 5 pmol EcoRI-linker DNA was always included into the reaction to activate PARP1 enzymatic activity. ADP-ribosylation assays with full-length or truncated histones were resolved by a 10-20% acrylamide gradient SDS-gel of 15 cm length (Amersham). Assays with GST-fusion proteins were resolved on standard 12% acrylamide mini-gels (Hoefer). Radiolabeled proteins were visualized by exposure to X-ray films or by quantification through the phospho-imager system (Molecular Dynamics).

For mass spectrometry, 22 nmol biotinylated H2A (aa 3-23), H2B (aa 18-37), H3 (aa 23-42), H4 (aa 1-22) or H4K16ac (aa 1-22) peptides were incubated with 10 pmol PARP1, 5 pmol annealed EcoRI-linker and 100 μM or 500 μM NAD^{+} for 15 min at 30°C in ADP-ribosylation buffer without protease inhibitors. The reaction was stopped by the addition of 3AB to a final concentration of 20 mM and subsequently 1 μg GST-ARH3 was added to the reaction and further incubated for 1 hour at 30°C. The samples were acetone precipitated and the pellet was dissolved in distilled water.

GST-pulldown

Glutathione-sepharose affinity beads were incubated with a bacterial extract of the GST-fusion protein expression in EBC-buffer. After extensive washing, the GST-beads were equilibrated with ADP-ribosylation buffer containing 50 mM NaCl. After

washing, 10 pmol purified PARP1 was added to the beads in a total volume of 300 µl ADP-ribosylation buffer. The protein mixture was incubated for 2 hour at 4°C on rolls to allow for protein-protein interaction. The samples were washed again with ADP-ribosylation buffer and resolved on standard SDS-PAGE and subsequent western blotting with anti-PARP1 antibody.

Microvolume C-18 reversed phase purification

22 nmol H4-peptide (aa 1-22) was incubated with 10 pmol PARP1, 5 pmol EcoRI-linker DNA and 100 nM ^{32}P-NAD^{+} in 25 µl ADP-ribosylation buffer for 15 min at 30°C. The reaction was stopped by the addition of 3AB to a final concentration of 20 mM. The C18 reversed phase ZIP-tip (Millipore) was pre-wetted with 100% Methanol and equilibrated with 3% (v/v) acetonitrile. The peptides were bound onto the column and subsequently washed extensively with 3% (v/v) acetonitrile. Bound peptides were eluted by 60% (v/v) acetonitrile directly into scintillation liquid. In the control reaction, peptides were added after the addition of 3AB to the reaction. Scintillation counts were measured and normalized to the control reaction and the relative increase in scintillation counts was calculated (cpm).

Mass spectrometry

ETD experiments were performed on a hybrid LTQ Orbitrap XL ETD mass spectrometer (Thermo Scientific, Bremen, Germany) coupled to an Eksigent nano LC system (Eksigent Technologies) and analyzed by reversed-phase liquid chromatography nanospray tandem mass spectrometry (LC-MS/MS).

Peptides were resuspended in 3% ACN and 0.2% formic acid, loaded from a cooled (10°C) Spark Holland autosampler (Emmen, Holland) and separated using an ACN/water solvent system containing 0.2% formic acid with a flow rate of 200 nL/min. Separation of the peptides was performed on a 10 cm long fused silica column (75 µm i.d.; BGB Analytik) in-house packed with 3 µm, 200 Å pore size C18 resin (Michrom BioResources, CA). Elution was achieved using a gradient of 3−48% ACN in 35 min, 48−80% ACN in 4 min and 80% ACN for 7 min.

One scan cycle was comprised of a survey full scan MS spectra from m/z 300 to m/z 2000 were acquired in the FT-Orbitrap with a resolution of R= 60‘000 at m/z 400, followed by up to four sequential data- dependent ETD MS/MS scans with

detection of the ETD fragment ions in the linear ion trap. AGC target values were 5^{e5} for full FTMS scans, 1^{e4} for ion trap MSn scans. Anion target value was 1^{e6} and supplementary activation was employed to enhance the fragmentation efficiency for doubly-charged precursors and charge state dependent ETD time was enabled. Data dependent decision tree was used in order to control ETD dissociation based on charge state and m/z. The ETD reaction time was set at 100 ms and the isolation width was m/z 2. For all experiments dynamic exclusion was used with one repeat count, 30 s repeat duration, and 10 s exclusion duration.

The instrument was calibrated externally according to the manufacturer's instructions. The samples were acquired using internal lock mass calibration on m/z 429.088735 and 445.120025. Spectra generated by ETD were processed using Mascot Distiller 2.2 (Matrix Science) and data was searched against a SwissProt human database using Mascot 2.2.0 to find best matching sequences. Detailed spectra analysis was done by manual evaluation.

Molecular dynamics

It is computationally prohibitive to dock the full-length histone tails to PARP1. Therefore, only the relevant tetra- and octapeptide segments of the histone tails (abbreviated H-peptides hereafter) were taken into account in the present study. A two-step procedure was used to investigate the binding of the H-peptides to PARP1 (PDB ID: 1A26). Preliminary binding modes of the flexible H-peptides into the rigid structure of the catalytic domain of PARP1 were obtained by an in-house developed docking program, which uses a combination of simulated annealing and genetic algorithm optimization of position, orientation, and rotatable bonds of the ligand (Zhao et al., unpublished). Explicit solvent molecular dynamics (MD) simulations of the H-peptide/PARP1 complexes were then used to investigate the structural stability of the poses obtained by docking. In both docking and MD simulations, the N-terminus and C-terminus of the H-peptides were capped by neutral groups (acetyl and N-methlyamide, respectively) to take into account the fact that they belong to a longer polypeptide chain. To reproduce physiological pH conditions, the side chains of aspartates and glutamates were negatively charged, those of lysines and arginines were positively charged, while all other residues were considered neutral. The MD simulations were performed with the program NAMD (23) using the all-atom CHARMM PARAM27 force field (24) and the TIP3P model of water (25). The H-

peptide/PARP1 complexes were inserted into a cubic water box, with a minimal distance of 12 Å between any solute atom and the boundary of the box. Chloride and sodium ions were added to neutralize the system and approximate a salt concentration of 150 mM. The water molecules overlapping with the solute atoms or the ions were removed, if the distance between the water oxygen and any atom of the complex or any ion was smaller than 2.4 Å. Periodic boundary conditions were applied to avoid finite-size effects. Electrostatic interactions were calculated within a cutoff of 12 Å, while long-range electrostatic effects were taken into account by the particle mesh Ewald summation method (26). Van der Waals interactions were treated with the use of a switch function starting at 10 Å and turning off at 12 Å, which is the default of the all-atom CHARMM force field. The temperature was kept constant at 300 K by the Langevin temperature control with a damping coefficient of 5 ps^{-1}, while the pressure was held constant at 1 atm by applying a pressure piston. Before the production runs, water molecules and ions were subjected to energy minimization for 6000 steps, and a 1-ns equilibration with harmonic constraints applied to the positions of the C-alpha atoms. The covalent bonds involving hydrogen atoms were constrained by means of the SHAKE algorithm, and the dynamics were integrated with a time step of 2 fs. Snapshots were saved every 2 ps for trajectory analysis. Two MD runs with different initial distribution of velocities were carried out for each of the H4 peptides AKRH and AKRHRKIL for a total simulation time of 150 ns for each peptide. Analysis of the trajectories was carried out with the programs CHARMM (27) and WORDOM (28).

Results

PARP1 modifies core histones

Recently, we reported the ADP-ribosylation of distinct lysine residues of PARP1 and PARP2 *in cis* (19,20). Since core histones were described earlier to be modified by PARP1 *in vitro* and *in vivo* ((16) and Suppl.Fig.1A,B), we set out to investigate which residues of H2A, H2B, H3 and H4 would be modified by PARP1, and possibly also by PARP2 *in trans.* First, human PARP1 and PARP2 were expressed and purified from insect cells using the baculovirus-system and were subsequently incubated with full-length histones isolated from calf thymus together with 100 nM radiolabeled NAD^+. Although automodification of both PARP1 and PARP2 was easily detectable, only PARP1 displayed detectable trans-ADP-ribosylation of all four core histones, indicating a clear difference in the substrate specificity between PARP1 and PARP2 (Fig. 1A). Similar experiments with bacterially expressed and purified single histone proteins revealed that, indeed, all four histones are modified by PARP1 (Fig. 1B).

PARP1 mono- and poly(ADP-ribosyl)ates amino-terminal tails of core histone proteins covalently

Earlier reports suggested that histones are mainly ADP-ribosylated at their amino-terminal tails (13,29). To test whether PARP1-mediated ADP-ribosylation occurred at the amino-terminal tails or at the globular histone folds, we incubated the globular domains of histones H2B, H3 and H4 together with PARP1 and compared their ADP-ribosylation to the full-length counterpart (Suppl.Fig. 2A). ADP-ribosylation of the globular domains was reduced in comparison to full-length histones, implying that indeed the amino-terminal tails are required for modification by PARP1. We then expressed the different histone tails as GST fusion proteins in bacteria and incubated them with purified PARP1 and radiolabeled NAD^+. PARP1 was able to modify all four histone tails, whereas comparable PARP2-mediated ADP-ribosylation of histone tails was not detectable (Fig. 1C and Suppl.Fig. 2B). This finding suggests that the core histone tails are substrates specifically for PARP1 but not for PARP2 *in vitro*. Previous reports indicated that histones can interact with poly(ADP-ribose) non-covalently via a PAR-binding motif (30). Since the tested histone tails we analyzed did not contain this motif, it is highly unlikely that the observed labeling represented non-covalently attached PAR. To exclude this notion experimentally, the histone tail fusion proteins were added to the ADP-ribosylation reaction either together with

PARP1 or after the enzymatic reaction had been stopped by addition of the PARP-inhibitor 3-aminobenzamide (3AB). The addition of the histone tails after the reaction did not result in their modification (Fig. 1D, right panel), implying that the observed ADP-ribosylation is a covalent modification. To test whether the observed modification is an enzymatic reaction, the reaction was repeated in presence of the PARP-inhibitor PJ34. Increasing amounts of PJ34 abolished trans-ADP-ribosylation of the H2B tail, as well as automodification of PARP1 (Fig. 1E). Similar results were obtained with a second PARP-inhibitor, DAM-TIQ-A (Fig. 1E). Taken together these results indicate that PARP1 catalyze the covalent ADP-ribosylation of histone tails.

PARP1 is a mono- and a poly(ADP-ribosyl) transferase (16). To determine whether the histone tails can be mono and/or poly(ADP-ribosyl)ated by PARP1, we incubated the histone tails with PARP1 in the presence of increasing amounts of NAD^+. Poly(ADP-ribosyl)ation was determined by immunoblot analysis using an anti-PAR antibody, which recognizes only polymers of ADP-ribose (PAR). Both automodification of PARP1 and poly(ADP-ribosyl)ation of the histones were detected, indicating that PARP1 can attach long polymers of ADP-ribose onto histone tails (Fig. 1F). Notably, the length of poly(ADP-ribose) chains of the histones increased proportionally to the amounts of NAD^+, which led to retarded migration of the modified proteins due to an increased molecular weight (Fig. 1F, filled asterisk). ADP-ribosylation was earlier described to occur on glutamates of H2B and H1 (11,15). These findings were never directly attributed to PARP1 nor were they experimentally confirmed by mass spectrometry or amino acid substitutions. The PARP1-mediated ADP-ribosylation we describe here occurred on the basic amino-terminal histone tails, most of which do not contain glutamates (Fig. 2A). One exception is the tail of histone H2B that contains one single glutamate. Mutation of this residue to alanine did not affect the levels of incorporated ADP-ribose onto the H2B tail by PARP1 (Suppl.Fig. 2C), suggesting that glutamates are dispensable and that additional residues can be efficiently ADP-ribosylated by PARP1 *in trans*. Furthermore, when we incubated poly-L-lysine or poly-L-glutamate with purified PARP1 and measured incorporated ADP-ribose, lysines but not glutamates were modified by PARP1 (Suppl.Fig. 2D). These findings are consistent with our previous reports (19,20) and provided additional evidences that lysines are likely the primary target sites for PARP1-mediated ADP-ribosylation.

Identification of ADP-ribose acceptor sites within histone tails

As the amino-terminal histone tails are frequently targeted by a variety of post-translational modifications with important physiological functions (6), we aimed at identifying the exact sites of PARP1-mediated ADP-ribosylation. To this end, we first generated a series of histone tail deletion mutants to test in ADP-ribosylation assays (Fig. 2A). Successive shortening of the histone tails invariably resulted in a loss of PARP1-mediated ADP-ribosylation and defined for each histone the region comprising putative ADP-ribose acceptor sites (Fig. 2B-E).

To directly identify the ADP-ribosylated amino acids within the histone tails by mass spectrometry, we used synthetic peptides covering the regions identified by our deletion strategy. We incubated these peptides with PARP1 in the presence of 100-500 μM NAD^+, stopped the reactions by addition of 3AB and subsequently treated the poly(ADP-ribosyl)ated peptides with ADP-ribosylhydrolase 3 (ARH3). ARH3 is known to possess PARG-like ADP-ribose glycohydrolase activity, which hydrolyzes ester linkages between ADP-ribose units (31). Since no negatively charged amino acids (E or D), which would allow the formation of an ester linkage, were present in the polypeptides (except for H2B E35), we rationalized that treatment of the modified polypeptides with ARH3 would leave the first ADP-ribose unit bound to the peptide. The ADP-ribosylated peptides were acetone precipitated and analyzed by liquid-chromatography coupled mass-spectrometry. In the presence of PARP1 and NAD^+, the attachment of a single ADP-ribose unit resulted in a mass shift of 541 Dalton (Fig. 3A-D). Fragmentation of ADP-ribosylated peptides with conventional CID (collision induced dissociation) fragmentation technique completely removed the ADP-ribose moiety from the peptides, not allowing the identification of specific amino acid acceptor sites (data not shown). In contrast, analysis of the modified peptides by ETD (electron transfer dissociation) resulted in an almost complete fragmentation of the multiple charged histone peptides, as indicated by the presence of c- and z- ions, which represent N- or C-terminal fragment ions, respectively (Fig. 3A-D, Suppl.Fig. 2E). Fragmentation of the mono(ADP-ribosyl)ated H2A peptide revealed specific ADP-ribosylation of K13, while H2B was mainly ADP-ribosylated at K30 (Fig. 3A,B). H3 was ADP-ribosylated at K27 and K37 (Fig. 3C and Suppl.Fig. 2E). For H4, mass spectrometric analysis identified K16 to be ADP-ribosylated by

PARP1 (Fig. 3D). Control reactions performed in the presence of 500 μM NAD^+ but without PARP1 or in the presence of 500 μM ADP-ribose and PARP1 did not result in specific ADP-ribosylation (data not shown). The identified sites of PARP1-mediated enzymatic ADP-ribosylation represent two known sites of frequent histone modification (H3K27 and H4K16) as well as novel modification sites (H2AK13, H2BK30 and H3K37). To verify the mass spectrometric data for one histone, the H4 tail was mutated at K16 to alanine and tested for ADP-ribosylation by PARP1. The mutated H4 tail showed severely reduced ADP-ribosylation in comparison to the wild-type H4 tail (Fig. 3E, filled asterisk). The reduction of ADP-ribosylation was not due to a reduced interaction of PARP1 with the mutated H4 tail, since wild-type and mutated histone tail fusion proteins were able to interact with PARP1 to comparable levels (Fig. 3F).

Modeling of the histone H4 tail reveals that R17 is critical for the interaction with the catalytic domain of PARP1

In order to test computationally, whether the tail of H4 could enter the catalytic cleft of PARP1, automatic docking followed by explicit solvent molecular dynamics (MD) simulations were performed with the crystal structure from chicken PARP1 (PDB ID: 1A26), which uses the sequence numbering of human PARP1 (see Methods). The MD simulations indicate that the H4 tetrapeptide segment AKRH (aa 15-18) binds in an extended conformation to the catalytic domain of PARP1 (Fig. 4A,B). Two stable salt bridges are observed in all MD runs: between H4K16 and PARP1 Glu988 in the catalytic cleft, and between H4R17 and PARP1 Glu756 (Asp756 in human PARP1) on a loop at the entrance of the cleft. These intermolecular salt bridges lock H4 into the catalytic domain of PARP1 like two stretched arms holding two points far away from each other. In all MD runs, a single water molecule inserts between the amino group of K16 and the carboxy group of Glu988 in the first 15 ns and remains between these two charged groups until the end of the MD simulations of the tetrapeptide (Suppl.Fig. 3). This water molecule occupies the same position as the water molecule that is close to Glu988 in the X-ray structure of PARP1 (water 37 in PDB code 1A26). There are two additional side chains interactions: a stacking interaction between the imidazole of H18 and the amide group of Gln759 is almost always present in all MD runs, while the hydrogen bond between the side chains of R19 and

Asn906 is not very stable. In contrast to the aforementioned intermolecular salt bridges and hydrogen bonds, the K20 side chain is always exposed to solvent and very flexible. Furthermore, the backbone polar groups of the histone do not seem to be involved in hydrogen bonds with PARP1. Importantly, in all MD simulations both the N-terminal and C-terminal methyl groups point towards the solvent, which would allow the rest of the H4 polypeptide chain to position itself close to the surface of PARP1 without steric clashes. Moreover, the MD runs with the H4 tetra- and octapeptide (aa 15-22) converge towards a common extended structure of the AKRH segment with the same side chain interactions. The convergence of multiple MD simulations and the agreement with the experimental results indicate that the binding mode obtained by docking and explicit water MD is reliable. To gain insight in the putative initiation step of ADP-ribosylation, the 10 ns snapshot of the MD simulation with the H4 tetrapeptide was used for docking NAD^+ into the donor site as previously published (32,33). Before docking, the nicotinamide was manually removed (Fig. 4C), which mimics the NADase activity of PARP1 and creates a reactive C1-atom of the ADP-ribose that is suggested to react with the substrate amino acid (19,34,35). Interestingly, the C1-atom of the ADP-ribose is only 3.7 Å away from the ε-amino group of H4K16 and 7.8 Å from the ε-amino group of Lys903. Moreover, the distance between the catalytic active Glu988 carboxy group and the ε-amino group of H4K16 is only 3.0 Å, which would potentially allow covalent ADP-ribosylation of H4K16 (Fig. 4C).

To test experimentally whether an arginine close to H4K16 is required for the interaction with PARP1, we mutated R17 (H4R17A) and analyzed the association with and the modification by PARP1. GST-pulldown experiments with recombinant PARP1 revealed that the interaction between PARP1 and the mutated H4 tail fusion protein was reduced (Fig. 4D), as well as its ADP-ribosylation by PARP1 (Fig. 4E). In agreement with the MD simulation and the mass spectrometry data, an H4K16A/R17A double mutant was completely defective for PARP1-mediated ADP-ribosylation (Fig. 4F). Since H4R17 was suggested by molecular modeling to interact with Asp756 of PARP1, we mutated Asp756 into a lysine (which is the corresponding amino acid at this position in PARP2) and tested this mutant for its ADP-ribosylation properties. The PARP1 mutant exhibited no defect in auto(ADP-ribosyl)ation (Suppl. Fig. 2F), indicating that Asp756 is not essential for automodification. This is

consistent with the fact that also PARP2 is able to modify itself, although it contains a lysine at the corresponding position. Interestingly, however, the PARP1 mutant was impaired in trans-ADP-ribosylation of full-length histones (Fig. 4G) and in the labeling of the H4 (1-22) peptide (Supp. Fig. 1G), confirming the importance of this residue for stabilization of the peptide in the catalytic cleft and subsequent trans(ADP-ribosyl)ation of H4.

Acetylation of K16 inhibits ADP-ribosylation of histone H4

Acetylation of H4K16 occurs frequently in eukaryotic cells and has been correlated with chromatin decompaction (6). If H4K16 was indeed an acceptor site for PARP1-mediated ADP-ribosylation, acetylation at that site should impair ADP-ribosylation. In order to test this hypothesis, we employed a H4 peptide (aa 1-22) chemically acetylated at K16. LC-coupled mass spectrometry of the H4K16ac peptide revealed that PARP1 was not any longer able to induce ADP-ribosylation of the acetylated peptide above background (Fig. 5A). Consistent with this result, PARP1 mediated ADP-ribosylation of both peptides (unmodified and acetylated) with radiolabeled NAD^+, followed by purification over a microvolume-C18 reversed phase column and subsequent measurement of incorporated radiolabeled NAD^+, provided evidence that ADP-ribosylation of the acetylated peptide was severely reduced (Fig. 5B). These results confirm that H4K16 is modified by PARP1 and show that acetylation of K16 severely impairs ADP-ribosylation of the H4 peptide. Together, our results led to the identification of ADP-ribose acceptor sites within the amino-terminal tails of the four core histones (Fig. 5C) and imply important cross-talks with other histone modifications such as acetylation or methylation.

Discussion

Here, we provide evidence that PARP1 covalently modifies the tails of all four core histones. We identified H2AK13, H2BK30, H3K27, H3K37, and H4K16 as specific target sites for PARP1-mediated ADP-ribosylation. Our conclusions are based on several observations: (i) mass spectrometric analyses of PARP1-mediated ADP-ribosylated peptides, (ii) loss of function experiments by site directed mutagenesis of the putative acceptor sites in recombinant histone tail fusion proteins, (iii) cross-talk of acetylation and ADP-ribosylation at the identified acceptor site in H4 and, finally, (iv) prediction of the interaction between the histone H4 tail and PARP1 by molecular dynamics and subsequent confirmation with mutated proteins.

Nearly 20 years ago, ADP-ribose acceptor sites were found in histones by biochemical approaches. Several laboratories identified glutamic acid residues in histone H1 and histone H2B to be modified when they incubated chromatin from rat liver with radioactive NAD^+ (11,13-15). At that time, no other PARP family member had been identified yet, and no knockout- or knockdown-system was available. Thus, it is possible that PARP1, other PARP-family members or even unrelated NAD^+ consuming enzymes were responsible for the modification at the identified glutamates. In fact, we could show here by mutational analyses, that E2 of H2B is dispensable for PARP1-mediated ADP-ribosylation and that additional amino acid residues are acceptors for ADP-ribose moieties. Consistent with this, we identify lysines in the amino terminal histone tails and in particular lysine 13 of H2A, lysine 30 of H2B, lysines 27 and 37 of histone H3, as well as lysine 16 of histone H4 as target sites for enzymatic ADP-ribosylation by PARP1, both by mass spectrometry and amino acid substitution. Therefore, we propose the ADP-ribosylation of the ε-amino group of lysines by PARP1 as a new canonical histone tail modification.

Remarkably, explicit solvent water MD revealed that the tetra- and octapeptides of H4 interact strongly with specific amino acid side chains of the catalytic cleft of PARP1, suggesting that specific binding of a relatively short segment of H4 is sufficient to allow poly(ADP-ribosyl)ation of the histone tail. The positively charged amino acid at the +1 position of the ADP-ribosylated residue formed a salt bridge with Glu756 of chicken PARP1, which corresponds to Asp756 in human PARP1. In contrast, the corresponding amino acid in PARP2 is a lysine at position 312. Although the catalytic domains between PARP1 and PARP2 are highly similar (18), the substrate specificity of those enzymes might be regulated by subtle

differences in the catalytic cleft. This could explain why PARP2 does not modify histones to a detectable extent at least *in vitro* (Fig. 1A, C and Suppl.Fig. 2B).

Application of novel mass spectrometry techniques allowed us to identify distinct amino acids as acceptors of ADP-ribose. We took advantage of the electron transfer dissociation technique (36), which allows the fragmentation of highly charged peptides, leaving most post-translational modifications intact. Recent publications describe the technical basis for the fragmentation of chemically ADP-ribosylated peptides by electron capture dissociation (ECD) (37) and the closely related electron transfer dissociation (ETD) (38). It is noteworthy, that, in contrast to other reports, we observed partial fragmentation of the ADP-ribose at the phosphodiester bond by application of ETD, as revealed by the presence of a (m/z 348) ion. However, conventional collision induced dissociation (CID) mass spectrometry of ADP-ribosylated H4 peptide did not reveal any ADP-ribose acceptor sites, since the ADP-ribose was cleaved off from the peptide during fragmentation. The commonly used CID, instead of ETD, might thus explain why numerous efforts to identify ADP-ribosylated residues failed in the past. Consequently, we would strongly recommend ETD as standard technique to detect ADP-ribosylated peptides. Of note, a previous study employing CID failed to detect ADP-ribosylated lysine residues in the catalytic PARP1 mutant E988Q (39). In summary, ETD can be expected to facilitate future investigations on ADP-ribosylated peptides, opening new opportunities to screen for ADP-ribosylated residues in a systems-biology setup.

Since poly(ADP-ribosyl)ated peptides cannot be detected by MS and PARP1 mainly attaches poly(ADP-ribose) to target proteins, we removed the poly(ADP-ribose) with ARH3, which degrades poly(ADP-ribose). However, this treatment was rather inefficient (data not shown), which could partly explain the observed low mono(ADP-ribosyl)ation of the histone peptides. Moreover, we cannot exclude that PARP1 modifies additional residues, which were not identified by these mass spectrometric analyses.

Our data provide strong evidence that PARP1-mediated ADP-ribosylation of histones occurs as post-translational modification at distinct lysine residues within the amino-terminal basic tails. From a chemical perspective, modification of a lysine residue by ADP-ribose results in an unstable Schiff base, which can undergo an Amadori rearrangement to form a stable ketoamine (19,40). It will be interesting to investigate whether histone lysine ADP-ribosylation can be reversed by a previously

identified but still poorly characterized ADP-ribosyl protein lyase (41). Since the attachment of ADP-ribose not only neutralizes the positive charge of the amino acid side chain, but instead reverses it into a negative charge, the functional consequences of lysine ADP-ribosylation can be assumed to be even more drastic than other modifications, such as acetylation. Therefore, the possible effects on chromatin architecture, histone dynamics, histone degradation, and histone variant incorporation may be dramatic. Possibly, ADP-ribosylation of histones interferes with other post-translational modifications of the histone tails. For example, H3K27 is methylated by EZH2 (enhancer of zeste homolog 2), which is in the polycomb group complex that is involved in maintenance of the inactive X-chromosome (42). Interestingly, PARP1 was demonstrated to participate in the maintenance of X-chromosome silencing as well (43). On the other hand, the amino-terminal tail of histone H4 was shown to be required for chromatin fiber formation, since the positively charged stretch between K16 and K20 makes internucleosomal contacts to two acidic patches on the carboxy-terminal α-helices of histone H2A (44). In addition to its function for chromatin topology, the stretch between K16 and K20 is required for the interaction with various non-histone modulators. For example, the ISWI-containing ATP dependent chromatin remodeler ACF solely engages histone H4, but is repelled, if H4K16 is acetylated (45,46). Furthermore, the chromatin remodeler Alc1 was shown to require the K16 to K20 stretch of H4 for its activity (47). Interestingly, recent reports provide evidence that the ATPase activity of Alc1 is highly stimulated by binding to poly(ADP-ribosyl)ated PARP1 (47,48). Whether ADP-ribosylated H4 would activate Alc1, remains to be investigated. Another intriguing possibility of how histone tail ADP-ribosylation could affect chromatin function is implied by a recent study showing that macrodomain-containing histone variants specifically bind to poly(ADP-ribose) generated after DNA damage (49). Using biochemical, crystallographic and state-of-the-art imaging techniques, it was shown that macroH2A1.1 senses PARP1 activation and directly binds poly(ADP-ribose) to cause a transient compaction of the chromatin. It will be interesting to investigate whether macrodomains preferentially bind to automodified PARP1 or also function as “readers” of poly(ADP-ribosyl)ated histone tails.

Taken together, the here presented work sheds new light on a well known but neglected histone modification and builds the basis for future investigations exploring the function of histone lysine ADP-ribosylation in chromatin dynamics, transcription,

DNA repair signaling and other nuclear processes influenced by histone modifications.

Funding

This work was supported in part by Swiss National Science Foundation Grant 31-122421 (to S.M. and M.A.) and the Kanton of Zurich (to M.O.H.).

Acknowledgements

We are grateful to Timothy Richmond (ETH Zurich, Switzerland) and Achim Leutz (Max-Delbrück-Centrum for Molecular Medicine, Berlin, Germany) for the generous provision of reagents and sequences. Brighton Samatanga (University of Zurich, Switzerland) is acknowledged for his technical support. We thank Raffaella Santoro (University of Zurich, Institute of Veterinary Biochemistry and Molecular Biology) for critical and constructive comments.

References

1. Kornberg, R.D. (1974) Chromatin structure: a repeating unit of histones and DNA. *Science*, 184, 868-871.
2. Davey, C.A., Sargent, D.F., Luger, K., Maeder, A.W. and Richmond, T.J. (2002) Solvent mediated interactions in the structure of the nucleosome core particle at 1.9 a resolution. *Journal of Molecular Biology*, 319, 1097-1113.
3. Luger, K., Mäder, A.W., Richmond, R.K., Sargent, D.F. and Richmond, T.J. (1997) Crystal structure of the nucleosome core particle at 2.8 A resolution. *Nature*, 389, 251-260.
4. Campos, E. and Reinberg, D. (2009) Histones: Annotating Chromatin. *Annu Rev Genet*.
5. Angelov, D., Vitolo, J.M., Mutskov, V., Dimitrov, S. and Hayes, J.J. (2001) Preferential interaction of the core histone tail domains with linker DNA. *Proc Natl Acad Sci USA*, 98, 6599-6604.
6. Kouzarides, T. (2007) Chromatin modifications and their function. *Cell*, 128, 693-705.
7. Ueda, K., Omachi, A., Kawaichi, M. and Hayaishi, O. (1975) Natural occurrence of poly(ADP-ribosyl) histones in rat liver. *Proc Natl Acad Sci USA*, 72, 205-209.
8. Otake, H., Miwa, M., Fujimura, S. and Sugimura, T. (1969) Binding of ADP-ribose polymer with histone. *J Biochem*, 65, 145-146.
9. Adamietz, P., Bredehorst, R. and Hilz, H. (1978) ADP-ribosylated histone H1 from HeLa cultures. Fundamental differences to (ADP-ribose)n-histone H1 conjugates formed into vitro. *Eur J Biochem*, 91, 317-326.
10. Minaga, T., Romaschin, A.D., Kirsten, E. and Kun, E. (1979) The in vivo distribution of immunoreactive larger than tetrameric polyadenosine diphosphoribose in histone and non-histone protein fractions of rat liver. *J Biol Chem*, 254, 9663-9668.
11. Ogata, N., Ueda, K. and Hayaishi, O. (1980) ADP-ribosylation of histone H2B. Identification of glutamic acid residue 2 as the modification site. *J Biol Chem*, 255, 7610-7615.
12. Boulikas, T. (1988) At least 60 ADP-ribosylated variant histones are present in nuclei from dimethylsulfate-treated and untreated cells. *The EMBO Journal*, 7, 57-67.
13. Burzio, L.O., Riquelme, P.T. and Koide, S.S. (1979) ADP ribosylation of rat liver nucleosomal core histones. *J Biol Chem*, 254, 3029-3037.
14. Riquelme, P.T., Burzio, L.O. and Koide, S.S. (1979) ADP ribosylation of rat liver lysine-rich histone in vitro. *J Biol Chem*, 254, 3018-3028.
15. Ogata, N., Ueda, K., Kagamiyama, H. and Hayaishi, O. (1980) ADP-ribosylation of histone H1. Identification of glutamic acid residues 2, 14, and the COOH-terminal lysine residue as modification sites. *J Biol Chem*, 255, 7616-7620.
16. Hassa, P.O., Haenni, S.S., Elser, M. and Hottiger, M.O. (2006) Nuclear ADP-ribosylation reactions in mammalian cells: where are we today and where are we going? *Microbiol Mol Biol Rev*, 70, 789-829.
17. Quénet, D., El Ramy, R., Schreiber, V. and Dantzer, F. (2009) The role of poly(ADP-ribosyl)ation in epigenetic events. *Int J Biochem Cell Biol*, 41, 60-65.
18. Amé, J.C., Rolli, V., Schreiber, V., Niedergang, C., Apiou, F., Decker, P., Muller, S., Höger, T., Ménissier-de Murcia, J. and de Murcia, G. (1999)

PARP-2, A novel mammalian DNA damage-dependent poly(ADP-ribose) polymerase. *J Biol Chem*, 274, 17860-17868.

19. Altmeyer, M., Messner, S., Hassa, P.O., Fey, M. and Hottiger, M.O. (2009) Molecular mechanism of poly(ADP-ribosyl)ation by PARP1 and identification of lysine residues as ADP-ribose acceptor sites. *Nucleic Acids Research*, 37, 3723-3738.
20. Haenni, S.S., Hassa, P.O., Altmeyer, M., Fey, M., Imhof, R. and Hottiger, M.O. (2008) Identification of lysines 36 and 37 of PARP-2 as targets for acetylation and auto-ADP-ribosylation. *Int J Biochem Cell Biol*, 40, 2274-2283.
21. Hassa, P.O., Haenni, S.S., Buerki, C., Meier, N.I., Lane, W.S., Owen, H., Gersbach, M., Imhof, R. and Hottiger, M.O. (2005) Acetylation of poly(ADP-ribose) polymerase-1 by p300/CREB-binding protein regulates coactivation of NF-kappaB-dependent transcription. *J Biol Chem*, 280, 40450-40464.
22. Hassa, P.O., Buerki, C., Lombardi, C., Imhof, R. and Hottiger, M.O. (2003) Transcriptional coactivation of nuclear factor-kappaB-dependent gene expression by p300 is regulated by poly(ADP)-ribose polymerase-1. *J Biol Chem*, 278, 45145-45153.
23. Kale, L., Skeel, R., Bhandarkar, M., Brunner, R., Gursoy, A., Krawetz, N., Phillips, J., Shinozaki, A., Vraradarajan, K. and Schulten, K. (1999) NAMD2: Greater Scalability for Parallel Molecular Dynamics. *Journal of Computational Physics*, 151, 283-312.
24. MacKerell, A.D., Bashford, D., Bellott, M., Dunbrack, R.L., Evanseck, J.D., Field, M.J., Fischer, S., Gao, J., Guo, H., Ha, S. *et al.* (1998) All-Atom Empirical Potential for Molecular Modeling and Dynamics Studies of Proteins. *J . Phys. Chem. B*, 102, 3586-3616.
25. Jorgensen, W.L., Chandrasekhar, J. and Madura, J.D. (1983) Comparison of simple potential functions for simulating liquid water. *J . Phys. Chem. B*, 79, 926-936.
26. Darden, T., York, D. and Pedersen, L. (1993) Particle mesh Ewald: An N.log(N) method for Ewald sums in large systems. *J. Chem. Phys.* , 98.
27. Brooks, B.R., Brooks, C.L., Mackerell, A.D., Nilsson, L., Petrella, R.J., Roux, B., Won, Y., Archontis, G., Bartels, C., Boresch, S. *et al.* (2009) CHARMM: the biomolecular simulation program. *J Comput Chem*, 30, 1545-1614.
28. Seeber, M., Cecchini, M., Rao, F., Settanni, G. and Caflisch, A. (2007) Wordom: a program for efficient analysis of molecular dynamics simulations. *Bioinformatics*, 23, 2625-2627.
29. Jump, D.B., Sudhakar, S., Tew, K.D. and Smulson, M. (1980) Probes to study the effect of methyl nitrosourea on ADP-ribosylation and chromatin structure at the subunit level. *Chem Biol Interact*, 30, 35-51.
30. Pleschke, J.M., Kleczkowska, H.E., Strohm, M. and Althaus, F.R. (2000) Poly(ADP-ribose) binds to specific domains in DNA damage checkpoint proteins. *J Biol Chem*, 275, 40974-40980.
31. Oka, S., Kato, J. and Moss, J. (2006) Identification and characterization of a mammalian 39-kDa poly(ADP-ribose) glycohydrolase. *J Biol Chem*, 281, 705-713.
32. Ruf, A., Rolli, V., de Murcia, G. and Schulz, G.E. (1998) The mechanism of the elongation and branching reaction of poly(ADP-ribose) polymerase as derived from crystal structures and mutagenesis. *J Mol Biol*, 278, 57-65.

33. Ruf, A., de Murcia, G. and Schulz, G.E. (1998) Inhibitor and NAD+ binding to poly(ADP-ribose) polymerase as derived from crystal structures and homology modeling. *Biochemistry*, 37, 3893-3900.
34. Alvarez-Gonzalez, R., Pacheco-Rodriguez, G. and Mendoza-Alvarez, H. (1994) Enzymology of ADP-ribose polymer synthesis. *Mol Cell Biochem*, 138, 33-37.
35. Bürkle, A. (2005) Poly(ADP-ribose). The most elaborate metabolite of NAD+. *FEBS J*, 272, 4576-4589.
36. Syka, J.E.P., Coon, J.J., Schroeder, M.J., Shabanowitz, J. and Hunt, D.F. (2004) Peptide and protein sequence analysis by electron transfer dissociation mass spectrometry. *Proc Natl Acad Sci USA*, 101, 9528-9533.
37. Hengel, S.M., Shaffer, S.A., Nunn, B.L. and Goodlett, D.R. (2009) Tandem mass spectrometry investigation of ADP-ribosylated kemptide. *J Am Soc Mass Spectrom*, 20, 477-483.
38. Zee, B.M. and Garcia, B.A. (2010) Electron transfer dissociation facilitates sequencing of adenosine diphosphate-ribosylated peptides. *Anal Chem*, 82, 28-31.
39. Tao, Z., Gao, P. and Liu, H. (2009) Identification of the ADP-Ribosylation Sites in the PARP-1 Automodification Domain: Analysis and Implications. *J Am Chem Soc*.
40. Cervantes-Laurean, D., Jacobson, E.L. and Jacobson, M.K. (1996) Glycation and glycoxidation of histones by ADP-ribose. *J Biol Chem*, 271, 10461-10469.
41. Oka, J., Ueda, K., Hayaishi, O., Komura, H. and Nakanishi, K. (1984) ADP-ribosyl protein lyase. Purification, properties, and identification of the product. *J Biol Chem*, 259, 986-995.
42. Heard, E. (2005) Delving into the diversity of facultative heterochromatin: the epigenetics of the inactive X chromosome. *Curr Opin Genet Dev*, 15, 482-489.
43. Nusinow, D.A., Hernández-Muñoz, I., Fazzio, T.G., Shah, G.M., Kraus, W.L. and Panning, B. (2007) Poly(ADP-ribose) polymerase 1 is inhibited by a histone H2A variant, MacroH2A, and contributes to silencing of the inactive X chromosome. *J Biol Chem*, 282, 12851-12859.
44. Zhou, J., Fan, J.Y., Rangasamy, D. and Tremethick, D.J. (2007) The nucleosome surface regulates chromatin compaction and couples it with transcriptional repression. *Nat Struct Mol Biol*, 14, 1070-1076.
45. Clapier, C.R., Längst, G., Corona, D.F., Becker, P.B. and Nightingale, K.P. (2001) Critical role for the histone H4 N terminus in nucleosome remodeling by ISWI. *Molecular and Cellular Biology*, 21, 875-883.
46. Shogren-Knaak, M., Ishii, H., Sun, J.-M., Pazin, M.J., Davie, J.R. and Peterson, C.L. (2006) Histone H4-K16 acetylation controls chromatin structure and protein interactions. *Science*, 311, 844-847.
47. Ahel, D., Horejsi, Z., Wiechens, N., Polo, S., Garcia-Wilson, E., Ahel, I., Flynn, H., Skehel, M., West, S., Jackson, S. *et al.* (2009) Poly(ADP-ribose)-Dependent Regulation of DNA Repair by the Chromatin Remodeling Enzyme ALC1. *Science*.
48. Gottschalk, A., Timinszky, G., Kong, S., Jin, J., Cai, Y., Swanson, S., Washburn, M., Florens, L., Ladurner, A., Conaway, J. *et al.* (2009) Poly(ADP-ribosyl)ation directs recruitment and activation of an ATP-dependent chromatin remodeler. *Proc Natl Acad Sci USA*.

49. Timinszky, G., Till, S., Hassa, P., Hothorn, M., Kustatscher, G., Nijmeijer, B., Colombelli, J., Altmeyer, M., Stelzer, E., Scheffzek, K. *et al.* (2009) A macrodomain-containing histone rearranges chromatin upon sensing PARP1 activation. *Nat Struct Mol Biol*.

Figure Legends

Figure 1: PARP1 covalently modifies all four core histone tails

(A) PARP1 trans-ADP-ribosylates histones isolated from calf thymus. 10 pmol recombinant PARP1 or PARP2 were incubated for 15 min (PARP1) or 30 min (PARP2) at 30°C with 5 pmol EcoRI-linker DNA, 100 nM radiolabeled NAD^+ and 20 μg extracted histones from calf thymus. The reaction was stopped by addition of SDS-lysis buffer and the proteins were resolved on a 10-20% SDS-PAGE gradient gel. The gel was stained with Coomassie-R250 and incorporated ^{32}P was visualized by autoradiography. (B) Recombinant expressed and purified histones (3 μg) were ADP-ribosylated by PARP1 as in Figure 1A. (C) 1.5 μg of each purified GST-histone tail were used in PARP1 or PARP2 mediated trans-ADP-ribosylation reactions for 5 minutes at 30°C. (D) 1.5 μg of each purified GST-histone tail were used in PARP1 mediated trans-ADP-ribosylation reactions for 5 minutes at 30°C. Histone tails were either included during the reaction (pre) or added after the reaction had been stopped with a 100-fold excess of 3-aminobenzamide over radiolabeled NAD^+ (post) to exclude non-covalent interaction of the histone tails with PAR. (E) Trans-ADP-ribosylation of the H2B tail is inhibited by the PARP-inhibitors PJ34 (0.01 μM-100 μM) and DAM-TIQ-A (10 μM). (F) GST-histones were incubated with PARP1, EcoRI linker and increasing concentrations of NAD^+ (0, 10, 100, 400 μM) for 10 min at 30°C. Poly(ADP-ribose) formation was assessed through western blotting with anti-PAR (LP-96-10) antibody. Unmodified GST-histone tails are marked by an empty asterisk, PARylated GST-histone tails are marked by a filled asterisk.

Figure 2: Confining the regions of putative ADP-ribose acceptor sites

(A) Schematic representation of the deletion strategy for GST-histone tails to identify the minimal ADP-ribosylated domain. (B-E) Trans-ADP-ribosylation of the indicated GST-histone deletion mutants by PARP1 with 100 nM ^{32}P-NAD^+.

Figure 3: Mass spectrometric analysis of ADP-ribosylated histone peptides

(A) Extracted ion chromatogram of the biotin tagged H2A (aa 3-23) peptide incubated with 500 μM NAD^+ and PARP1. The precursor masses of unmodified H2A peptide (2395.34 Da) and ADP-ribosylated H2A peptide (2936.40 Da) were plotted in a range of 10 ppm over time. ETD fragment spectrum of quintuple charged precursor mass of

ADP-ribosylated H2A peptide (638.51 m/z) at K13, as indicated by the sequence plot. The spectrum shows next to the 2 major peaks of unfragmented charge reduced precursor masses $(M+5H)^{n+}$ an almost complete series of N-terminal and C-terminal fragment ions (c-ions, z-ions, respectively). (B) Extracted ion chromatogram of the biotin tagged H2B (aa 18-37) peptide incubated with 500 μM NAD^+ and PARP1 as in (A). ETD fragment spectrum of ADP-ribosylated H2B peptide (797.89 m/z) at K30, indicated by the sequence plot. (C) Extracted ion chromatogram of the biotin tagged H3 (aa 23-42) peptide incubated with PARP1 as in (A). ETD fragment spectrum of ADP-ribosylated H3 peptide (590.29 m/z) at K27, indicated by the sequence plot. (D) Extracted ion chromatogram of the biotin tagged H4 (aa 1-22) peptide incubated with 100 μM NAD^+ and PARP1. ETD fragment spectrum of ADP-ribosylated H4 peptide (621.30 m/z) at K16, as indicated by the sequence plot. (E) Trans-ADP-ribosylation of the GST-H4 histone tail wild-type or K16A mutant by PARP1. (F) GST-pulldown of wild-type and mutated GST-histone H4 tails with recombinant PARP1. The GST-histone tails are marked by an asterisk.

Figure 4: Histone H4 interacts with PARP1 by salt bridges with acidic residues in the catalytic domain

(A) Representative snapshot of the binding mode saved after 10 nanoseconds (ns) MD simulation of the H4 tetrapeptide AKRH. (B) Enlarged view of the catalytic cleft for the same snapshot as in (A). Amino acids in close proximity of the H4 peptide are highlighted. PARP1 and the H4 tetrapeptide are shown in surface render and sticks, respectively. The surface is colored according to atomic elements with carbon, oxygen and nitrogen in green, red, and blue, respectively. Carbon atoms of the H4 tetrapeptide are in cyan. (C) ADP-ribose was docked into the donor-site of PARP1 catalytic domain after 10 ns MD simulation of the H4 tetrapeptide. Amino acids in close proximity of the H4 peptide are highlighted. The orientation is rotated by about 180°C with respect to (A,B). (D,) GST-pulldown of wild-type and mutated GST-histone H4 tail with recombinant PARP1 and subsequent western blot with anti-PARP1 antibody. GST-histone tails are indicated by an asterisk. (E,F) Trans-ADP-ribosylation of wild-type and mutated GST-H4 tails with PARP1 and radiolabeled NAD^+. Coomassie stains of the input and autoradiographies are shown. (G) Trans-

ADP-ribosylation of calf-thymus extracted histones by PARP1 wild-type or PARP1 D756K mutant as in Fig. 1A.

Figure 5: ADP-ribosylation of the H4 peptide is impaired by H4K16 acetylation
(A) Elution profile of biotinylated H4 peptide (aa 1-22) and biotinylated H4K16ac peptide (aa 1-22) incubated with 100 μM NAD^+ for 15 min without PARP1 (- PARP1) or in the presence of PARP1 (+ PARP1) and subsequent ARH3 treatment. Acetone precipitated peptides were run on a LC-MS/MS with a C18-reversed phase column and subsequent detection by mass-spectrometry. (B) Histone H4 (aa 1-22) and acetylated H4K16ac (1-22) peptides were ADP-ribosylated with PARP1 for 15 min at 30°C with 100 nM ^{32}P-NAD^+. The peptides were purified by microvolume-C18 reversed phase columns, eluted into scintillation liquid and counted for incorporated ^{32}P. Relative increase of counts per minutes was calculated over background (peptides added after termination of the reaction by 3AB). (C) Overview of the identified ADP-ribose acceptor sites within the amino-terminal core histone tails.

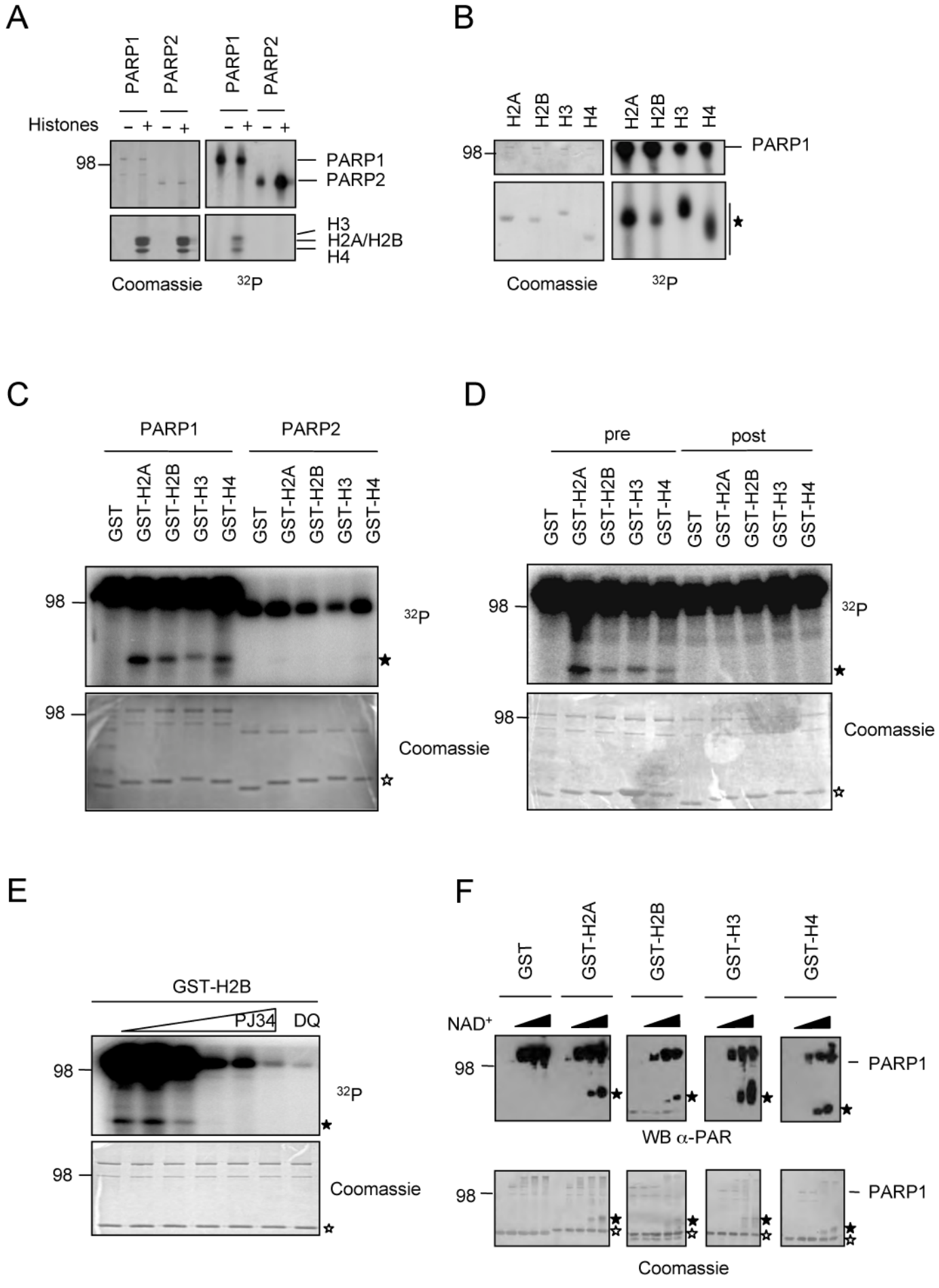
A
PARP1
PARP2
PARP1
PARP2
Histones
- + - + - + - +
98
PARP1
PARP2
H3
H2A/H2B
H4
Coomassie
32P
B
H2A
H2B
H3
H4
H2A
H2B
H3
H4
98
PARP1
Coomassie
32P
C
PARP1
PARP2
GST
GST-H2A
GST-H2B
GST-H3
GST-H4
GST
GST-H2A
GST-H2B
GST-H3
GST-H4
98
32P
98
Coomassie
D
pre
post
GST
GST-H2A
GST-H2B
GST-H3
GST-H4
GST
GST-H2A
GST-H2B
GST-H3
GST-H4
98
32P
98
Coomassie
E
GST-H2B
PJ34
DQ
98
32P
98
Coomassie
F
GST
GST-H2A
GST-H2B
GST-H3
GST-H4
NAD+
98
PARP1
WB α-PAR
98
PARP1
Coomassie

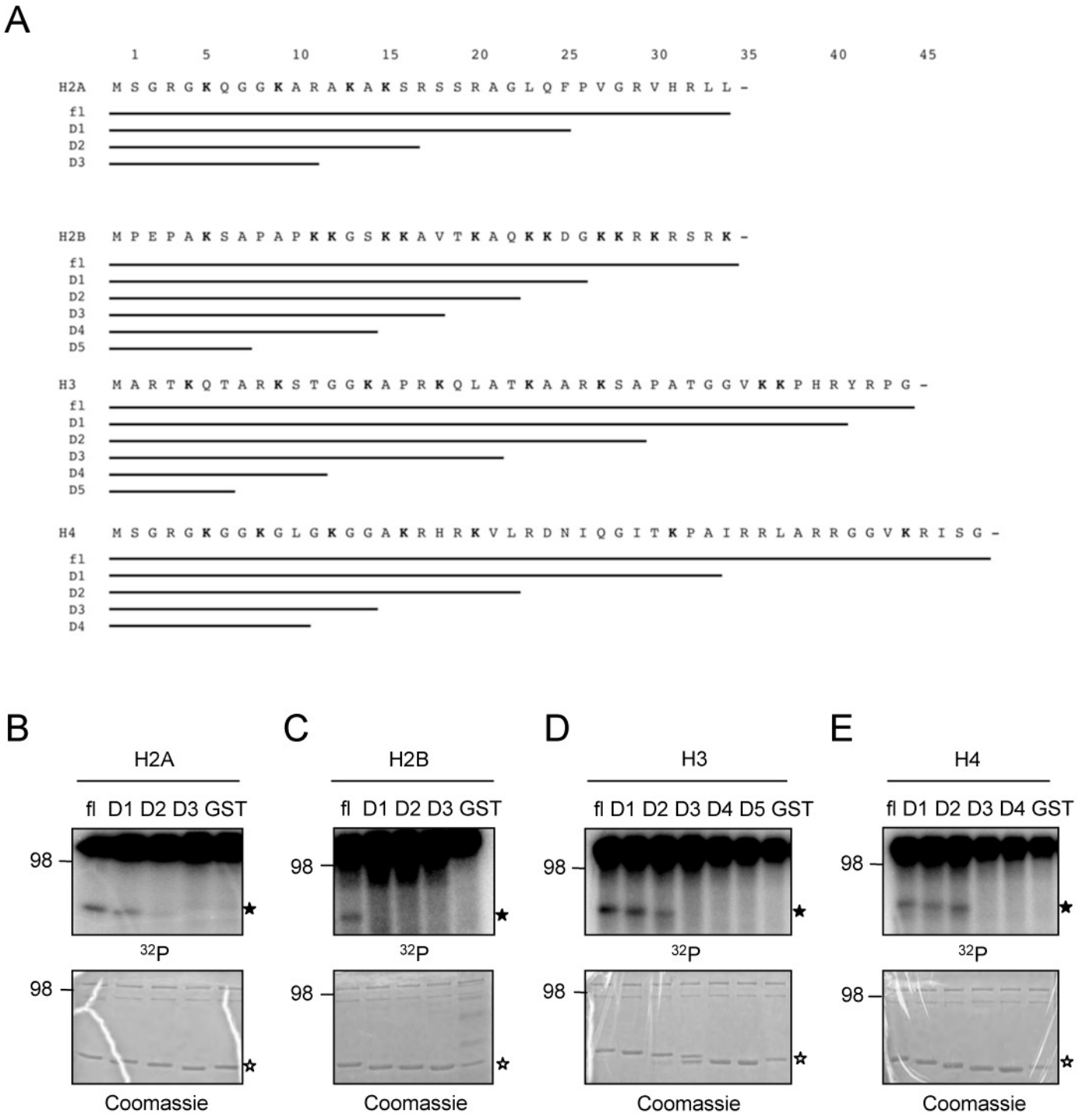
A
1 5 10 15 20 25 30 35 40 45
H2A M S G R G K Q G G K A R A K A K S R S S R A G L Q F P V G R V H R L L –
f1
D1
D2
D3
H2B M P E P A K S A P A P K K G S K K A V T K A Q K K D G K K R K R S R K –
f1
D1
D2
D3
D4
D5
H3 M A R T K Q T A R K S T G G K A P R K Q L A T K A A R K S A P A T G G V K K P H R Y R P G –
f1
D1
D2
D3
D4
D5
H4 M S G R G K G G K G L G K G G A K R H R K V L R D N I Q G I T K P A I R R L A R R G G V K R I S G –
f1
D1
D2
D3
D4
B
H2A
fl D1 D2 D3 GST
98
32P
98
Coomassie
C
H2B
fl D1 D2 D3 GST
98
32P
98
Coomassie
D
H3
fl D1 D2 D3 D4 D5 GST
98
32P
98
Coomassie
E
H4
fl D1 D2 D3 D4 GST
98
32P
98
Coomassie

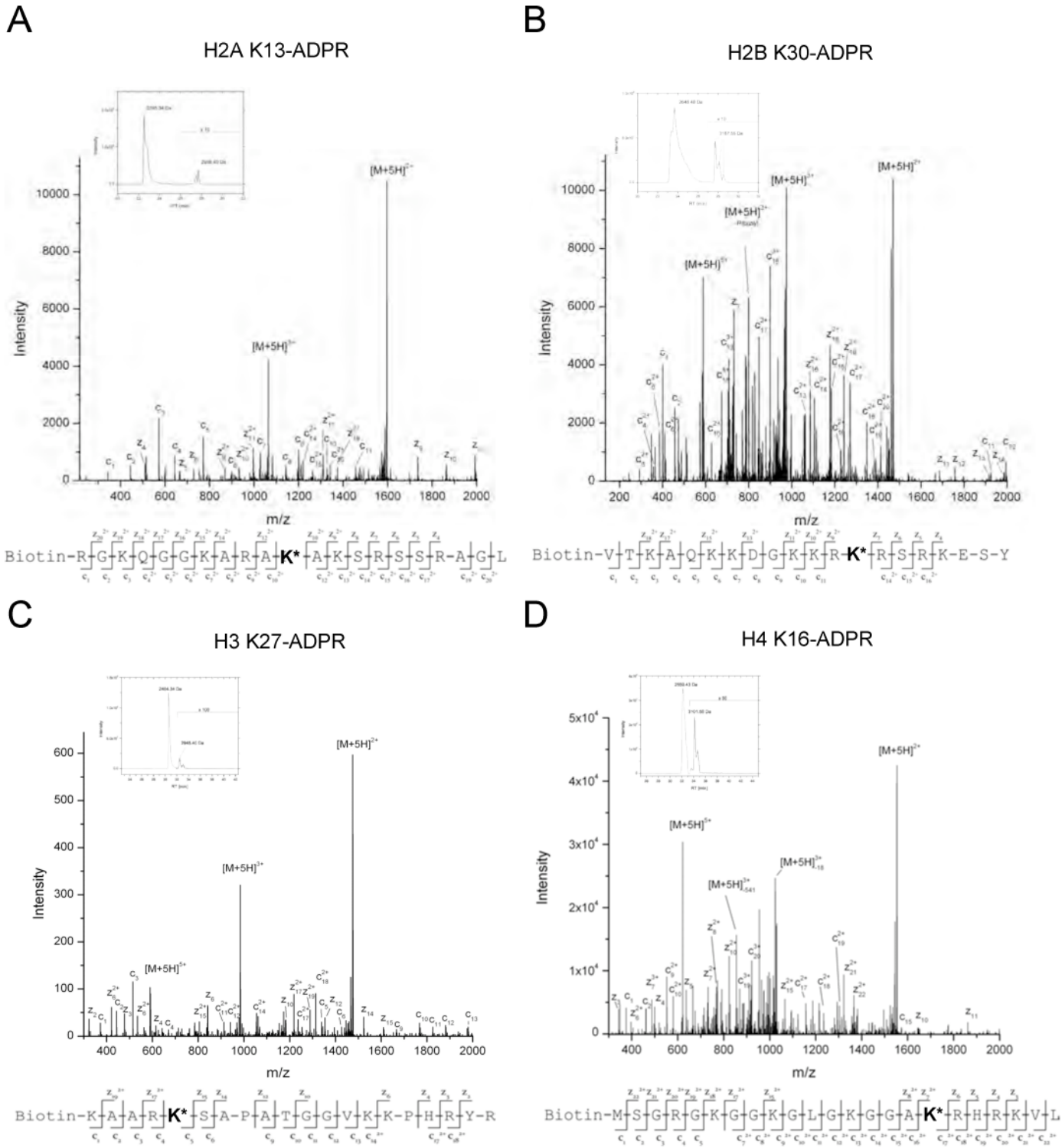
A
H2A K13-ADPR
Intensity
m/z
[M+5H]2+
[M+5H]3+
Biotin-R-G-K-Q-G-G-K-A-R-A-K*-A-K-S-R-S-S-R-A-G-L
B
H2B K30-ADPR
Intensity
m/z
[M+5H]2+
[M+5H]3+
[M+5H]4+
Biotin-V-T-K-A-Q-K-K-D-G-K-K-R-K*-R-S-R-K-E-S-Y
C
H3 K27-ADPR
Intensity
m/z
[M+5H]2+
[M+5H]3+
[M+5H]4+
Biotin-K-A-A-R-K*-S-A-P-A-T-G-G-V-K-K-P-H-R-Y-R
D
H4 K16-ADPR
Intensity
m/z
[M+5H]2+
[M+5H]3+
Biotin-M-S-G-R-G-K-G-G-K-G-L-G-K-G-G-A-K*-R-H-R-K-V-L
E
H4 D2 wt
H4 D2 K16A
H4 D2 wt
H4 D2 K16A
98
PARP1
Coomassie
32P
F
GST
H4 D2 wt
H4 D2 K16A
GST
H4 D2 wt
H4 D2 K16A
98
PARP1
Coomassie
WB α-PARP1

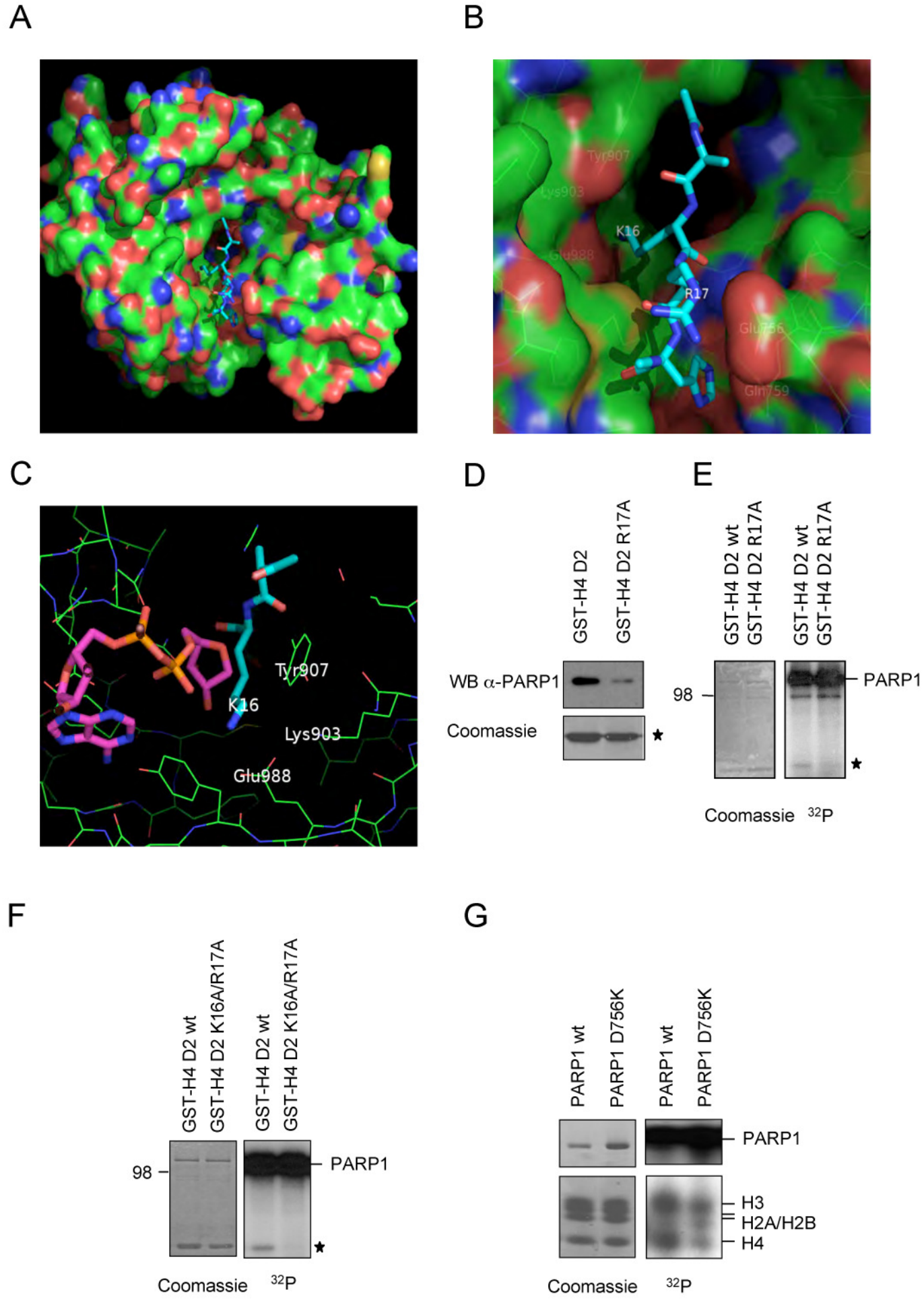
A
B
Tyr907
Lys903
K16
Glu988
R17
Glu756
Gln759
C
Tyr907
K16
Lys903
Glu988
D
GST-H4 D2
GST-H4 D2 R17A
WB α-PARP1
Coomassie
E
GST-H4 D2 wt
GST-H4 D2 R17A
GST-H4 D2 wt
GST-H4 D2 R17A
98
PARP1
Coomassie 32P
F
GST-H4 D2 wt
GST-H4 D2 K16A/R17A
GST-H4 D2 wt
GST-H4 D2 K16A/R17A
98
PARP1
Coomassie 32P
G
PARP1 wt
PARP1 D756K
PARP1 wt
PARP1 D756K
PARP1
H3
H2A/H2B
H4
Coomassie 32P

A

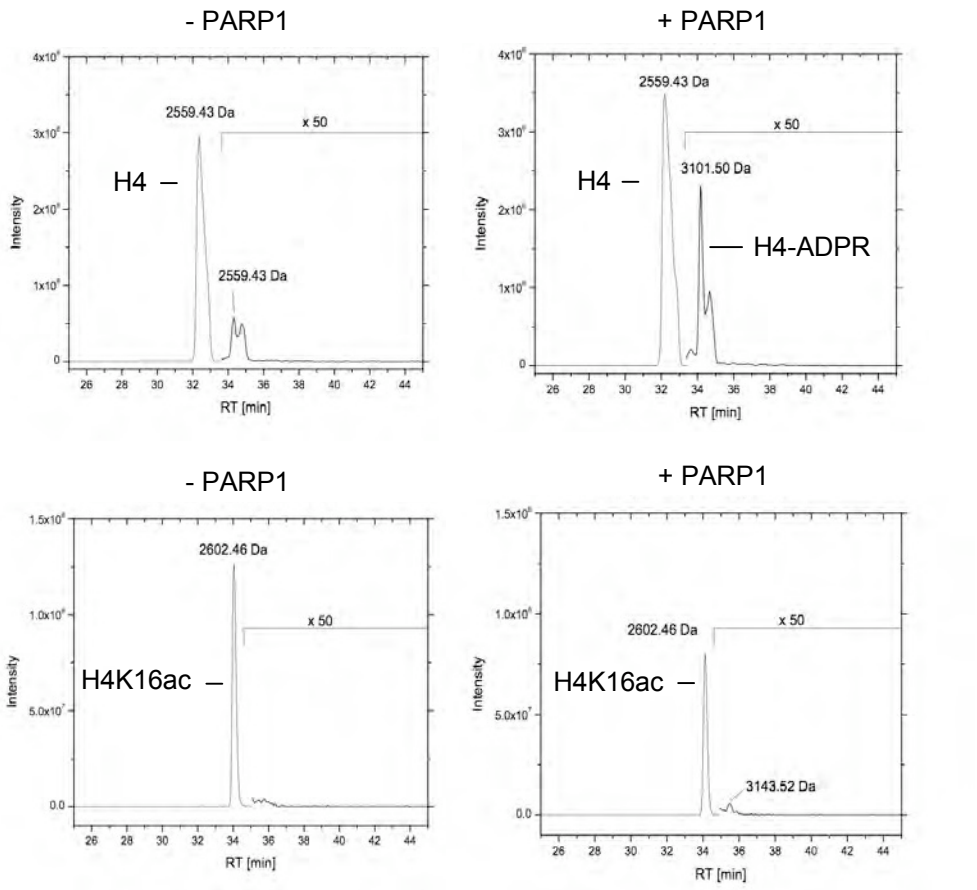
- PARP1
+ PARP1
2559.43 Da
x 50
H4 –
3101.50 Da
H4-ADPR
Intensity
RT [min]
- PARP1
+ PARP1
2602.46 Da
x 50
H4K16ac –
3143.52 Da
Intensity
RT [min]

B

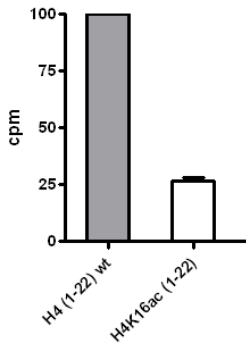
cpm
100
75
50
25
0
H4 (1-22) wt
H4K16ac (1-22)

C

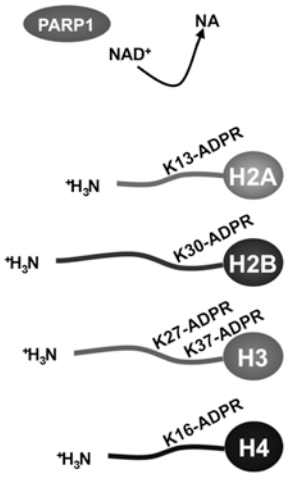
PARP1
NA
NAD+
K13-ADPR
H2A
K30-ADPR
H2B
K27-ADPR
K37-ADPR
H3
K16-ADPR
H4

Supplementary Methods

Cell culture, transfection of siRNA and overexpression of PARP1

HEK293T cells were grown in DMEM Glutamax-1 (Invitrogen), supplemented with 10% (v/v) fetal calf serum (Invitrogen) and 50 units/ml penicillin and 50 μg/ml streptomycin (Sigma). Cells were grown in 5% CO_2 and 37°C in a humidified incubator. HEK293T cells were transfected with RNAi-max (Invitrogen) and siRNA directed against PARP1 (Qiagen, Cat.No. S102662989) or control siRNA (Qiagen, Cat.No. S103650318) for 48 hours. Overexpression of PARP1 was performed by transfection of HEK293T cells by standard Calcium-Phosphate precipitation method with a pcDNA3-HA-PARP1 expression vector or an empty vector control, respectively. 8 hours after transfection the medium was replaced and the cells were grown for another 20 hours before they were harvested.

ADP-ribosylation of isolated nuclei

Nuclei were isolated from 5x 10^6 HEK293T cells by the addition of cold hypotonic lysis buffer (5 mM HEPES pH 7.4, 0.5% NP-40, 85 mM KCl, 1 μg/ul Pepstatin, Leupetin, Bestatin). After 2 minutes of incubation, the nuclei were centrifuged for 4 min at 7000g and washed twice with suspension buffer (33.3 mM Tris-HCl pH 7.8, 40 mM $MgCl_2$, 1 μg/ul Pepstatin, Leupetin, Bestatin). The pellet was resuspended in permeabilization buffer (38.3 mM Tris-HCl pH 7.8, 42.1 mM $MgCl_2$, 0.53 mM EDTA, 13.9 mM β-Mercaptoethanol, 1 μg/ul Pepstatin, Leupetin, Bestatin), supplemented with 400 μM etheno-NAD^+ (Sigma Aldrich) or 4 mM PJ34 (Enzo Life Science) and incubated for 20 min at 37°C at 900 rpm in a rotator. After centrifugation the pellet was resuspended in SDS-lysis buffer and run on a 18% SDS-PAGE. Western blotting was performed with anti Ig4 antibody hybridoma serum (kindly provided by Dr. R. Santella, Columbia University, USA) in a vacuum blot apparatus (Millipore SNAP i.d).

Supplementary Figures

Supplementary Figure 1:

PARP1 poly(ADP-ribosyl)ates chromatin associated histones. (A) HEK293T cells were depleted of PARP1 and nuclei were prepared. The nuclei were incubated with 400 μM etheno-NAD^+ at 37°C for 20 min and lysed in SDS-lysis buffer. Western blotting was performed with the Ig4 antibody, which specifically recognizes the etheno-group of NAD^+. (B) HEK293T cells were transiently transfected with HA-PARP1 (ov. PARP1) or with an empty vector (control). Nuclei were prepared and incubated with 400 μM etheno-NAD^+ in presence or absence of the PARP-Inhibitor PJ34.

Supplementary Figure 2:

(A) Trans-ADP-ribosylation of histone tails by PARP1. 1.5 μg of full-length and truncated histones were incubated with 10 pmol PARP1 and 100 nM ^{32}P-NAD^+ for 15 min at 30°C. His-tagged H2B (36-122) was generated by PCR and cloned into pET3a with NdeI and BamHI restriction enzymes. The protein was expressed in inclusion bodies, solubilized, purified by a nickel-column and dialyzed against water. The other histones were expressed and purified as in Luger K. et al, 1997, JMB, 272, 301-311. (B) Identical to Fig. 1C of the main manuscript. The automodification of PARP2 was adjusted to the automodification of PARP1 by ImageQuant-Software. (C) Trans-ADP-ribosylation of H2B is not impaired in an H2B E2A mutant, in which the only glutamic acid residue is substituted by an alanine. Shown are autoradiographs and Coomassie stained gels. (D) Poly-L-lysine but not poly-L-glutamate are modified by hPARP1. Poly-L-amino acids were coupled onto cyanogen-bromide activated agarose beads over night as suggested by the provider (Sigma-Aldrich). Excess poly-L-amino acids were washed away and unoccupied reactive sites were blocked over night. The beads were washed and equilibrated in PARP1 reaction buffer. Reactions were performed for 5 minutes at 30°C in the presence of 100 nM radiolabeled NAD^+. The beads were washed 3 times in PARP1 reaction buffer containing 500 mM NaCl before scintillation counts in two different channels were determined. (E) Extracted ion chromatogram of the biotin tagged H3 (23-42) peptide, ADP-ribosylated by PARP1. ETD fragment spectrum of ADP-ribosylated

H3 peptide (590.29 m/z) at K37, indicated by the sequence plot. (F) Automodification of wild-type PARP1 and PARP1 D756K mutant for 10 min at 30°C in presence of activating DNA (EcoRI-linker) and 100 nM ^{32}P-NAD^{+}. Shown is an autoradiography and the coomassie stained gel. (G) Histone H4 (aa 1-22) peptide was ADP-ribosylated with PARP1 or PARP1 D756K mutant for 15 min at 30°C with 100 nM ^{32}P-NAD^{+}. The peptides were purified by microvolume-C18 reversed phase columns, eluted into scintillation liquid and counted for incorporated ^{32}P. Relative increase of counts per minutes was calculated over background (peptides added after termination of the reaction by 3AB) and the counts obtained for wild-type PARP1 were set to 100.

Supplementary Figure 3:

Time evolution of intermolecular salt bridges and side chain dihedral angles of PARP1 Tyrosine residues in the catalytic cleft.

A

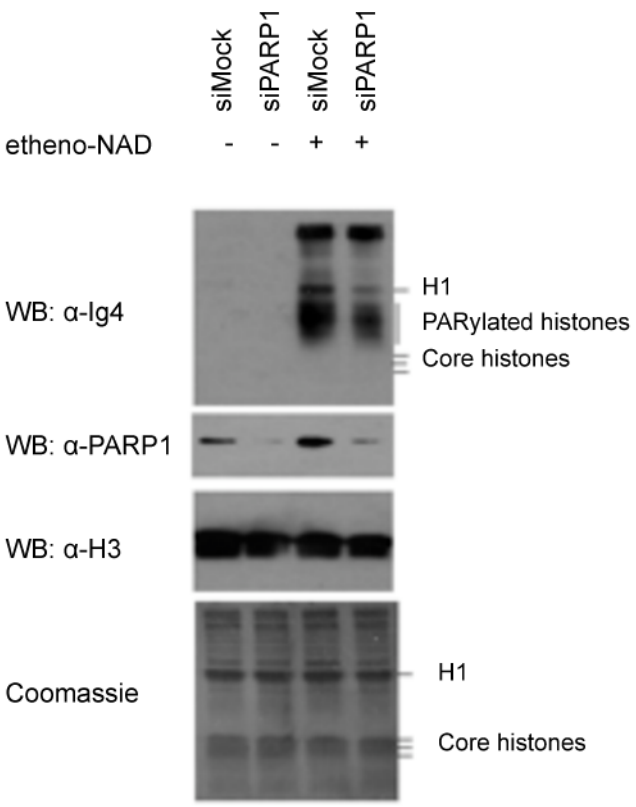
siMock
siPARP1
siMock
siPARP1
etheno-NAD
- - + +
WB: α-Ig4
H1
PARylated histones
Core histones
WB: α-PARP1
WB: α-H3
Coomassie
H1
Core histones

B

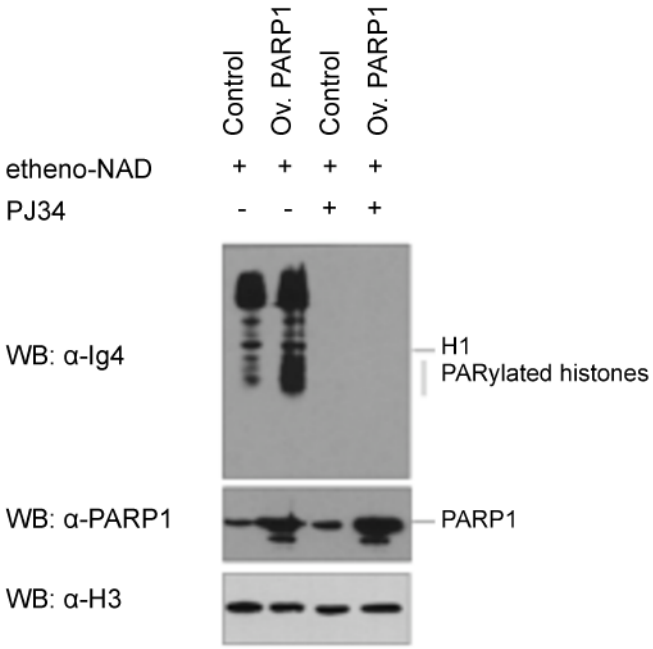
Control
Ov. PARP1
Control
Ov. PARP1
etheno-NAD
+ + + +
PJ34
- - + +
WB: α-Ig4
H1
PARylated histones
WB: α-PARP1
PARP1
WB: α-H3

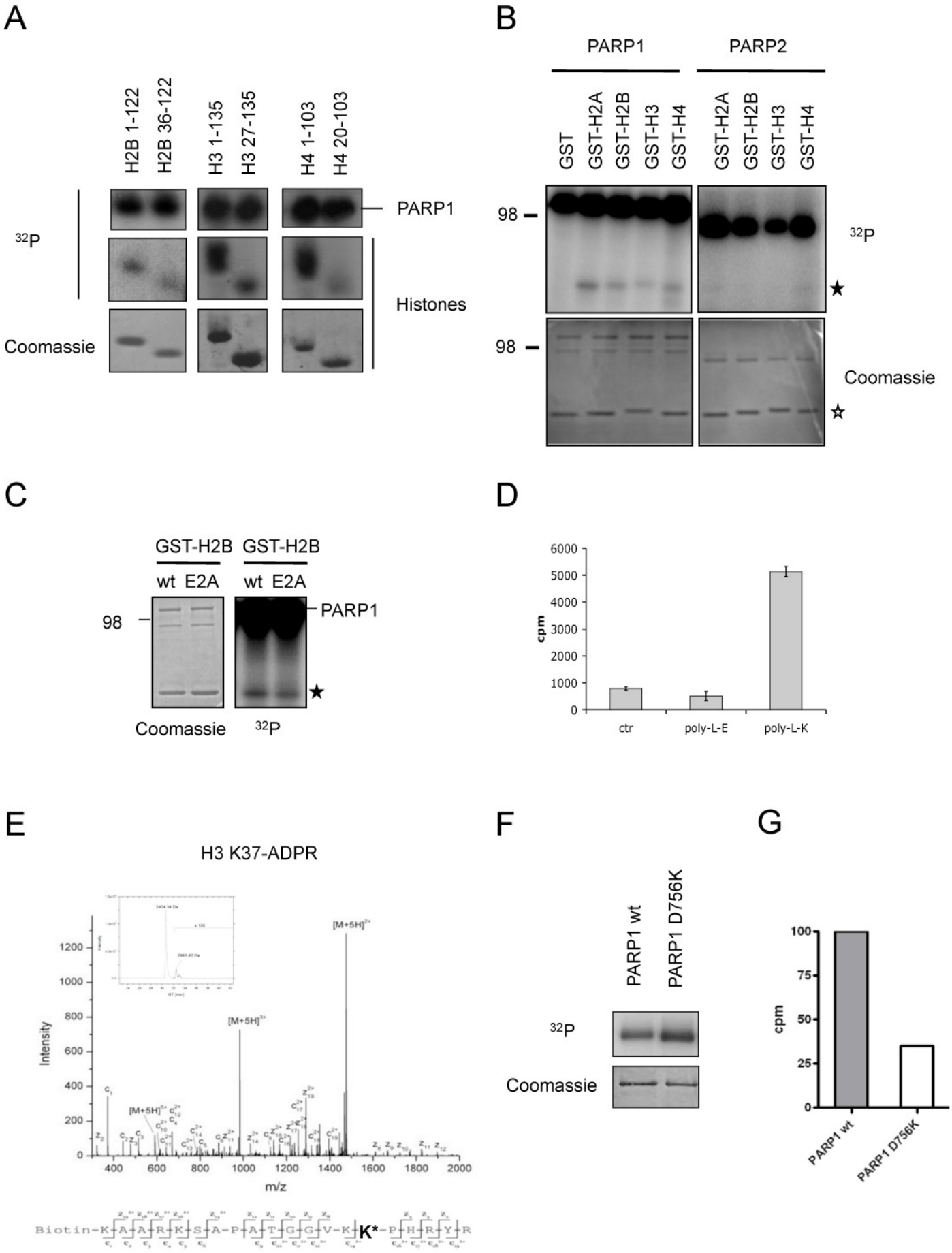
A
H2B 1-122
H2B 36-122
H3 1-135
H3 27-135
H4 1-103
H4 20-103
32P
PARP1
Histones
Coomassie
B
PARP1
PARP2
GST
GST-H2A
GST-H2B
GST-H3
GST-H4
GST-H2A
GST-H2B
GST-H3
GST-H4
98
98
32P
Coomassie
C
GST-H2B
GST-H2B
wt
E2A
wt
E2A
98
PARP1
Coomassie
32P
D
cpm
6000
5000
4000
3000
2000
1000
0
ctr
poly-L-E
poly-L-K
E
H3 K37-ADPR
Intensity
m/z
[M+5H]5+
[M+5H]5+
[M+5H]5+
Biotin-K-A-A-R-K-S-A-P-A-T-G-G-V-K-K*-P-H-R-Y-R
F
PARP1 wt
PARP1 D756K
32P
Coomassie
G
cpm
100
75
50
25
0
PARP1 wt
PARP1 D756K

Time evolution of intermolecular salt bridges and side chain dihedral angles of PARP1 Tyr residues in the catalytic cleft